A Methodology for Design and Adaptation of Infrastructure Under Deep Climate Uncertainty

by

Mohammad Michael Barkhori Mehni

A thesis

presented to the University of Waterloo

in fulfillment of the

thesis requirement for the degree of

Doctor of Philosophy

in

Civil Engineering

Waterloo, Ontario, Canada, 2023

Examining Committee Membership

The following served on the Examining Committee for this thesis. The decision of the Examining Committee is by majority vote.

External Examiner: Dr. Samer Adeeb
                               Professor, Dept. Of Civil and Environmental Engineering
                               University of Alberta

Internal-External Member: Dr. Gordon Savage
                               Professor, Dept. Of Systems Design Engineering
                               University of Waterloo

Internal Members: Dr. Bruce MacVicar
                               Associate Professor, Dept. Of Civil and Environmental Engineering
                               University of Waterloo

                               Dr. Kunho Eugene Kim
                               Assistant Professor, Dept. Of Civil and Environmental Engineering
                               University of Waterloo

Supervisors: Dr. Mahesh Pandey
                               Professor, Dept. Of Civil and Environmental Engineering
                               University of Waterloo

                               Dr. Scott Walbridge
                               Professor, Dept. Of Civil and Environmental Engineering
                               University of Waterloo

Author's Declaration

I hereby declare that I am the sole author of this thesis. This is a true copy of the thesis, including any required final revisions, as accepted by my examiners.

I understand that my thesis may be made electronically available to the public.

Abstract

Proper decision-making in design, and adaptation management of infrastructure is essential, in the face of environmental uncertainties. As and example, current climate change models yield a range of widely diverging projections, rendering the allocation of climate change readiness investments increasingly complicated. While a severe climate change scenario may necessitate extensive adaptation investments, realization of a mild or moderate environment after costly system modifications or early adoption of costly adaptation measures would also result in a sense of loss. An alternative approach is resorting to adaptive solutions that commence with reduced costs until the environmental circumstances become more evident.

With the goal of minimizing the sense of loss associated with decision-making, this research integrates the concept of regret into a decision-making framework. Regret serves as a quantifiable metric, capturing decision-makers' desire to mitigate the sense of loss resulting from making incorrect choices. Additionally, the framework incorporates the potential of gaining information over time about climate as it occurs through a dynamic programming scheme.

The research encompasses three studies. Firstly, common design and decision-making approaches are evaluated within the context of climate change. Specifically, an investigation into the nonstationary effects of wind load on structural reliability under the impact of climate change was conducted using several methods. The findings reveal that, under the worst scenario, the lifetime probability of failure can

be around twice as high as the baseline without climate change. However, such a scenario-based analysis is not conclusive in decision-making.

To facilitate decision-making in the face of deep climate uncertainty, an innovative methodology is developed and then tested in a second study on bridge corrosion management. In this study, the methodology offers a straightforward decision-making approach when considering the implementation of costly corrosion protection measures in an unknown environment. Additionally, a sensitivity analysis aids in discerning project types and determining the optimal course of action, whether it involves waiting or investing in field testing.

Finally, the third study is an application of the methodology in the context of climate change by addressing the design and managed adaptation of a river-crossing bridge exposed to climate change-induced scour. The study showcases how the methodology can assess trade-offs among different design options and determine the optimal course of action, given the uncertainties surrounding future climate scenarios. By evaluating the trade-offs between inaction and costly adaptations, the research identifies conditions under which a wait-and-see approach is effective and when incorporating design flexibilities for future adaptations is warranted. Furthermore, the method's performance is evaluated, and a comparison of various decision-making methods for adaptation is presented. The analysis demonstrates that in the case study, incorporating the potential for information arrival can yield up to $3.5 million in benefits, where an indirect cost of failure amounts to $10 million. Consequently, this framework empowers designers and asset managers to navigate the uncertainties of climate change in their decision-making processes effectively.

The outcomes of this research contribute to the advancement of decision-making approaches for infrastructure design and adaptation in the face of climate uncertainties. By integrating deep uncertainties into decision-making processes and proposing an innovative methodology, this research assists infrastructure owners, managers, and policymakers in enhancing the resilience and long-term sustainability of infrastructure systems in an uncertain future climate.

Acknowledgements

My deepest appreciation goes to my supervisor, Prof. Scott Walbridge, and Prof. Mahesh Pandey. Their unwavering support and invaluable guidance have been instrumental throughout my academic journey. Prof. Walbridge, akin to a second father, not only served as an exemplary leader in academia but also provided mentorship that transcended into various facets of my life.

I would like to extend my gratitude to the esteemed committee members, Profs. Bruce MacVicar, K. Eugene Kim, Gordon Savage, and Samer Adeeb for agreeing to be on my committee. Their insightful comments and constructive feedback significantly contributed to the refinement of my work.

Special thanks go to Profs. James Craig and Bill Annable for their time and critical guidance, essential in navigating the challenges of my research.

Heartfelt appreciation goes to my family members, Noorallah, Mehrangiz, Hamed, Moen, Fatemeh, Moeeneh, Mehdi, and Shirin, whose unwavering moral support played a pivotal role, especially during challenging times.

I am genuinely thankful of my colleagues and research group members, Ali Chehrazi, Laurent Gerin, Melanie Perreault, Carol Liang, Rakesh Ranjan, Michelle Chien, Eduardo Fontes, Abdullah Abdelbadie, Jun Seo Lee, Mi Zhou, Maryam Shirinchi, Mahmoud Trimech, and Mohammad Tolou Kian. Their collective support has propelled me to this significant milestone in my academic and professional journey.

Dedication

This thesis is dedicated to my loved one, Asal.

Table of Contents

List of Figures

xvi

List of Tables

Nomenclature and Abbreviations

CDF	Cumulative distribution function
DAPP	Dynamic adaptive pathway planning
LCC	Life cycle cost
LRFD	Load and resistance factor desing
MCS	Monte Carlo simulation
MR	Minimax regret
PCIC	Pacific climate impacts consortium
Plan	A detailed timeline for performing a sequence of actions
Policy	A set of rules that a decision-maker uses to map from states to actions for maximizing its expected cumulative reward. In comparison with plans, policies are broader in scope and provide a framework for decision-making.
RDM	Robust decision making
SDEMRD	Stochastic differential equation with mean-reverting drift
WDR	Wind to dead load ration
WV	Waiting value

List of Notations

A Wind exposure area

$A(t)$ The action set available at time interval $[t, T]$

a Action choice

$\tilde{a}(t)$ Plan determined through the stochastic information arrival method

a_* Scatter parameter of Gumbel distributed extreme wind event with return period of * years

$a^c(t)$ Optimal action found at time t using classical MR method

a_c Analysis coefficient for the conversion of the wind load into a load effect

$a_s^d(I)$ Best scenario-based action according to deterministic information arrival method

C_e Wind exposure coefficient

C_g Wind gust coefficient

C_h Wind horizontal effect coefficient

$c_{sa\tau}$ Element of cost matrix for taking action a at time τ under scenario s

$c_s^c(t)$ Scenario based cost of decision-making at time t using classical MR method

$c_s^d(I)$ Scenario based cost for waiting for information arrival at time I using deterministic information arrival method

COV_* Coefficient of variation of random variable *

D Random variable representing dead load

D_{50} Median grain size

dz Increment of a standard Winner Process: $dz = \varepsilon\sqrt{dt}$

$F()$ CDF of the information arrival time

$F_L()$ Cumulative distribution function (CDF) of demand, L

Fr Froude number

Fy Yielding strength

G Limit state function

g Gravitational constant

h_b Vertical bridge opening height before scour

h_{s0} Horizon at the initial time under scenario s

h_t Flow depth above the bottom of the bridge superstructure

h_u Upstream channel flow depth

h_{ue} Effective approach flow depth under the bridge

h_w Height of the weir flow overtopping the bridge

k_1 Correction factors for pier nose shape

k_2 Correction factors for flow angle of attack

k_3 Correction factors for bed condition

K_u A constant factor for calculation of $y_{s,SFCS}$

L	Demand
M_D	Nominal value of dead load flexural effect on the bridge component
M_R	Nominal flexural resistance of the bridge component
M_W	Nominal value of wind load flexural effect on the bridge component
m_D	Random variable for dead load flexural effect on the bridge component
m_R	Random variable for flexural resistance of the bridge component
m_W	Random variable for wind load flexural effect on the bridge component
P_i	Annual probability of failure of the ith year under maximum annual wind loading
$P_I(t_i)$	Probability of information arrival between t_{i-1} And t_i
$P_I'(t_i)$	Probability of no information arrival between t_{i-1} and t_i
P_{T_j}	Cumulative probability of failure through the jth year of service
p	Design horizontal wind load pressure
p_f	Probability of failure
q	Air pressure
R	Random variable representing resistance or capacity
$R^{\text{c}}(t)$	Regret of decision-making at time t using classical MR method
$R^{\text{d}}(I)$	Regret of decision-making at time $t = I$ using deterministic information arrival method

$R_S^d(I)$ — Scenario based regret for waiting for information arrival at time I using deterministic information arrival method

$R_{sa\tau}$ — Element of regret matrix for taking action a at time τ under scenario s

S — Scenario variable

T — Planning horizon

t — Time

t_0 — Break even time when $V^d(t_0, t_0) = 0$

U — Subtraction of the dead load from resistance: $U = R - D$

V — Wind velocity

$V^d(t, I)$ — The value of information update at I based on available action choices at time 0 (i.e., the construction phase)

$V^d(0, I)$ — The value of information update at a time $I = t$ based on available action choices at decision-making time, t

$V^s(t)$ — An expectation of the waiting value for information arrival

V_{ue} — Effective average approach velocity under the bridge

v — Streamflow velocity

var_* — Variance of random variable *

$\bar{V}_{10}$ — 10-year wind speed in design code

$\bar{V}_{100}$ — 100-year wind speed in design code

W	Random variable representing wind load
X	A variable representing the stochastic process of maximum annual streamflow
$y_{s,pc}$	Pile cap scour depth
$y_{s,pg}$	Pile group scour depth
$y_{s,pier}$	Pier scour depth
$y_{s,SFCS}$	Submerges flow contraction scour depth
z_*	Normalization of random variable * by dividing it with its nominal value
z_{Mod}	Normalized random variable representing model errors in the prediction of the exact value of resistance.
α	Persistence or instantaneous drift rate of the stochastic streamflow process
α_D	Dead load factor
α_L	Load factor
α_W	Wind load factor
β	Reliability index
ε	A random variable following the normal distribution: $\varepsilon \sim N(0,1)$
$\lambda(t)$	Time-varying occurrence rate of the loading
ρ	Density of air

μ Trend slope of the stochastic streamflow process

μ_* Central tendency of Gumbel distributed extreme wind event with return period of * years

σ Instantaneous variance of the stochastic streamflow process

σ_* Standard deviation of random variable *

τ Time of exercising a chosen action

$\tau^c(t)$ Time of exercising $a^c(t)$ based on decision-making at time t

$\tau_s^d(I)$ Time of exercising $a_s^d(I)$

ϕ_R Resistance load factor

Ω Phase change time, a time after construction beyond which adaptation would not be reasonable even with having the information that the worst scenario is occurring

$\mathcal{A}$ Constant for corrosion rate

$\mathcal{B}$ Constant for corrosion rate

$\mathcal{C}$ Thickness loss due to corrosion

$\mathcal{L}(t)$ Time-dependent reliability

$\mathcal{R}(X)$ Correlation matrix, in which $X = [x_1, x_2,, \ldots, x_n]$ is the vector of random variables in different years (e.g., wind load effect in successive years of service) and the element $r_{x_i x_j}$ defines the correlation between variables in i^{th} and j^{th} year.

$\mathcal{S}$ Section modulus

$*_n$ Nominal value of parameter *

$\overline{*}$ Mean of random variable *

Chapter 1. Introduction

1.1 Extent of Impact

Different climate systems regulate the natural environment of our planet. Any disturbance to the harmony of these systems, natural or human-made, is a threat not only to natural ecosystems but also socio-economic ecosystems through complex cascading effects. In recent years, changes in the average temperature compared to historical data have provided strong evidence of climate change, attributed to the increase of greenhouse gas (GHG) emissions. The Intergovernmental Panel on Climate Change (IPCC) predicts a temperature rise of 1.5°C to 4°C above the 1850-1900 average, by the end of the 21st century (Stocker et al., 2014). While global climate models predict a temperature rise of almost two times the global average for Canada, the changes in northern regions can be more intense, affecting the coverage of permafrost in those regions and imposing severe risk to many infrastructure systems such as foundations of buildings, roads, and bridges. Temperature changes can also influence deterioration and degradation rates of infrastructure. Additionally, due to expected changes in climate systems, precipitation patterns/frequency and tornado and high-wind events severity are expected to change. In general, it is predicted that dry lands around the equator will become drier, and wet areas will become wetter. In Canada, with high confidence, the annual precipitation and rainfall are predicted to increase with global warming over the 21st century (Cannon et al., 2020). Accordingly, changes in precipitation and wind speed may result in an increase in driving rain wind pressures (DRWP) by ~5 to 22% over the six Canadian regions with a larger effect in British Columbia and the North at the +3°C global warming level. With the increase of surface temperature in the future and poleward shift of the 0° isotherm,

1

the frequency and amount of ice accretion will change particularly in winter, with a decrease in southern North America and an increase in northern North America. The magnitude of this increase could be considerable and risky for buildings and infrastructure in latitudes higher than 50° North (see (Cannon et al., 2020)).
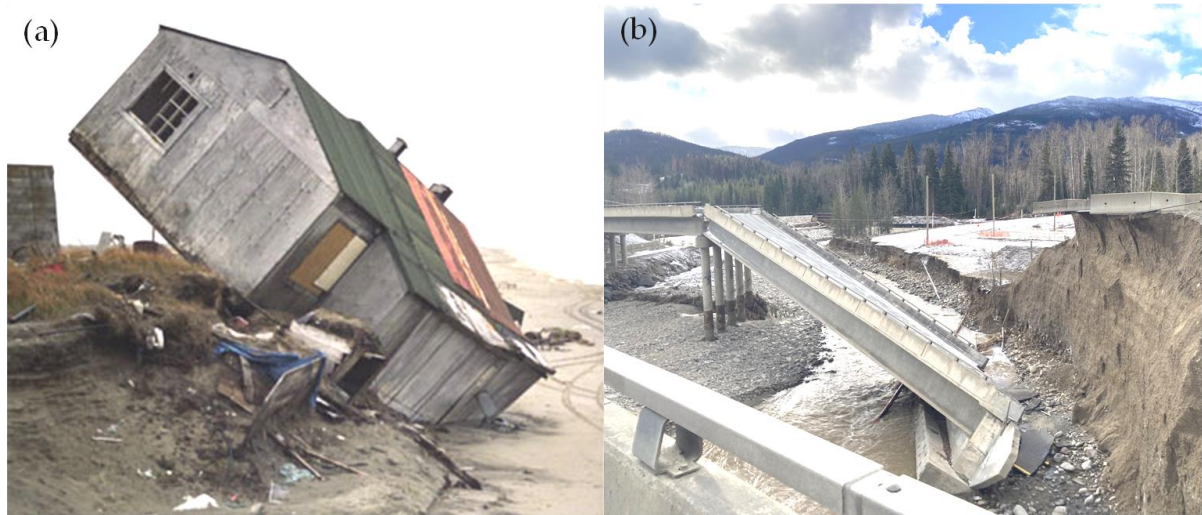
Figure 1-1. Examples of climate change effects on built environment. (a): melting ground and sea ice destroying a village in Alaska, U.S. (Issues - Global Warming | Impact Zones - U.S. Alaska, n.d.), and (b): damage to the Coquihalla Highway in BC, Canada (Judd, 2021).

These changes in climatic variables may have a significant effect on the reliability, performance, and life cycle cost of infrastructure systems (see Figure 1-1). For instance, changes in precipitation patterns can cause flooding events and failures of bridges. An analysis of previous data on the failure of 500 bridges in the U.S. between 1989 and 2000 has shown that above 50% of failures are related to scour and foundation instabilities (Wang et al., 2017; Wardhana & Hadipriono, 2003). Another study on the failure of bridges in the U.K. estimates that depending on the location of the bridges, the risk of failure due to scour will increase 3 to 50% compared to the

current risk level by the 2080s (Bastidas-Arteaga & Stewart, 2019). The occurrence of tornadoes and high-wind events accompanied by rain or ice accretion threatens buildings and infrastructure systems such as bridges and power transmission and distribution lines. While climatic conditions can impact the lifespan and capacity of power lines, power losses related to weather conditions can be highly costly. A historical analysis of disasters in the United States has shown that storm and weather-related events like ice, high winds, flooding, and lightning strikes have been the cause of 78% of major power outages (based on 1333 events from 1992 to 2010 (Mills, 2012)) with an equivalent repair cost of $270 million per year (Johnson, 2005). Moreover, wind-driven rain events could threaten existing buildings and their contents. Therefore, consideration of climate change in the design and adaptation of infrastructure systems will be critical for addressing these concerns.

1.2 Research Gaps

Infrastructure systems, including transportation networks, bridges, buildings, and utilities, play a critical role in supporting economic activities and ensuring the well-being of communities. However, these systems are designed based on historical climate data and assumptions of stationarity, or in other words assumption that future climate conditions will be similar to the past. The uncertainties associated with climate change challenge this traditional approach and require a re-evaluation of infrastructure design, construction, and management practices.

The conventional approach to managing infrastructure risks relies on a combination of deterministic models and probabilistic assessments that use historical data. However, these approaches become less reliable in the face of climate change,

3

where future climate projections are uncertain and may deviate significantly from historical patterns. The inherent deep uncertainties associated with climate change make it challenging to accurately predict future climate scenarios, which are crucial for making informed decisions regarding infrastructure design, adaptation, and maintenance.

Addressing the impacts of climate change on infrastructure safety requires new decision-making frameworks that can account for these so-called deep uncertainties in developing the adaptive design and management strategies. These frameworks should allow decision-makers to evaluate alternative design options, assess trade-offs, and prioritize investments to minimize risks and possible future regrets.

Another aspect of climate change uncertainty is that it will likely decrease over time as a result of scientific advancements, statistical data, and monitoring weather patterns (van der Pol, van Ierland, et al., 2017). For example, some studies suggest meaningful learning about some important aspects of climate change will take 20–50 years to occur (Lee et al., 2017; Urban et al., 2014). This possibility leads to some questions. One question is whether inaction and waiting for such information is worth the risk of adverse climate change driven events. Another important question is around the value of implementation of costly design flexibilities.

1.3 Motivation

The impacts of climate change pose significant challenges for infrastructure planning and decision-making. As uncertainties surrounding future climate scenarios persist, there is a growing need for effective strategies to address these uncertainties and make informed decisions regarding the design and adaptation of infrastructure

systems. Traditional approaches to decision-making may be inadequate in dealing with deep uncertainties and the evolving risks associated with climate change. Therefore, there is a pressing motivation to explore new decision-making tools and methodologies that can better capture the complexities of climate change uncertainties and support more robust and adaptive infrastructure design and management. With this motivation, this research investigates decision-making approaches that can guide the design and adaptation of infrastructure systems. By exploring the advantages and limitations of different methods, this research contributes to the development of a design and planning framework leading to more resilient and sustainable infrastructure systems that can withstand the challenges of a changing climate.

1.4 Objectives

The thesis aims to investigate and address several key research objectives that are central to the topic of design and adaptation in the context of climate change. These research objectives include:

- *Develop a design and adaptation framework using a regret-based decision-making approach*: Traditional optimization-based approaches are inadequate in dealing with uncertainties in climate change scenarios where the likelihood of various possible outcomes is unknown. By employing a non-probabilistic decision-making tool, the thesis seeks to overcome this limitation and provide more robust design and adaptation strategies that are better suited for the uncertainties of climate change.

- *Exploring the wait-and-see design and adaptation management paradigm:* Recognizing the evolving nature of climate change information, a new design paradigm based on the wait-and-see concept can be beneficial. In traditional approaches, infrastructure is designed and built based on assumptions of stationery or known trends in demand. However, in the face of climate change uncertainty, adopting a wait-and-see approach allows for the consideration of delaying extensive safety investments and incorporating future adaptation flexibility into the initial design.

- *Minimizing hindsight regret:* Given the inherent uncertainties of climate change, decisions and planning must be made with imperfect information. To mitigate the potential regret associated with these decisions, the thesis focuses on defining objective functions that minimize the regret as knowledge on climate change evolves. This approach aims to improve decision-making under uncertain conditions.

- *Assessing the trade-offs and implications of a wait-and-see approach:* One important aspect is determining the value of inaction and waiting for additional information versus implementing early and potentially costly adaptation measures. The thesis aims to analyze the conditions under which employing a wait-and-see approach is effective and when it is reasonable to implement design flexibilities to accommodate possible future adaptations.

By addressing these research questions, the thesis seeks to advance our understanding of decision-making in the face of climate change uncertainties. The findings will contribute to the development of more effective design and adaptation

strategies that can enhance the resilience of infrastructure systems and minimize the potential negative consequences of climate change.

1.5 Overview

Chapter 1: Introduction

This chapter introduces the research problem, its significance, and the objectives of the study. It sets the stage for the subsequent chapters by highlighting the need to address uncertainties related to climate change and the importance of decision-making tools in this context.

Chapter 2: Literature Review

The second chapter offers a comprehensive examination of the sources of uncertainty associated with climate change. It categorizes these uncertainties into distinct elements and assesses their relative significance. Moreover, this chapter explores the decision-making tools available within the context of climate change and presents contemporary approaches to design and management.

Chapter 3: Methodology

Chapter three begins by providing a detailed explanation of the methodology, illustrated through straightforward examples. It subsequently formulates the methodology and delves into its essential properties, laying the groundwork for its application in later chapters.

Chapter 4: Assessment of Climate Change Effects

The fourth chapter aims to demonstrate several possible approaches for considering non-stationary (e.g., increasing) load effects in the reliability analysis of

structures. the study focuses on assessing the impact of nonstationary wind loading, a key climatic stressor, on the performance of a structural element situated in London, Ontario, Canada. The presented approaches may serve as useful practical tools for aiding code-writers and decision-makers to assess the effects of changes in climatic stressors on the failure risk and life cycle cost associated with new and existing civil infrastructure.

Chapter 5: Application - Steel Bridge Corrosion Protection

Chapter five utilizes the developed framework in chapter three to evaluate various strategies for safeguarding steel bridges against unexpected corrosion degradation in weathering steel highway structures. It demonstrates the practical application of the methodology in addressing a critical issue in infrastructure resilience. Given the high variability in microclimate conditions around a bridge, this chapter delves into the complexities of preserving weathering steel under deep uncertainty, exacerbated by climate change effects on road salt usage. The chapter explores strategies for choosing optimal corrosion management options and action times using the developed methodology, with an emphasis on adapting to various possible futures rather than relying on singular expectations.

Chapter 6: Application - Bridge Scour Safety Investments

Chapter six explores the challenges posed by uncertainties associated with climate change for bridge managers, particularly concerning flood protection measures for vulnerable bridges. It delves into the issue of scour, the erosion of riverbed material around bridge foundations, and its expected exacerbation due to climate change impacts on local climate patterns and river flow regimes. This chapter

investigates whether inaction and waiting for more information is justifiable when facing climate-driven risks and the value of implementing costly design flexibilities. To address these questions, the proposed framework is employed to design a bridge in British Columbia, Canada. The methodology models the arrival of new information as a stochastic event with a predefined probability distribution, allowing for the evaluation of trade-offs between different design options in the presence of deep uncertainties associated with climate change.

Chapter 7: Conclusions and Future Research Directions

The final chapter, chapter seven, synthesizes the key findings of the study and draws conclusions based on the research outcomes. It also offers insights into potential avenues for future research, emphasizing the continued relevance and significance of the research in the broader context of climate change and related challenges.

Chapter 2. Literature Review

2.1 Introduction

Climate change presents significant challenges to common decision-making tools in civil infrastructure design and management. The complexities of the climate problem introduce uncertainties that are only partially addressed by current analytical tools. While it is acknowledged that the climate is changing, the precise extent, rate, and implications of these changes remain unclear. Uncertainties in this context stem from both scientific gaps and our limited comprehension of how the socio-economic system will evolve in response to climate changes over the next few centuries. These uncertainties cannot be easily quantified or expressed probabilistically, falling into the realm of deep uncertainty rather than simple "risk," as described by (Knight, 1921).

Consequently, the conventional expected utility framework offers limited usefulness. This chapter aims to comprehensively examine the sources of uncertainty related to climate change. It separates these uncertainties into different elements and comments on their relative importance. Additionally, it discusses the available decision-making tools in this context and presents current methods for design and management. By addressing the uncertainties surrounding climate change, this chapter enhances understanding of their implications for decision-making in civil infrastructure asset design and management. With this background, robust and adaptive strategies can then be developed to mitigate the risks and impacts of climate change on infrastructure systems.

2.2 Sources of Uncertainty

Human emissions of greenhouse gases are the primary cause of the observed global temperature changes throughout the 20th century. Recent advancements in climate change detection and attribution science have established this fact unequivocally (IPCC, 2007). The continued release of greenhouse gases such as CO_2 into the atmosphere will bring about further alterations to the climate. However, the magnitude and speed of the global climate's response to atmospheric composition changes are still unknown. This quantitative information is fundamental in shaping policy responses to the climate crisis.

Climate science provides insight on this regard; however, not as much as to comprehend when, where, and how much the climate will change. To better understand this, consider the case of estimates of climate sensitivity, perhaps the most studied among the climate science community. Climate sensitivity is a measure of the long-term average surface warming as a result of doubling of the atmospheric concentration of CO_2, in equilibrium. Estimates of the probability distribution for climate sensitivity for various research studies are presented in Figure 2-1 (Heal & Millner, 2014). The figure presents a lot of discrepancies among the studies. To comprehend the source of the variabilities, it would be helpful to know how these estimates are produced. Climate sensitivity is derived by running climate models. These models can be complex, with a lot of uncertainty about their parameters and initial conditions. Therefore, the scientists run the models under various configuration of the parameters and initial conditions. Subsequently, they weigh the output for each of these configurations according to the likelihood of the considered value of parameters. There is not a single method of assigning these likelihoods nor does there

exist a single best climate model that anyone agrees upon. One more important point is that the predictions of the models are not independent, as they are based on related data. As a result, it is not possible to assume they are equally likely. On the other hand, it is impossible to determine their dependency on each other (Heal & Millner, 2014). Therefore, it would be very difficult to interpret such variation between predictions in a probabilistic framework without imposing strong subjective judgments on the combination of various estimates (Knutti, 2010; Knutti et al., 2010). In conclusion, although climate models provide predictions about the future, the information they provide is ambiguous with no gold standard that everyone agrees upon. The climate sensitivity problem discussed here is on the top of the hierarchy of uncertainties and provides a rough image of the scale of the climate change problem.

Climate change projections are not exact predictions of what will happen. They are subject to various sources of uncertainty that affect their accuracy and reliability. The main contributors to the total uncertainty can be decomposed into the following categories:

- Scenario uncertainty: The future emissions of greenhouse gases and other human activities that affect the climate system are unknown and depend on social, economic, technological, and political factors that are hard to predict (Hawkins & Sutton, 2011; Katz et al., 2013).

- Model uncertainty: Different climate models may have different assumptions, simplifications, parameterizations, and resolutions that affect how they represent the physical processes and feedbacks in the climate system (Katz et al., 2013; Knutti & Sedláček, 2012) (Knutti & Sedláček, 2012).

- Internal variability: The natural fluctuations of the climate system due to chaotic dynamics and nonlinear interactions between its components can cause deviations from the long-term trends (Katz et al., 2013).

- Observational uncertainty: The historical data used to calibrate and evaluate the climate models may have errors or gaps due to measurement limitations or quality control issues (Katz et al., 2013).
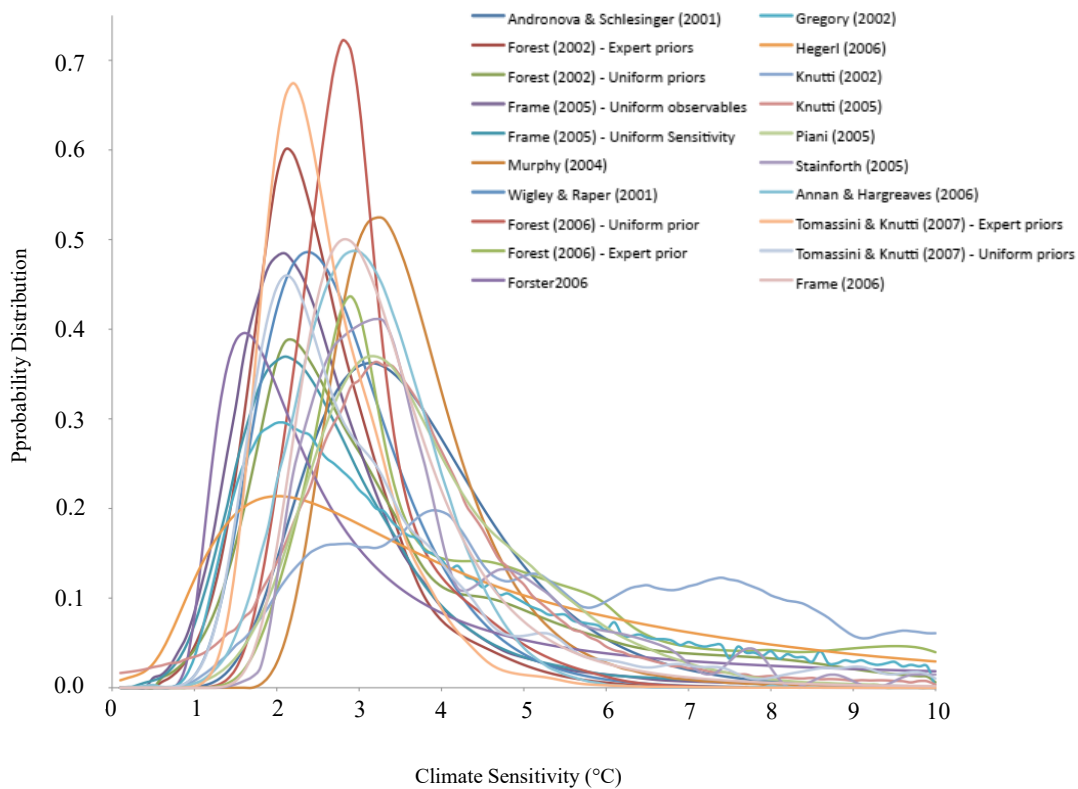
Figure 2-1: Estimates of the probability distribution for climate sensitivity (Heal & Millner, 2014).

(Hawkins & Sutton, 2011) have done a study on the contribution of emissions scenario uncertainty, model uncertainty, and internal variability in the total

13

uncertainty based on the lead time of projection. Figure 2-2 shows how this decomposition for temperature change (ignoring observational uncertainty). When dealing with short lead times – less than 20 years, internal variability and model uncertainty are the primary sources of unpredictability. This observation is not surprising given that the climate system is inherently chaotic, thus rendering it sensitive to initial conditions. Furthermore, regional predictions are particularly sensitive to internal variability, which contributes significantly to total uncertainty for lead times of 60 years or more. At the global level, model uncertainty is the dominant source of unpredictability for projections spanning 20 to 50 years. This is reflective of the diversity of predictions generated across various climate models. However, beyond the 50-year mark, the uncertainty in emissions scenarios becomes the primary driver of long-term unpredictability. This is because it is shaped by the policies that are ultimately adopted, which have significant implications for the rate of greenhouse gas emissions.

In summary, the interplay of internal variability, model uncertainty, and emissions scenario uncertainty all contribute to the overall uncertainty of climate projections, and their relative importance varies with lead time. These findings are critical for decisionmakers, who must balance the desire for long-term predictability against the need to make decisions in the face of significant uncertainty.
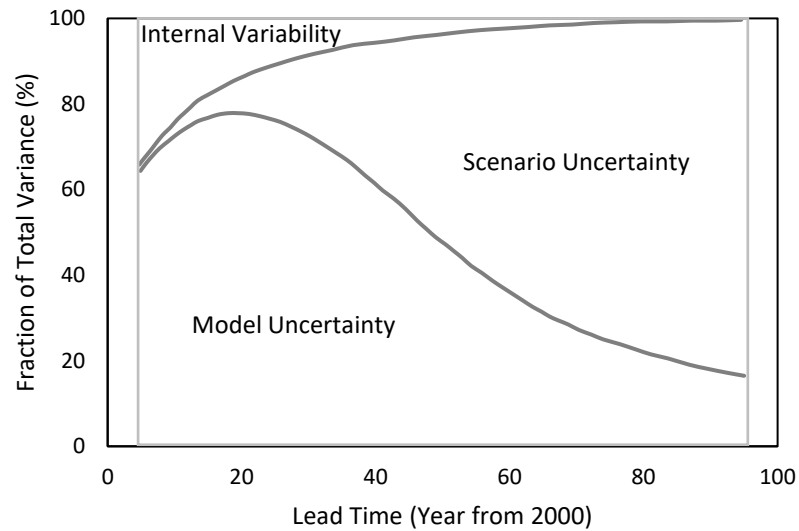
Figure 2-2. Sources of uncertainty in temperature predictions as a function of lead time, from

(Hawkins & Sutton, 2011).

2.3 Infrastructure, Climate Change, and Deep Uncertainty

According to a recent report by The Financial Accountability Office of Ontario, adapting public transportation infrastructure due to climate change could increase costs between $110 billion to $229 billion by 2100, depending on emissions scenarios (Afroz et al., 2022). The climate change uncertainty poses challenges to infrastructure managers in investing in protection and adaptation measures. This uncertainty makes it difficult to assess risks and trade-offs, prioritize actions, evaluate alternatives, and monitor outcomes. For instance, one of the primary reasons for bridge failure globally is scour, or the removal of riverbed material from the bridge foundations caused by water flow. This issue is expected to be exacerbated by the impacts of climate change, which affects local climate patterns and river flow regimes that may increase the risk of bridge failure. So far determining the level of these changes in climate has been

15

elusive. Deterministic approaches are appropriate for defining optimum management plans for a clear and relatively certain future, which is not the case in this problem with very different and uncertain projections of river flow processes. Future climate projection is a complex task due to the interplay of various factors, including solar radiation, greenhouse gas emissions, and natural variability. Additionally, there is a limited amount of historical data available, making it challenging to understand past climate responses and make accurate predictions about future changes.

Despite these challenges, scientists have made significant progress in developing models to predict the impacts of climate change by using data from various sources, including satellites, weather stations, and ocean buoys. However, the models are limited by the quality of data and the accuracy of assumptions used in the simulations, leading to high levels of uncertainty referred to as deep uncertainty, or ambiguity, mostly in economics literature (Etner et al., 2012).

Deep uncertainty is a term that describes a situation where decision makers and stakeholders face multiple plausible future scenarios that are influenced by complex and interrelated factors, such as natural variability, human behavior, technological innovation, and policy choices. In such a situation, decision makers and stakeholders do not know or cannot agree on how likely these scenarios are to occur, what consequences they would have for natural and human systems, or what values should guide their decisions. A formal probabilistic representation of deep uncertainty is a challenging task. Figure 2-3 provides a summary of four uncertainty levels between determinism and total ignorance as distinguished by (Walker et al., 2010). This summary highlights the distinction between deep uncertainties (Levels 3 and 4, depicted in the right two columns) and the more manageable uncertainties

encountered in statistics and scenario analysis with known probabilities (Levels 1 and 2, shown in the left two columns).

Deep uncertainty challenges the traditional expected utility theory for decision making, a gold standard for normative models in decision analysis field. Traditional decision and risk analyses make extensive use of models to predict the probable consequences of alternative decisions, but this approach faces four major obstacles when dealing with model uncertainty: poor knowledge of underlying state or scenario probabilities, conflicting beliefs about the probabilities among stakeholders, and uncertainties or conflicts about values and preferences to be encoded in the utility function used to evaluate different consequences (Cox, 2012).
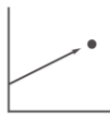
		Level 1	Level 2	Level 3	Level 4
				Deep Uncertainty	
	Context	A clear enough future	Alternative futures (with probabilities)	A multiplicity of futures	Unknown future
	System Model	A single system model	A single system model with a probabilistic parameterization	Several system models, with different structures	Unknown system model; know we don't know
	System Outcomes	A point estimate and confidence interval for each outcome	Several sets of point estimates and confidence intervals for the outcomes, with a probability attached to each set	A known range of outcomes	Unknown outcomes; know we don't know
	Weights of Outcomes	A single estimate of weights	Several sets of weights with a probability attached to each set	A known range of weights	Unknown weights; know we don't know

Figure 2-3. A suggested taxonomy of four levels of uncertainty between determinism to total ignorance (Walker et al., 2010)

17

2.4 Decision Theory and Deep Uncertainty

In engineering design, decision theory provides a framework for analyzing alternatives and selecting between choices. Therefore, to assess and improve engineering design and management frameworks, it would be worthwhile to begin exploring the realm of decision theory.

2.4.1 Expected Utility Framework

The dominant model for economists who deal with uncertainties is the expected utility framework of von Neuman and Morgenstern (vNM). It presupposes a well-defined set of outcomes, an exogenous probability distribution over them, and preferences over lotteries that can be represented by expected utilities. Nevertheless, this model does not adequately capture the uncertainties pertaining to climate change.

One challenge is a lack of a well-defined set of potential states of the world. Even today there may be implications of climate change that we are not considering. A simple example is reducing or stopping of the Gulf Stream – considered as a severe but improbable outcome of climate change, which was not even identified as a possibility until late 20th century (Broecker, 1997).

Another issue with the von Neumann-Morgenstern (vNM) framework is the lack of access to objective probabilities. To address this issue, the theory of Subjective Expected Utilities (SEU) proposed by (Savage, 1972) offers a traditional solution. This theory posits that rational decisions can be made under ambiguity or even absence of information by assuming subjective probabilities and selecting actions that maximize the expectation of a utility function. In essence, SEU provides a universal solution for all uncertain situations, regardless of the source of the probabilities.

However, empirical investigations, primarily by (Allais, 1953) and (Ellsberg, 1961), have revealed that human behavior violates a critical axiom of SEU known as the "Sure Thing Principle" (Gilboa, 2009). Ellsberg's research (Ellsberg, 1961) demonstrated that people treat objective unknown risks (e.g., the probability of flipping a fair coin and obtaining heads) differently from ambiguity or unknown uncertainties (e.g., the probability of flipping an unknown biased coin and obtaining heads). Therefore, while SEU offers a straightforward solution, its assumptions are not always consistent with human decision-making behavior (Heal & Millner, 2014; Malik et al., 2010).

Of course, the views on this topic have been widely debated. There are arguments that the fact that people are ambiguity averse should not be a part of the decision policy. On the contrary, some decision theorists believe that: SEU is not universally applicable (Binmore, 2008), subjective probabilities cannot always represent the state of knowledge (Gilboa et al., 2008), and ambiguity aversion is rational when dealing with low-quality information (Gilboa et al., 2009). Ultimately, there is no definitive answer regarding the applicability of SEU and the impact of ambiguity aversion on decision-making. With this background, it would be worthwhile to explore methods other than SEU for decision making under deep uncertainty.

2.4.2 Alternatives to Utility Framework

Over the past few decades, following the work of (Schmeidler, 1989) and (Gilboa & Schmeidler, 1989), there has been a significant expansion in the literature regarding decision-making under deep uncertainty. These methods are derived

through satisfying primitive choice axioms. Some scholars argue that the diversity of these approaches may lead to a fallback to the traditional SEU method, as it may not be clear how one of them should be selected. However, it is crucial not to be overwhelmed by the variety of methods and instead explore different avenues to address deep uncertainties (Heal & Millner, 2014). A thorough review of these methods is provided in (Etner et al., 2012). A short list of the most promising ones is provided in Table 2-1, which is adopted from (Heal & Millner, 2014). These methods can best be discussed with the aid of Figure 2-4. The A_i is a collection of alternatives one of which must be selected by the decision maker. The set $S = \{s_1, \dots, s_n\}$ contains the possible scenarios. Here u_{ij} is the utility of selecting alternative A_i when the actual scenario is s_j. An uncertainty is introduced since the decision maker is unaware of the actual scenario prior to choosing a preferred alternative.

$$
\begin{array}{c}
\\
A_1 \\
A_i \\
A_m
\end{array}
\begin{array}{ccc}
S_1 & S_j & S_n \\
\left(\begin{array}{ccc}
 & & \\
 & u_{ij} & \\
 & &
\end{array}\right)
\end{array}
$$

Figure 2-4. Basic utility matrix

Table 2-1. Alternatives to Expected Utility Theory

20

Name	Reference	Rule
Non-probabilistic Approaches		
Maxmin	(Wald, 1949)	$\max_i[\min_j u_{ij}]$
α-Maxmin	(Arrow & Hurwicz, 1972)	$\max_i[\alpha \min_j u_{ij} + (1 - \alpha) \max_j u_{ij}]$
Minmax Regret	(Savage, 1972)	$\min_i[\max_j\{(\max_{i'} u_{i'j}) - u_{ij}\}]$
Multiple Prior Approaches		
Maxmin EU	(Gilboa & Schmeidler, 1989)	$\max_i[\min_p \mathrm{E}_p(u_{ij})]$
Smooth Ambiguity	(Klibanoff et al., 2005)	$\max_i[\mathrm{E}_p\phi(\mathrm{E}_p(u_{ij}))]$
Variational Preference	(Maccheroni et al., 2006)	$\max_i[\min_p\{\mathrm{E}_p(u_{ij}) + C(p)\}]$

Note: In this table, p is the set of the probability of distributions in the superset ($\mathcal{P}$), and E denotes the expectation operator. In the smooth ambiguity approach, ϕ is a second order utility function (Heal & Millner, 2014).

The methods can be categorized into non-probabilistic and multiple prior approaches. For more details on the multiple prior approaches the reader is referred to (Heal & Millner, 2014). Non-probabilistic decision-making approaches include Maximin, a pessimistic approach that selects an action that maximizes a minimum utility. This method assigns to each alternative its worst payoff and then selects the alternative with the best of these worst payoffs. The α-Maxmin approach introduces an α factor to give the decision-maker leverage for their pessimism level. The Minimax Regret (MR) approach is like the other two approaches, but the decision-maker seeks to minimize the emotion of regret when realizing they made a wrong decision as the future unfolds.

2.4.3 Regret Derivation and Advantages

To drive the regret values for the MR approach, the following procedure is taken:

1. For each scenario, s_j, calculate the utility of the best possible action as $U_j = \max_i[u_{ij}]$

2. For each alternative/scenario pair A_i and s_j calculate regret $r_{ij} = U_j - u_{ij}$

3. For each alternative A_i calculate $R_i = \max_j[r_{ij}]$

4. Select alternative A_{i*} such that $R_{i*} = \min_i[R_i]$

Note that in this procedure, r_{ij} are the components of the regret matrix, and U_j is referred to as the "horizon" under s_j.

According to (Heal & Millner, 2014), the MR approach aligns more closely with human behaviour under deep uncertainty. Additionally, Minimax Regret is advantageous over the other two methods in capturing the benefits of a wait-and-see approach. In this regard, an illustrative example is provided in the following.

Consider the following example adopted from (Savage, 1951) with some modifications. Consider a situation where you must decide whether to carry an umbrella or wait for some time and watch the weather report on TV. For simplicity, let's assume there are only two possible outcomes: future rain or future shine. To analyze the potential consequences of each decision, the following table can be considered:

Table 2-2. Consequences of actions for different states

	State	
Act	Rain	Shine
Carry	Inconvenience and wet feet	Inconvenience and slight embarrassment
Don't carry	Miserable drenching	Convenience
Wait	Inconvenience, wet feet, and late	Convenience, but late

For the sake of comparison, it might be reasonable to express the consequence in terms of utility values such as presented in Table 2-3. In this table the horizon (i.e., the best action given the scenario) under each scenario is indicated with a star. Based on the utility values, regret of taking each action is determined based on this procedure and presented in Table 2-4. For better understanding, consider the case of waiting when the Rain is in the future state. In this situation, waiting results in a regret of 1, which is the difference of 3 as the utility of waiting and 4 as the horizon of the Rain Scenario. Subsequently, taking the MR approach would result in waiting, while considering the utility values given here, employing the Maximin approach results in carrying the umbrella. The reason is that waiting comes at a price, and paying this price reduces the minimum possible utility of waiting below all the other options. This issue in nature is similar to the issue of adaptation of infrastructure under deep uncertainties of climate change.

The issue of adaptation of infrastructure under deep uncertainties of climate change has the same nature. The uncertainty, however, will eventually decrease as a result of scientific advancements, statistical data, and monitoring weather patterns (van der Pol, van Ierland, et al., 2017). For example, some studies suggest meaningful learning about some important aspects of climate change will take 20–50 years to occur (Lee et al., 2017; Urban et al., 2014). This possibility leads to some questions. One question is whether inaction and waiting for such information is worth the risk of adverse climate change driven events. Another important question is around the value of implementation of costly design flexibilities.

Table 2-3. Utility of actions for different states

	State	
Act	Rain	Shine
Carry	4*	5
Don't carry	-10	10*
Wait	3	9

Table 2-4. Regret of actions for different states

Act	State	
	Rain	Shine
Carry	0	5
Don't carry	14	0
Wait	1	1

2.5 Methods of Design, Management, and Policies

Departing from the decision theory, this section first discusses the traditional design methods in stationary climate, then it explores the alternative design and planning methods that can be applied in a non-stationary climate.

2.5.1 Traditional Design Methods in Stationary Climate

Structural design generally involves making decisions about variables including dimensions and other specifications related to the structure. The approaches for the determination of these decision variables are versatile. In what follows, the design methods included in the international standard ISO 2394 (ISO, 2015) are provided with some detail.

2.5.1.1.1 Risk-informed Approach (Level 4)

In the Risk-informed (Level 4) approach, the principle of decision theory is directly applied for optimization and design of individual structures. In this regard, considering a simplified example of a component based on LCO, the total expected

costs $E[C_{tot}(\theta)] = C_c(\theta) + E[C_f] \cdot P_f(\theta)$ represents the societal preference. Here, $Cc(\theta)$ is the added cost of safety as a function of the vector of design parameters, (e.g., height of cross-section), while the product of the expected consequence of failure $E[C_f]$ and the probability of failure $P_f(\theta)$, represent the risk of failure in monetary units. As the costs of the added safety increase, while the risk of failure decreases with the design parameter, their summation generally forms a convex function whose minimum corresponds to the optimal solution maximizing the utility. It is noteworthy that while this approach provides the most optimal solution for an individual structure, it is rarely used for multiple reasons. Usually, there is a lack of information in design codes about hazards, their consequences, and probabilities of failures. Moreover, simpler methods (as provided in the following sections) are available that produce reasonably optimal results with much less computational effort (Baravalle & Köhler, 2019).

2.5.1.1.2 Reliability-Based Approaches (Levels 3 and 2)

In Levels 3 and 2 approaches, the design parameters are determined to satisfy requirements provided in design codes in the form of the reliability index β_{sys}, which has a one-to-one relation to the probability of failure P_f, where $P_f = \Phi(\beta_{sys})$ and $\Phi()$ is the standard normal cumulative density function. The design solution is determined by applying reliability methods to find the vector of design parameters, θ, that yields the required P_f.

Here, the reliability index is calibrated by code writers to provide an optimal level of safety for a class of structures. The structures included in a class are not identical but similar in terms of characteristics that affect their optimum design point (i.e. $C_c(\theta)$, $E[C_f]$, and $P_f(\theta)$). Although the individual structures designed with this

approach are not optimal, the method simplifies the design process by providing a β, which aims to optimally regulate the design approach (Baravalle & Köhler, 2019).

2.5.1.1.3 Semi-Probabilistic Approach (Level 1)

In the Level 1 approach, the decision problem is further simplified by avoiding the reliability analysis. Instead, the appropriate safety level is ensured by calibrating safety factors that consider the probability and consequences of failure. These safety factors include partial safety factors, load combination factors and modification factors, such as those that can be found in modern LRFD based codes. The calibration of the safety factors is usually divided into two tasks for simplicity. In the first task, the optimum component reliability index, β_{comp}, is determined through a procedure similar to the one described for level 2 and 3 codes. In the second task, the safety factors are calibrated based on β_{comp} through reliability-based code calibration. In this regard, an appropriate design should satisfy $f(\theta, S_f) \geq 0$, where S_f is the vector of safety factors (Baravalle & Köhler, 2019).

2.5.2 Design and Adaptation in the Face of Climate Change

This section is an overview of the assessment of the most common, design and adaptation approaches in the face of a changing climate. Currently, despite an abundance of guidance on how to tackle risks associated with deep uncertainties, the literature on adaptation of infrastructure to climate change is limited. In this respect, the current recommendations include creating organizations, systems, and infrastructure that are robust, flexible, and able to recover quickly; conducting trials to test potential enhancements and learning from any setbacks or experiences; and proactively gathering feedback and local insights to modify plans as circumstances

change. However, the practical challenge lies in determining the most effective means of executing these suggestions in practice. Those who advocate for increased learning, adaptability, and resilience in risk analysis may struggle to implement these changes or to gauge their success (Cox, 2012).

2.5.2.1 High-level Qualitative Method

For high level screening or where in-depth analysis incurs substantial costs and data availability is constrained, the utilization of qualitative methodologies can offer a justifiable approach. Within this context, the inception of the PIEVC Protocol was initiated by Engineers Canada in 2005, in collaboration with co-funding from NRCan (Natural Resources Canada). Over an extended period, the protocol underwent rigorous validation and refinement, a process facilitated through the execution of comprehensive case studies. This "learn by doing" approach spanned an extensive array of infrastructure categories and ownership entities, ranging from expansive urban centers to smaller local communities. The developmental phase culminated in 2012 with the release of Version 9, coinciding with the cessation of co-funding assistance from NRCan (Sandink & Lapp, 2021).

The PIEVC Protocol stands as a qualitative framework for identifying and evaluating potential risks within a screening-level climate assessment context. Its origins can be traced back to the CAN/CSA Standard Q850-97 (R2009) Risk Management: Guideline for Decision-Makers (Canadian Standards Association, 2009). Unlike quantitative risk assessment tools, the protocol doesn't demand exhaustive or comprehensive data for conducting an assessment. However, this approach involves a trade-off, as it doesn't yield quantitative risk estimations but

instead offers "risk scores" that can be categorized into different levels, characterized qualitatively using designations like high, medium, and low risk.

The protocol furnishes a broad comprehension of climate-related risks, often sufficient to facilitate informed decision-making concerning adaptation and resilience strategies, particularly applicable to smaller-scale infrastructure and communities. Additionally, it serves as a valuable precursor to more intricate quantitative risk evaluations, channeling attention towards pivotal areas necessitating deeper, data-intensive analysis before informed actions and budgetary allocations can be determined.

2.5.2.2 Time-Dependent Reliability Method

The current design practices for engineered components and systems typically assume that loads and resistance remain stationary throughout their lifespan. However, with the anticipated changes in weather stressors over the lifespan of infrastructure systems, it is necessary to develop methods that capture the non-stationary nature of loading to accurately assess future reliability and service life.

In the field of analyzing historical environmental data, the annual maxima (AM) and peaks over threshold (POT) methods are widely employed. The AM method utilizes the Gumbel and generalized extreme value (GEV) distributions, while the POT method employs the generalized Pareto distribution. To address non-stationarity, where data characteristics change over time, (Coles, 2001) introduced modified versions of these distributions by incorporating time-dependent parameters. This approach has gained significant popularity as the preferred method for modeling non-stationary data in the existing literature.

However, the existing literature on this topic is limited, and new approaches are emerging. For instance, (Pandey & Lounis, 2023) proposed a stochastic load process model that explicitly models the frequency and intensity of the load and analyzes their effects on the extreme value distribution. This approach provides an accurate solution for the maximum load distribution within a finite time frame, leveraging the advancements in modern digital instrumentation that provide high-resolution meteorological data. Importantly, it does not rely on asymptotic arguments as used in the annual maxima and POT methods. However, despite the advancement of reliability-based methods, these methods does not offer conclusive results when faced with various possible climate change scenarios, as the presence of large uncertainties complicates decision-making regarding proactive reinforcement of systems (Pandey & Lounis, 2023).

2.5.2.3 Optimization Based Methods

In the face of deep uncertainties, to identify investment options with good performance, the applications of new decision-making tools rather than designing against a single projection have been gaining wider acceptance in engineering. Currently, there is a heated discourse on the methods of tackling the evolving risks and uncertainties in large infrastructure projects in a changing climate (Hallegatte, 2009; Hallegatte et al., 2012; Marchau et al., 2019), including robust decision making (RDM) (Kwakkel et al., 2016), real options analysis (RO) (Morel, 2020), and dynamic adaptive pathways planning (DAPP) (Haasnoot et al., 2013, 2020). RDM provides a measure for selecting between different concrete actions, designs, or plans, while RO and DAPP fall under the category of policy-making. In policy-making, a decision-

maker (so called agent) crafts a forward-looking strategic perspective, undertakes some near-term actions, and establishes a framework to guide future actions. As such a policy allows for dynamic adaptation of a system over time in response to shifting conditions.

2.5.2.3.1 Robust Decision Making

With the presence of multiple scenarios, a shift from usual cost benefit analysis toward robust decision-making tools is observed and recommended (Dittrich et al., 2016). In this context, Minimax and Maximax are among the most widely used non-probabilistic, robust optimization formulations (Cox, 2012). These methods are mostly helpful in local scale studies such as those in the context of climate change adaptation, as they do not require likelihood information (Cox, 2012). For example, Mondoro et.al (Mondoro et al., 2018) used RDM to combine the performance under scenarios in a so called gain-loss framework for quantifying the advantages of postponing adaptation investments.

2.5.2.3.2 Real Option

Real Option (RO) and Flexibility in Design are two related methods that can be used to plan for adaptation to climate change. RO is a decision-making tool that involves evaluating the value of maintaining the flexibility to change a design or plan in response to changing conditions. Flexibility in Design is a design approach that emphasizes the importance of creating designs that can be easily modified or adapted over time. RO analysis is suitable where adaptive management strategies are available to cope with the evolving demand. RO analysis originated from financial options analysis (Kwakkel et al., 2016), and received a Nobel Prize in Economic Science in

1997. On the contrary to decision-making based on LCC, which suggests investing when the total profit, W, is greater than the investment cost, I, in the context of RO, an investment is recommended if W is greater than I plus a hidden cost of V for losing the option to invest later. The value of delaying an uncertain investment is then referred to as the option value.

Since the 1990s, RO has found its way into design and management of infrastructure systems in the presence of uncertainty due to analogies of infrastructure management decisions and financial market interventions (Dittrich et al., 2016; Haasnoot et al., 2013, 2020; Morel, 2020). This new perspective of RO in (re)design of infrastructure systems is known as "Real 'in' Options (RIO) analysis" (Mondoro et al., 2018), which is slightly different from its traditional application.

The traditional perspective of RO in finance treats the system configuration as a black box. For instance, it can help decide on investing in a stock now or in the future. Whereas the new perspective of RO in (re)design of infrastructure systems, manipulates technical characteristics of system in response to reduction of uncertainty through future learning. Therefore, for RIO, the availability of technical characteristics of system including technical details of options and their interdependencies is necessary. RIO provides the rational means of quantifying the value of flexibility built into infrastructure systems, helping with identifying worthwhile flexibilities, and expanding the horizon for considering flexible designs (Guthrie, 2019). In the context of climate change, RIO and Flexibility in Design can help planners assess the potential risks and uncertainties associated with climate change impacts and develop designs that are resilient and adaptable. For example, a building that is designed with flexible walls or modular components can be easily modified in response to changing weather

patterns or rising sea levels. This approach can help reduce the costs and risks associated with adapting to climate change.

In the context of climate change, RO can help identifying and evaluating real options that can be exercised to adjust a plan or investment in response to changing conditions. In this way, RO can aid planners assess the potential risks and uncertainties associated with climate change impacts and develop adaptive strategies that can be adjusted over time. For example, a real option for adapting to climate change might include the ability to switch to drought-resistant crops or to build infrastructure that can withstand extreme weather events.

Despite these benefits and the expectation that some forms of climate change uncertainty will decrease over time (Lee et al., 2017; Urban et al., 2014), the literature on the integration of adaptation planning and learning remains limited in the face of an evolving climate (Guthrie, 2019). Specifically, illustration on application of RO as a supplementary method for risk management decision making in the context of climate change has been mostly missing, likely due to criticisms on its reliance on traditional probability calculations (de Neufville, 2019). However, in recent years, endeavours on exploiting RO benefits in the context of climate change adaptation have been revived (Stroombergen & Lawrence, 2022). For example, Stromberg and Lawrence (Stroombergen & Lawrence, 2022) suggest a cut-off probability method for using RO in DAPP and RDM frameworks.

Guthrie (Guthrie, 2019) provides a simplified approach to incorporating RO in assessing investment in climate change adaptation. In his research, he employs a binomial tree model to climate-change adaptation problems and gradually updated

the likelihood of the true climate regime using a Bayesian updating scheme driven by observations of extreme events. van der Pol et al. (van der Pol et al., 2014) analyses the flood protection investments assuming an initial distribution for the likelihood of various scenarios and assumes the information of the true scenario arrives in two settings: in a certain time or in an stochastic event. In both of these methods, however, employing subjective probabilities at least in the initial stage of decision-making is inevitable before more knowledge on the likelihood of adverse events is evident. This can pose problems where the likelihood of these subjective probabilities is controversial between different stakeholders, and where an immediate decision at the time being is required, such as designing and managing bridges at a time being. In this research, to avoid the issue of subjective probabilities, dynamic programming is used, which is the essence of Real Option formulations.

2.5.2.3.3 Dynamic Programming

The dynamic programming technique rests on The Bellman's Principle of Optimality (Bellman, 1952; Dreyfus, 2002): "An optimal policy has the property that whatever the initial state and initial decision are, the remaining decisions must constitute an optimal policy with regard to the state resulting from the first decision". In this context, van der Pol et al. (van der Pol, Gabbert, et al., 2017) introduced a method for avoiding subjective probabilities by combining Bellman's Principle of Optimality with MR in a decision tree, where the uncertainty is allowed to be reduced in an event of arrival of information in a single date. However, expectation of occurrence of information arrival in a predetermined date does not seem realistic in the context of climate change.

The current study contributes to the literature on adaptive design and management by applying dynamic programming and MR decision criterion to adaptation strategies under emerging information on climate change. In the provided framework, the information arrival is modelled as a stochastic event with a predefined probability distribution. Furthermore, it provides a framework for determining the situations where the developed method is effective in either postponing the adaptation projects, or implementation of flexibility in the initial design.

Chapter 3. Methodology

3.1 Introduction

In this chapter a methodology for determining adaptation strategies under emerging information on climate change is first explained in detail with simple illustrative examples. A formulation of the methodology is then provided, and lastly, its properties are discussed. The methodology employed herein considers deep uncertainty in choosing the optimum management strategy subject to the possibility of emerging information.

3.2 Methodology Steps

Using established theories in decision making, this research provides a framework for investigating low regret and flexible decision making in the design and management of a system. The framework involves a three-stage procedure as follows:

- Identification:

The first stage identifies the potential strategies, or in-service flexibility, in the considered system and identifies their cost components and possible benefits. In-service flexibility is achieved by employing system configurations that allow system modifications after establishment of an initial configuration. As such, three steps are completed, including:

1) identifying possible scenarios,
2) identifies actions for mitigating vulnerabilities from possible future scenarios, and
3) determining the costs and benefits of the actions for each scenario.

- Economic Analysis of Adaptation Options:

In the second stage, economic indicators are evaluated for each of the scenarios. As such, the climate change scenario uncertainty is detached, and the evaluation can be performed through common tools such as probabilistic analysis tools and Monte Carlo simulation (MCS). The evaluation results in different failure cost values under each scenario, as each scenario produces different levels of risk. Having the risk and cost of adaptation determined in the previous stage, the lifecycle cost of each strategy will be identified in terms of the expected Life Cycle Cost (LCC), which is the summation of discounted adaptation and failure costs accruing over a planning horizon.

- Comparison Across All Future Scenarios and Policies:

Once the LCCs of various strategies under all possible scenarios are determined, a comparison should be performed to identify the most appropriate strategy across all future scenarios. In so doing, MR across all possible scenarios is chosen as the performance measure of the various strategies. In this approach we first obtain a regret matrix R. Here, the purpose is to reduce the hindsight regret with respect to what could have been done in the first place. This is an important consideration as regret criteria is context dependent (Yager, 2004) as explained in Section 3.3.

3.3 Context-Dependency of Regret

This feature implies that the MR approach is not indifferent to irrelevant alternatives. As the following example (adopted from (Yager, 2004)) illustrates, the removal of a non optimal alternative can change the choice of best alternative. In this

figure, with the presence of option A_3, the low regret choice is A_2, while in absence of A_3, the optimal choice is A_1.

In Presence of A_3

	Utility Matrix				Regret Matrix			
	S_1	S_1	S_3		S_1	S_1	S_3	
A_1	0	10	4	A_1	10	0	6	10
A_2	5	2	10	A_2	5	8	0	8 ←
A_3	10	5	1	A_3	0	5	9	9
Horizon	10	10	10					

In Absence of A_3

	Utility Matrix				Regret Matrix			
	S_1	S_1	S_3		S_1	S_1	S_3	
A_1	0	10	4	A_1	5	0	6	6 ←
A_2	5	2	10	A_2	0	8	0	8
Horizon	5	10	10					

Figure 3-1. Example of choice based on the context in regret-based decision-making (Adopted from (Yager, 2004)*)*

Conceptually what seems to happen here is that the removal of A_3 changes the perspective (context) of the decision maker. With this removal, there would be smaller possibilities associated with the Scenario s_1. This led to realizing that regret associated with the selection of A_1 in the case of s_1 is smaller than the first case. This in turn resulted in A_1 becoming more appealing. Therefore, here considering this property of regret, the objective is defined such that the decision-maker does not change his

38

decision as some irrelevant options, such as implementing a safety measure during construction, expire as time passes by.

For better understanding of this concept in the context of adaptation of infrastructure, consider the following example. Assume a bridge adaptation problem in which the owner choses to the option of modifying the bridge in 30 years for reducing regret. When the time of modification comes after 30 years, the options of modifying the bridge earlier (e.g. in year 20) are expired. However, the decision of the bridge owner should not be changed with this understanding. To achieve this, the bridge owner is reminded of all the options they had available in year zero of decision-making.

3.4 Regret Matrix

The analysis begins with the LCC matrix with elements $c_{sa\tau}$, representing the life cycle cost associated with taking action $a \in A$ at time $\tau \in [0, T]$ (in the interval between construction and end of the planning horizon) under scenario $s \in S$. As mentioned earlier, regret is context dependent. This property of regret means that the regret can change with the change of context and such a change may result in inconsistency of the decision-making if the context is not defined properly (please refer to (Yager, 2004) for more detail). Here the context is defined as the realm of possible actions that the decision-maker could have chosen at time zero, i.e., the construction/design time. This consideration ensures that the context remains constant as time passes by, and the decision-maker feels regret by comparing what they have done with what could have been done at time zero. Accordingly, the decision-maker's regret takes the form of Equation (3-1):

$$R_{sa\tau} = c_{sa\tau} - h_{s0} \tag{3-1}$$

where h_{s0}, the horizon at the initial time under scenario s, represents the cost associated with the best action possible at time zero and is determined according to the following minimization equation:

$$h_{s0} = \min_{a,\tau}(c_{sa\tau}) \tag{3-2}$$

Note here that as the costs are inversely related to utility, the maximization in the MR formulation is changed to minimization.

For each strategy, regret may significantly vary across various future scenarios. Furthermore, assumptions about the possibility of new information affect the decision-making among the adaptive strategies. Here, with regards to the possibility of information update, three different assumptions are evaluated and compared: classical MR, deterministic information arrival, and stochastic information arrival. In the following, these three methods are distinguished with superscripts of c, d, and s.

3.5 Classical MR

Assuming that at time t the objective is the minimization of regret by choosing between the action set $A(t)$ available at time interval $[t, T]$ (i.e., the time interval between t and the end of the planning horizon T), the classical application of MR takes the form of Equation (3-3). The findings of realizing this objective are denoted with superscript "c" and are: the optimum action $a^c(t)$ at time $\tau^c(t)$ resulting a minimax regret (i.e., minimization of maximum possible regret) of $R^c(t)$ with scenario-based utility of $c_s^c(t) = c_{sa^c\tau^c}$.

Objective: $R^c(t) = \min\limits_{\tau} \left(\min\limits_{a} \left(\max\limits_{s} R_{sa\tau} \right) \right)$ (3-3)

Find: $a^c(t)$, $\tau^c(t)$, $R^c(t)$, $c_s^c(t)$

3.6 Deterministic Information Arrival

Now, assume that the information on the actual scenario is expected to arrive at future time I, and the objective is postponing the decision-making until I for regret minimization. With this assumption, the objective function takes the form of Equation (3-4). Solving the optimization function delivers the optimum scenario-based course of action $a_s^d(I)$, which should be taken at time $\tau_s^d(I)$.

Objective: $R_s^d(I) = \min\limits_{\tau} \left(\min\limits_{a} R_{sa\tau} \right)$ (3-4)

Find: $a_s^d(I)$, $\tau_s^d(I)$, $R_s^d(I)$, $c_s^d(I)$, $R^d(I)$

where $\tau \in [I, T]$ (meaning that the action can be taken at or after time I), and

$c_s^d(I) = c_{sa_s^d \tau_s^d} = R_s^d(I) + h_{s0}$ (3-5)

Solving the optimization function delivers the optimum scenario-based course of action $a_s^d(t)$, which should be taken at time $\tau_s^d(t)$. Accordingly, the scenario based LCC and regret are determined as $c_s^d(I)$ and $R_s^d(I)$, leading to a minimax regret of $R^d(I)$ according to the following equation:

$R^d(I) = \max\limits_{s} \left(R_s^d(I) \right)$ (3-6)

At a given time t, the monetary waiting value (WV) for a deterministic information arrival by a future time I can be captured by subtracting $R^c(t)$ and $R^d(I)$ as presented in the following equation:

$$V^d(t, I) = \max{(R^c(t) - R^d(I), 0)} \qquad\qquad (3\text{-}7)$$

The following values can be determined from this equation:

- $V^d(0, I)$: The value of information update at I based on available action choices at time 0 (i.e., the construction phase)

- $V^d(t, t)$: The value of information update at a time $I = t$ based on available action choices at decision-making time, t.

The former is important for a new construction, whereas the latter shows the value of instantaneous information update at t for an existing structure. As the WV declines over time, there would be break even times I_0 and t_0, when $V^d(0, I_0) = V^d(t_0, t_0) = 0$.

3.7 Stochastic Information Arrival

3.7.1 Overview

In practice, the exact time of information arrival may not be clear. Here, to improve the method in this regard a distribution for time of information arrival is considered. Here, an example of such a distribution with mean of $\bar{I} = 5$ years and COV of 0.5 is presented in Figure 3-2. The dash line indicates the PDF on the right-hand side axis, while the solid line represents the CDF of the distribution on the left-hand-side axis. In this figure, the CDF curve depicts the probability of having an information updating event by a determined time.

To consider the effect of the possibility of information arrival, the classical regret concept is implemented in a dynamic programming scheme. To understand the implication of doing this, a two-period adaptation problem can be considered according to Figure 3-3. For illustration, it is assumed there is a 60% probability of

information on the true scenario arriving before the beginning of the second period. In the beginning of the first period, t_0, the decision-maker has the following options:

- *A*: adapt, or

- *W*: wait for the information arrival.

    Whereas in the beginning of the second period, t_1, the decision-maker has the following options:

- *A*: adapt, or

- *A'*: do not adapt.
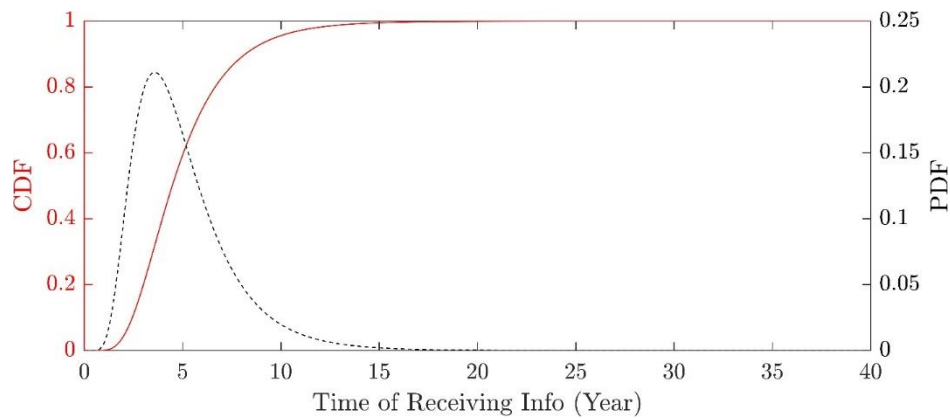
Figure 3-2. Lognormal probability distribution of stochastic event of information arrival with mean of $\bar{I} = 5$ years and COV of 0.5.

    With two possible scenarios, s_1 (adverse) and s_2 (favourable), the lifetime cost expectation of each option (*C*) and their relevant regret (*R*) is presented in Table 3-1. The procedure of deploying dynamic programming on the regret parameter is presented in Figure 3-3. Here the cases of having and not having information on the actual scenario at t_1 are distinguished with $P_I(t_1)$ and $P_I'(t_1)$ respectively. For each of

43

these cases, the regret of taking each action at t_1 under all scenarios is provided in the far-right boxes. Beginning from these boxes, the solution is derived in a backward process. Under the no information case, $P_I'(t_1)$, employing the classical MR results in adaptation (Option A) with regret values of 9 and 12 under Scenarios s_1 and s_2 respectively. However, under the case of information arrival ($P_I(t_1)$ path) the decision-maker chooses the optimal action according to the revealed true scenario. As such, under Scenario s_1, the decision-maker takes Option A with regret of 9, whereas under the other scenario, they take Option A' with regret of 0. Determination of these values is essential in finding the regret of waiting in the first period.

The regret of waiting is the expectation of the outcome under the cases of $P_I(t_1)$ and $P_I'(t_1)$ with 60 and 40% probabilities. For example, under scenario s_2, $R = 0 \times (0.6) + 12 \times (0.4) = 4.8$. Also, in this situation the course of action is undetermined, which is shown as $\tilde{A}$. Having these values, empowers the decision-maker to compare between waiting and immediate adaptation at t_0 with regret values of 0 and 11 under Scenarios s_1 and s_2 respectively. Subsequently, employing the MR approach results in choosing the waiting option over the immediate adaptation. It would be straightforward to find that classical MR results in immediate adaptation with maximum regret of 11. This indicates that the decision-maker should be willing to pay some amount to be flexible according to the Dynamic MR approach. Accordingly, the upper bound of willingness to pay for flexibility can be found as the difference in the maximum regret for the dynamic MR and classical MR approaches. Here, this difference is referred to as the Waiting Value (WV).

Table 3-1. Lifetime cost and regret of various options under two scenarios for the dynamic programming illustrative example.

Adapt at	Cost		Regret	
	S_1	S_2	S_1	S_2
T_0	184	26	0	11
T_1	193	27	9	12
Never	230	15	46	0
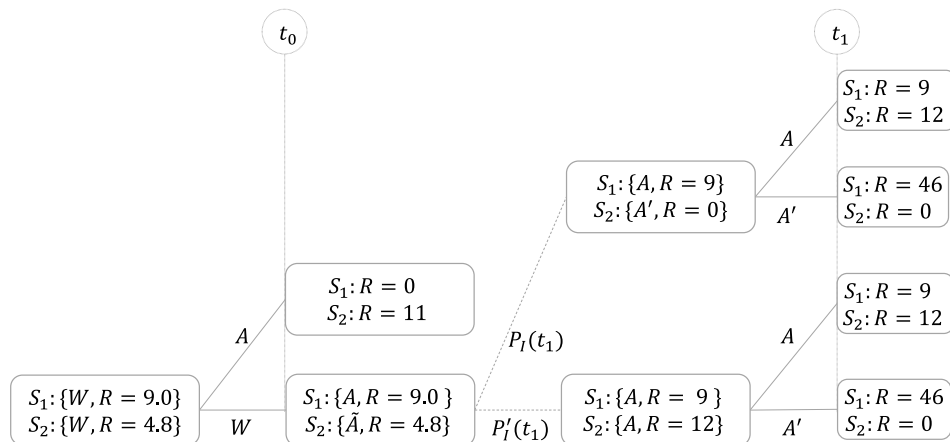
Figure 3-3. Illustration of dynamic programming of regret for two-period example.

It is noteworthy that employing Maximin in the dynamic programming framework results in immediate adaptation instead of waiting. For the sake of completeness, Figure 3-4 is presented, in which MR is substituted with Maximin approach. The reader is encouraged to follow the same steps to confirm that

employing Maximin in the Dynamic programming framework results in immediate adaptation instead of waiting.
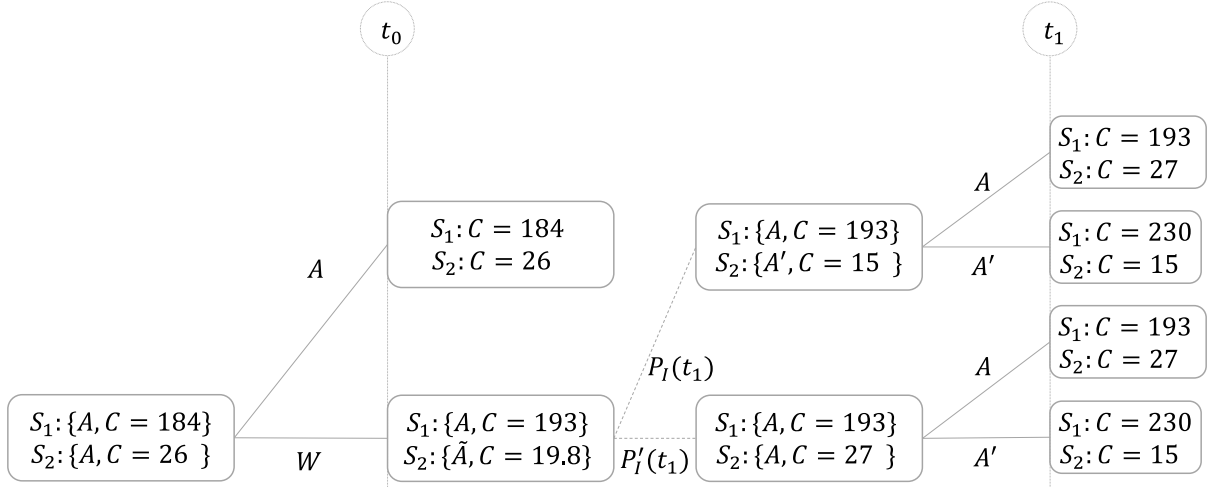
Figure 3-4. Illustration of Dynamic programming of Maximin cost on the two-period example.

Following the same procedure, the developed methodology is formulated as a multi-period decision-making procedure as illustrated in Figure 3-5. The probability of information arrival between t_{i-1} and t_i, can be formulated according to the following equation through the conditional probability rule:

$$P_I(t_i) = \left[\frac{F(t_i) - F(t_{i-1})}{1 - F(t_{i-1})} \right] \tag{3-8}$$

where $F()$ denotes the unconditional CDF of the information arrival time (see Figure 3-2). The reason for this equation is that the probability of information arrival is updated with no occurrence of information arrival until the beginning of each step. Accordingly, an expectation of the waiting value for information arrival can be determined through the following equation:

$$V^s(t) = R^c(t) - R^s(t) \tag{3-9}$$

In what follows, these procedures are formulated, and specifically, the formulations for continuous possibility of information arrival and adaptation are derived.
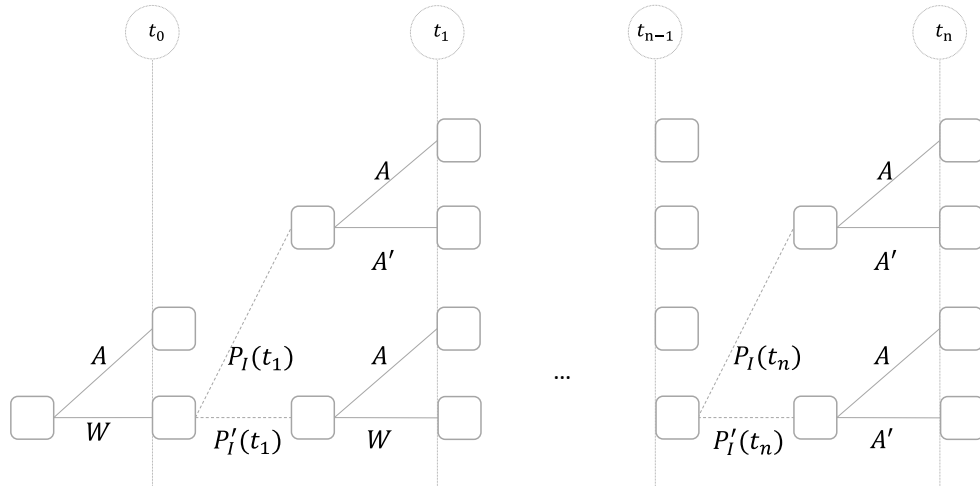
Figure 3-5. Illustration of dynamic programming of regret for a multi-period problem.

3.7.2 Equations

For driving the general equations consider a multi-period problem. For a decision-making time step t_i, if the actual scenario is already recognized (i.e., $I \leq t_i$) the manager can act according to Equation (3-4). Otherwise, if no information update happens at time step t_i, then the objective is to minimize the regret by deciding between:

a) waiting for the possibility of receiving the information in the future step, t_{i+1}, with the regret and scenario-based LCC of $R^s(t_{i+1})$ and $c_s^s(t_{i+1})$ respectively, or

b) planning blindly based on Equation (3-3) with $R^c(t_i)$.

As such, as the values corresponding to t_i are used in decision-making at t_{i-1}, a recursive approach is taken. The idea behind this dynamic programming approach is stated in Bellman's Principle of Optimality (Bellman, 1952; Dreyfus, 2002). Therefore, in this situation the optimal choice is:

$$\tilde{a}(t_i) = \begin{cases} Wait, \text{for } R^c(t_i) > R^s(t_{i+1}) \\ a^c(t_i), \text{for } R^c(t_i) \leq R^s(t_{i+1}) \end{cases} \tag{3-10}$$

With this basis, the maximum possible regret with no information at time t_i can be expressed as:

$$\tilde{R}(t_i) = \min\left[R^c(t_i), R^s(t_{i+1})\right] \tag{3-11}$$

and the net present value of the decision-making at t_i can be expressed as:

$$\tilde{c}_s(t_i) = \begin{cases} c_s^s(t_{i+1}) \text{ for } R^c(t_i) > R^s(t_{i+1}) \\ c_s^c(t_i) \text{ for } R^c(t_i) \leq R^s(t_{i+1}) \end{cases} \tag{3-12}$$

where $c_s^s(t_{i+1})$, the expectation of LCC of waiting longer than t_i for info update takes the following forms:

$$c_s^s(t_{i+1}) = c_s^d(t_{i+1}) \, P_I(t_{i+1}) + \tilde{c}_s(t_{i+1})[1 - P_I(t_{i+1})] \tag{3-13}$$

In this equation, $P_I(t_{i+1})$ is the probability of information update between t_i and t_{i+1} (i.e., $t_i < I \leq t_{i+1}$) and can be determined by applying the rule in Equation (3-8). Consequently, the relevant regret of the waiting longer is determined according to the following equation:

$$R^s(t_{i+1}) = \max_s(R_s^s(t_{i+1})) \tag{3-14}$$

where $R_s^s(t_{i+1}) = c_s^s(t_{i+1}) - h_{s0}$, in which h_{s0} is the horizon, as given in Equation (3-2).

As the time step size approaches zero, the following equations for differentiable segments of $c_s^s(t)$ are determined:

For $R^c(t) \leq R^s(t)$:

$$c_s^s(t) = c_s^d(t) P_I(t) + c_s^c(t)(1 - P_I(t)) \tag{3-15}$$

and

$$R_s^s(t) = R_s^d(t) P_I(t) + R_s^c(t)(1 - P_I(t)) \tag{3-16}$$

As $c_s^d(t) \leq c_s^c(t)$, it can be found that $c_s^s(t) \leq c_s^c(t)$, and therefore, $R_s^s(t) \leq R_s^c(t)$. With consideration of the given condition, $R^c(t) \leq R^s(t)$, it can be concluded that $R^s(t)$ is always bounded with $R^c(t)$. Further, it can be concluded that $R^c(t) = R^s(t) = R^d(t)$. With this conclusion, the given condition, $R^c(t) \leq R^s(t)$ can also be expressed as $t \geq t_0$.

On the other hand, for $R^c(t) > R^s(t) > R^d(t)$ (i.e., $t < t_0$), Equation (3-13) can be expanded as follows:

$$c_s^s(t_i)[1 - F(t_i)] - c_s^s(t_{i+1})[1 - F(t_{i-1})] + c_s^s(t_{i+1})[1 - F(t_{i-1})] \tag{3-17}$$
$$- c_s^s(t_{i+1})[1 - F(t_i)] = c_s^d(t_i)[F(t_i) - F(t_{i-1})]$$

Therefore, as the time step size approaches zero:

$$[F(t) - 1]d(c_s^s(t)) + c_s^s(t)d(F(t)) = c_s^d(t)d(F(t)) \tag{3-18}$$

Subsequently, Equation (3-19) gives the differential equation of value of waiting longer than t if no information arrives by this time,

$$\frac{d(c_s^s(t))}{dt} = \frac{[c_s^s(t) - c_s^d(t)]f(t)}{[1 - F(t)]} \tag{3-19}$$

in which, $f()$ is the PDF of time of arrival of the information. An expectation of the waiting value for information arrival can be determined according to Equation (3-9).

3.8 Adaptive Decision-Making Policy Categories

For the developed methodology, adaptation policy can be categorized. Depending on the various costs, an adaptation policy can fall under one of the following seven types:

- Category 1:

This case involves projects with very cheap adaptation procedures. In such cases, in a new construction project, adapting during construction is recommended to avoid accessibility costs (costs of field application, such as permits, scaffolding, sand blasting and transportation of the equipment). For an existing structure ($t > 0$), however, when the opportunity of so doing is missed, investment on finding information on the actual scenario is reasonable. If information update happens before t_0, adaptation can occur according to the revealed scenario. Otherwise, adapting immediately at t_0 is suggested.

- Category 2:

Similar to Category 1, this case involves projects with very cheap adaptation procedures. The difference, however, is that here the accessibility cost is so high that for an existing structure, adaptation is not suggested.

- Category 3:

This category involves inexpensive adaptation projects where avoiding immediate adaptation during construction is suggested against the recommendation of classical implementation of MR, when an information update is expected before I_0. Otherwise, if no information is received before t_0, adaptation is suggested.

- Category 4:

In this situation, the adaptation cost is such that lingering adaptation until $a^c(0)$ is cost effective due to discounting effect. However, an information arrival indicating adversary scenario may result in adaptation earlier than planned.

- Category 5:

In this case adaptation is so costly that is not recommended when ignoring the possibility of receiving information. Otherwise investing in finding information on the actual scenario and building flexibility into the design may be reasonable. If information indicating the occurrence of an adversary scenario is received before t_0, adapt under the worst scenario. If no information is received, adaptation is not suggested. In this situation specifically, the waiting value counts as the summation of the value of investment on finding information as well as the value of building flexibilities into the design that otherwise would not have been reasonable when the WV is omitted.

- Category 6:

In this case adaptation is so costly that is not recommended unless further information suggesting the realization of an adversary scenario is provided before construction.

- Category 7:

Adaptation is too expensive to be considered.

A flowchart for finding the decision category and subsequent procedures is provided in Figure 3-6 and Figure 3-7. In the flowchart, the variable Ω is referred to as the phase change time, a time after construction beyond which adaptation would not be reasonable even with having the information that the worst scenario is occurring.
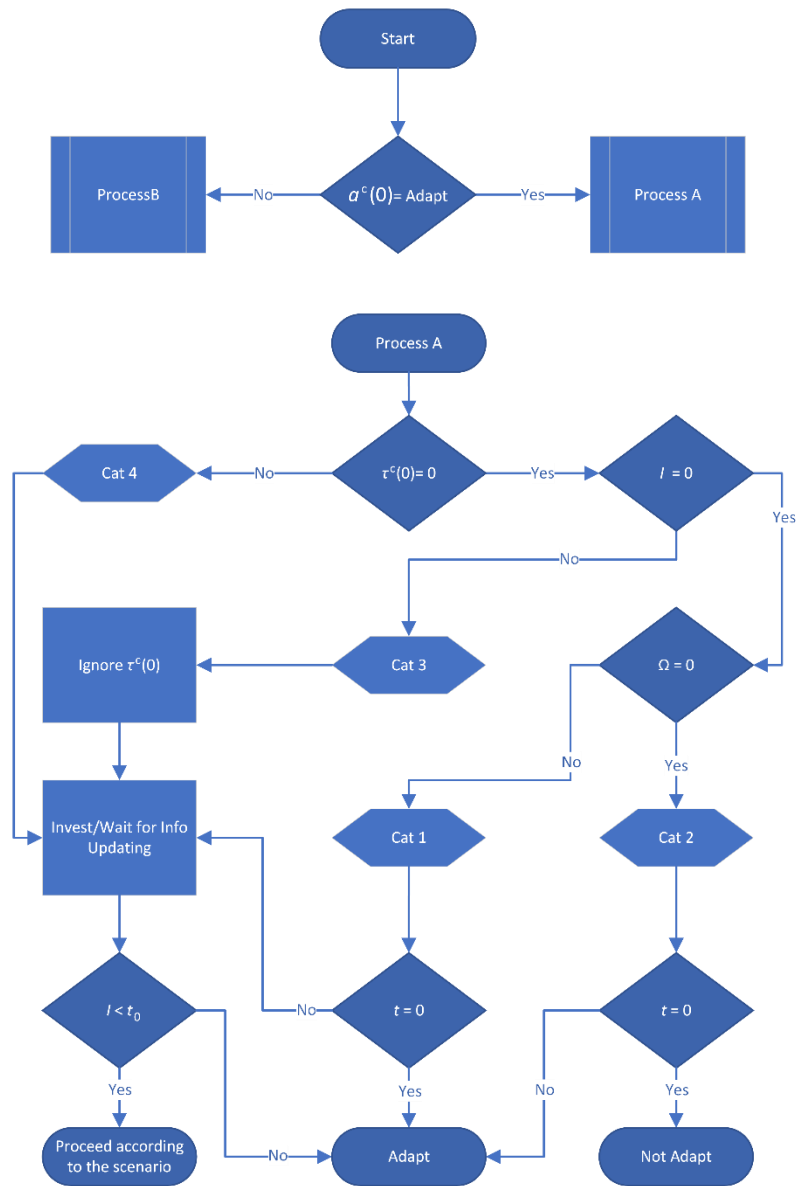
Figure 3-6. (Part 1) Flowchart of determining the decision category and subsequent procedures.
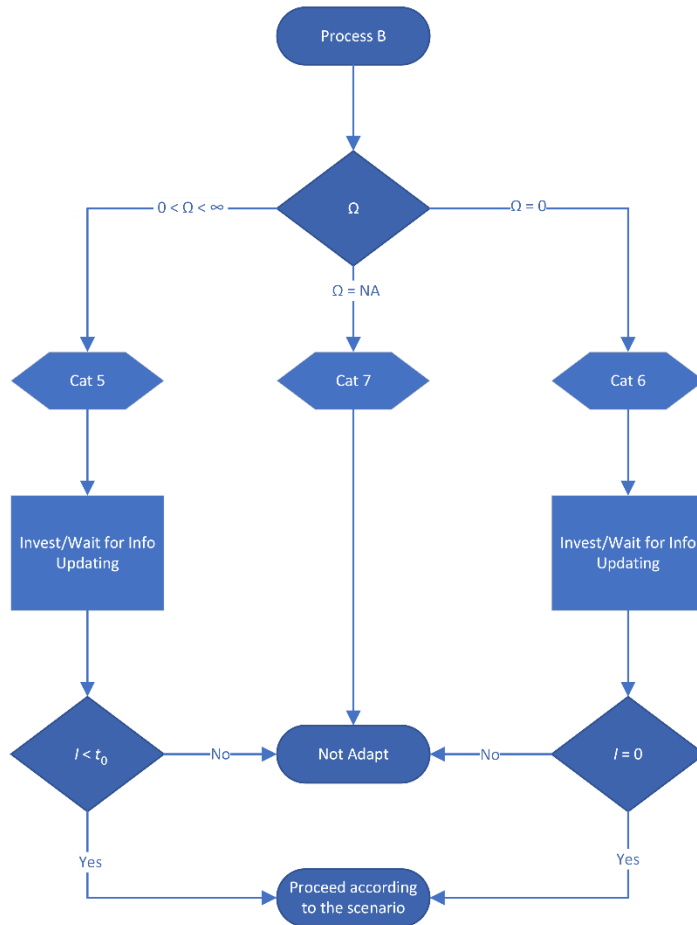
Figure 3-7. (Part 2) Flowchart of determining the decision category and subsequent procedures.

Chapter 4. Reliability Based Design under Non-Stationary Climate Change

4.1 Introduction

In this chapter, the effects of nonstationary wind loading, as one of the climatic stressors on the performance of a structural element located in London, Ontario, Canada is investigated. It is assumed that the element is a flexural member on a bridge. Nevertheless, the employed method is general and applicable to other structural elements and load types. In this example, wind pressure and dead load effects are the only stressors, and strength deterioration is negligible during the service life. The element is designed based on the Load and Resistance Factor Design (LRFD) approach and fails when the stochastic values of wind and dead load surpass the randomly distributed resistance.

4.2 Reliability Analysis in a Changing Climate

4.2.1 Failure Probability and Design Load Factors

To appropriately design engineered components and systems, it is crucial to account for the uncertainties associated with the demands placed on these components or systems and their capacity to tolerate these demands. Reliability methods can be employed to address this need as discussed in Section 2.5.1.1.2. In this context, defining the limit state function as the subtract of demand, L, and capacity, R, (i.e., $G = R - L$) failure occurs when $G \leq 0$ (Shayanfar et al., 2018). Various reliability methods, such as Monte Carlo Simulation (MCS) and first and second-order reliability methods, exist for assessing the probability of structural failure.

Nevertheless, due to the complexity of applying these methods in general engineering practice, alternative approaches like LRFD (Load and Resistance Factor Design) are developed and incorporated into design codes to ensure safety.

4.2.2 Load Factors and Reliability Index

This section reviews the mathematical relation of load factor and reliability index (β), which is related to the probability of failure as illustrated in Figure 4-1 through the following equation:

$$p_f = \Phi(-\beta) \tag{4-1}$$
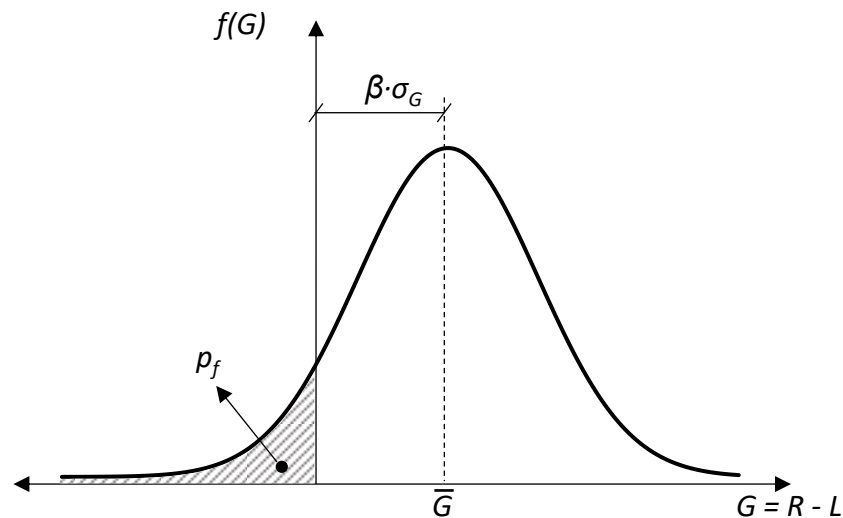
Figure 4-1. Illustration of the relationship between p_f and β

In general design problems, the demand on the engineered component or system usually involves a combination of different loads, each of which is given its load factor in modern design codes. The simultaneous presence of dead and wind load effects on a structure is a simple example of such a condition. In this regard, the limit sate function can be redefined as $G = R - (D + W)$ where D and W are random

56

variables representing dead and wind load effects. Accordingly, given the nominal design values (denoted with the 'n' subscript) and load and resistance factors, the reliability index can be mathematically computed through the following equation:

$$\beta = LN\left(\omega \sqrt{\frac{1+COV_{z_W}^2}{1+COV_{z_U}^2}}\right) \Big/ \sqrt{LN\left[(1 + COV_{z_W}^2)(1 + COV_{z_U}^2)\right]} \tag{4-2}$$

Here, $U = R - D$, and ω is given in Equation (4-3), in which α_W, α_D and ϕ_R denote wind load factor, dead load factor and resistance factor, respectively. The procedure for derivation of these equations is provided in Appendix **A.1**.

$$\omega = \frac{\bar{z}_R}{\bar{z}_W \phi_R}\left[\alpha_W - \frac{D_n}{W_n}\left(\frac{\phi_R \bar{z}_D}{\bar{z}_R} - \alpha_D\right)\right] \tag{4-3}$$

Please note that in this analysis, the lognormally distributed random variables for load and resistance are replaced by normalized variables for simplification:

$$z_R = \frac{R}{R_n}, z_W = \frac{W}{W_n}, z_D = \frac{D}{D_n}, z_U = \frac{U}{U_n} \tag{4-4}$$

Also, the mean value of each variable is denoted by a bar (e.g. $\bar{z}_D$) while their coefficient of variation is denoted with a COV (e.g. COV_{z_D}), and their standard deviation is shown by σ (e.g. σ_{z_D}).

4.2.3 Time-Dependent Reliability Analysis

As discussed in Chapters 1 and 2 of this thesis, the design of engineered components and systems is generally based on an assumption of stationarity of loads and resistance over their lifetime. However, the anticipated alterations in weather stressors throughout the lifespan of infrastructure systems necessitate an approach that can effectively capture the pertinent non-stationary characteristics of loading

when calculating future reliability and service life. In this regard, Equation (4-5) provides the time-dependent reliability (i.e., the probability of survival) of ageing structures in the presence of non-stationary loads and degradation during a time interval of (0,t) (Li et al., 2015):

$$\mathcal{L}(t) = EXP\left\{-\int_0^t \lambda(\tau)[1 - F_L(R(\tau))]d\tau\right\} \tag{4-5}$$

where $F_L()$ represents the cumulative distribution function (CDF) of demand. While $\lambda(\tau)$ and $R(\tau)$ respectively denote the time-varying occurrence rate of the loading and resistance functions. depending on the considered hazard type, parameters of $F_L()$ can be redefined so that the occurrence of loading forms a Homogenous Poisson Process with the time-independent occurrence rate, λ. In such a case, by discretizing time to years, the Equation (4-5) can be simplified as follows:

$$\mathcal{L}(t) = EXP(-\sum_{i=1}^N \lambda P_i) \tag{4-6}$$

in which N is the number of years in a time interval of $(0, t)$, and $P_i = P(G < 0)$ denotes the probability failure during the ith year or the probability that limit state, G, is crossed in that year. Here, P_i is computed through a mathematical approach using Equations (4-1) and (4-2). With the help of the models and formulations provided here, the following sections endeavor to illustrate the climate change effects on safety of the built environment through several examples.

4.3 Limit state, Load, and Resistance Models

4.3.1 Limit State Function and Design Load Combination

According to the Canadian highway bridge design code (CSA Group, 2019) a bridge component with nominal flexural resistance M_R can be designed according to the following condition:

$$\phi M_R > \alpha_W M_W + \alpha_D M_D \tag{4-7}$$

where M_W and M_D are nominal values for the wind and dead load flexural effects on the component, and α_W, α_D, and ϕ represent the wind load, dead load, and resistance factor, respectively. Considering the load effect and factor values in Table 4-1, a component with the nominal resistance of M_R = 505 kN·m is satisfactory according to Equation (4-7).

Table 4-1. Load and Load factors

α_W	α_D	ϕ	M_W	M_D
1.4	1.1	0.95	200 kN·m	200 kN·m

The component fails when the stochastic values of wind and dead load surpass the randomly distributed component resistance. The limit state function can be defined as:

$$G = m_R - (m_D + m_W) = z_{m_R} M_R - (z_{m_D} M_D + z_{m_W} M_W) \tag{4-8}$$

where, bias coefficients z_{m_R}, z_{m_D}, and z_{m_W} are the normalized random variables for defining the variability of the loads and resistance. In the next section, the procedure for calculating the mean and standard deviation of these parameters is presented.

4.3.2 Load and Resistance Models

4.3.2.1 Resistance Model

The flexural resistance of the component is assumed to be a linear function of $Fy \cdot S$, where Fy and S are the yielding strength of the used material and section modulus with related bias coefficients of z_{Fy} and z_{S}, respectively. The component resistance model exhibits error in the prediction of the exact value of resistance, which can be represented with the random variable z_{Mod}. Therefore, the combined bias coefficient for resistance can be calculated as follows:

$$z_{m_R} = z_{Mod} z_{Fy} z_S \tag{4-9}$$

Assuming independence of variables in Equation (4-9), the mean of z_{m_R} can be computed, using the following equation:

$$\bar{z}_{mR} = \bar{z}_{Mod} \bar{z}_{Fy} \bar{z}_S \tag{4-10}$$

Also, the variance and COV of z_{m_R} can be calculated using Equations (4-11) and (4-12) respectively:

$$var_{m_R} = \prod_{i=1}^{3}(var_{Z_i} + \bar{z}_i^2) - \prod_{i=1}^{3} \bar{z}_i^2 \tag{4-11}$$

where var_{Z_i} and $\bar{z}_i^2$ represent variance and mean of variables z_{Mod}, z_{Fy}, and z_S and:

$$COV_{m_R} = \frac{\sqrt{var_{m_R}}}{\bar{z}_{m_R}} \tag{4-12}$$

Table 4-2 presents the values of mean and COV of the variables used to define the resistance model (CSA, 2007).

Table 4-2. Resistance model Parameters.

Variable	Mean	COV
z_{Fy}	1.06	0.051
z_S	0.99	0.021
z_{Mod}	1.09	0.045
z_{m_R}	1.14	0.071

4.3.2.2 Dead Load Model

The bias factor of the dead load is assumed to have a mean of 1.03 and COV of 0.08, based on (CSA, 2007; Nowak & Grouni, 1994).

4.3.2.3 Wind Load Model

According to (CSA, 2007), the design horizontal wind load pressure can be calculated as:

$$p = C_e C_g C_h q \tag{4-13}$$

where C_e, C_g, and C_h are exposure, gust effect, and horizontal effect coefficients and q is the air pressure, which is related to the wind velocity (V) through the following equation:

$$q = \frac{1}{2}\rho V^2 = CV^2 \tag{4-14}$$

in which ρ is the density of air. If the V is in km/h, the constant $C = 0.05$ can be used to compute the q in Pa. Defining a_c as the analysis coefficient for the conversion of the wind load into a load effect and A as the exposure area, the general equation for the wind load effect is:

$$m_W = a_c C_e C_g C_h C V^2 A \qquad (4\text{-}15)$$

According to (CSA, 2007), the mean and COV of the wind bias coefficient can be computed using the following equations:

$$\bar{z}_{mW} = \bar{z}_{a_C} \bar{z}_{C_e} \bar{z}_{C_g} \bar{z}_{C_h} \bar{z}_C \bar{z}_{V^2} \bar{z}_A \qquad (4\text{-}16)$$

$$COV_{z_{mW}} = \sqrt{COV_{z_{a_C}}^2 + COV_{z_{C_e}}^2 + COV_{z_{C_g}}^2 + COV_{z_{C_h}}^2 + COV_{z_C}^2 + COV_{z_{V^2}}^2 + COV_{z_A}^2} \qquad (4\text{-}17)$$

The statistical values of the parameters used in this study to define wind loading are adopted from (CSA, 2007) and presented in Table 4-3. It is noteworthy that the values for z_{V^2} in this table represent climate conditions in the Year 2000.

Table 4-3. Statistical parameters used in defining wind load.

Variable	Mean	COV
z_C	1.00	0.025
z_{C_e}	1.00	0.080
z_{a_C}	1.00	0.050
z_A	1.00	0.000
z_{V^2}	0.332	0.587
z_{C_h}	0.71	0.140
z_{C_g}	1.02	0.075
z_{mW}	0.24	0.616

The values defining the distribution of wind velocity during extreme events mostly rely on statistical analyses of historical weather data. However, new studies predict the deviation of these values from historical data in future decades. The

following section discusses the procedure used for the computation of the parameters of the wind velocity distribution.

4.3.2.3.1 Wind Velocity

According to (Kupper, 1971) the probability distribution of maximum hourly wind speeds can be modelled with an Extreme Value Type I (or Gumbel) distribution, as follows:

$$F_V(v) = P(V \leq v) = EXP\{-EXP[-a(v-\mu)]\} \tag{4-18}$$

where a and μ are the scatter and central tendency of the distribution. The mean $\bar{V}$ and standard deviation σ_V of the distribution can be computed using Equations (4-19) and (4-20).

$$\sigma_V = 1.282/a \tag{4-19}$$

$$\bar{V} = \mu + 0.577/a \tag{4-20}$$

Indicating the return period of the extreme wind event in the subscript (e.g., a_1, μ_{100}), the statistical parameters of the annual maximum hourly wind speed (i.e., a_1, μ_1) can be calculated through (CSA, 2007):

$$a_1 = \frac{LN\left(\frac{100}{10}\right)}{\bar{V}_{100}-\bar{V}_{10}}, \ \mu_1 = \bar{V}_{10} - \frac{LN(10)+0.577}{a_1} \tag{4-21}$$

where values of $\bar{V}_{10}$ and $\bar{V}_{100}$ are available in the design codes (e.g. the Canadian highway bridge design code (CSA Group, 2019)).

4.3.2.3.2 Square of Wind Velocity

The preceding section establishes the distribution for the 75-year wind velocity. However, Equation (4-14) indicates that the reference wind pressure is dependent on the square of the wind velocity, necessitating a transformation from the distribution of wind velocity to the distribution of the square of wind velocity. Given that load and resistance typically follow lognormal distributions, it is reasonable to fit a lognormal distribution to the square of the velocity. This procedure initiates with determining the parameters of the maximum hourly wind speed, denoted as a_N and μ_N, and generating data for the wind speed and then its square based on the cumulative distribution function (CDF) of maximum hourly wind speed as specified in Equation (4-18). Subsequently, a lognormal distribution can be fitted to the upper tail (right-hand side) of the generated data using the probability paper plotting method.

4.3.3 Non-stationary wind speed model

Environment and Climate Change Canada (ECCC) has recently researched the regional projections of changes in climate design values for a range of future Canadian climate states to facilitate the development of climate-resilient codes and standards for Canada's Buildings and Core Public Infrastructure (B&CPI) (Cannon et al., 2020). From this project, changes in climate design variables are provided for certain levels of changes in global temperature. For instance, Figure 4-2 shows the projected changes of 10-year hourly wind pressures for different Canadian regions as a function of changes in average global temperature (ΔT) relative to 1986-2016. In this figure, lines denote the median of the predicted percent change for each region of the country,

while areas represent the 25th and 75th percentiles of the distributions for each region (Cannon et al., 2020).
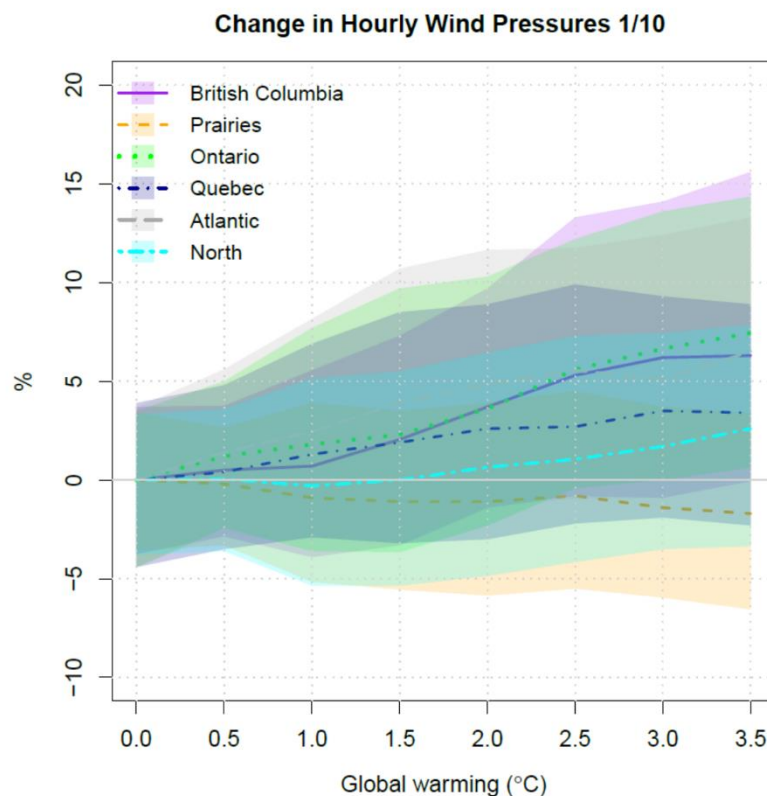
Figure 4-2. Projected changes in 10-year level hourly wind pressures for different Canadian regions (Cannon et al., 2020).

4.3.4 Timing of Global Warming

This method of presenting future projections provides a simple way of decoupling uncertainties about regional projections (or internal variability) from forcing scenarios and the timing of global warming. The regional projections are based on CanRCM4 LE, a regional climate model, while global scale analysis for calculating the timing of global warming is estimated based on CMIP5, a multi-model,

multi-scenario ensemble of GCMs. Table 4-4 provides the mean times at which a certain level of global warming is irreversibly exceeded (Cannon et al., 2020). Figure 4-3 shows the spline curves fitted to this data. As can be seen, for the RCP2.6 curve the temperature increases 0.5°C by 2023 and then remains almost constant through 2100. On the other hand, the RCP4.5 and RCP6.0 projections are almost linear and the same through 2070, after which the RCP6.0 projection separates with a more intense slope. The RCP8.5 predicts the most intense temperature change. According to this scenario, the temperature change will reach around 4°C in 2100. Changes of common design parameters used for building and bridges in Canada are provided in (Cannon et al., 2020) for different global warming levels. Figure 4-4 shows spline curves fitted to this data for London, Ontario for changes in the 10- and 100-year wind pressures as a function of the global warming level. In the following section, this data is used to predict changes in structural reliability.

Table 4-4. Mean time of irreversibly exceeding a certain level of global warming (Cannon et al., 2020).

ΔT	CanESM2 LE	RCP8.5	RCP6.0	RCP4.5	RCP2.6
+0.5°C	2012		2023		
+1.0°C	2025	2035		2046	–
+1.5°C	2036	2047		2070	–
+2.0°C	2047	2059	2087	–	–
+2.5°C	2057	2069	–	–	–
+3.0°C	2066	2080	–	–	–
+3.5°C	2076	2090	–	–	–
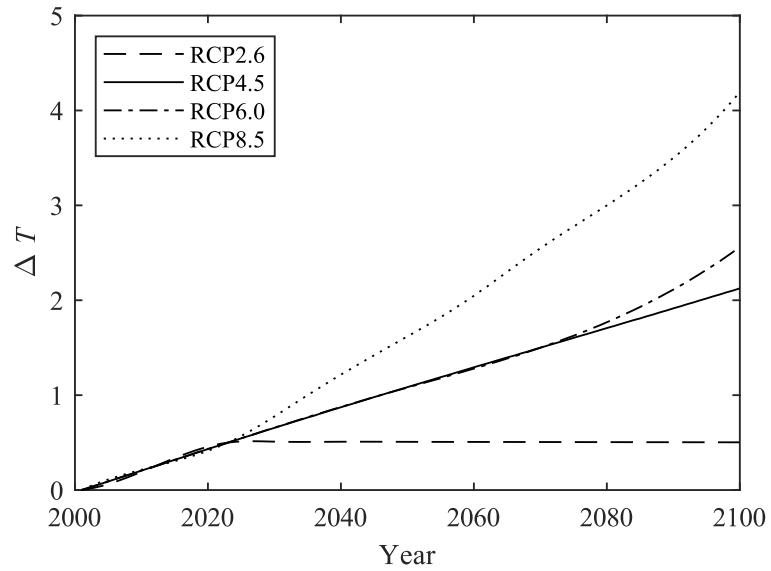
Figure 4-3. Global temperature changes for various RCPs.
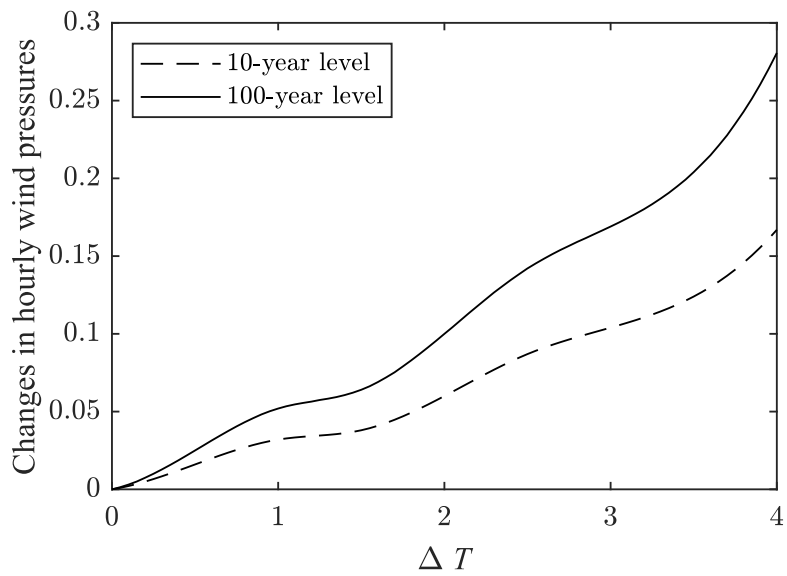
Figure 4-4. Changes in wind pressures for London, Ontario as a function of global temperature change.

4.3.5 Changes in hourly wind pressure

In this section, probabilities of failure of the case study structure are calculated with various climate change scenarios considered. To calculate the changes in wind pressure during the 21st century, the RCP curves of global temperature changes (Figure 4-3) are combined with curves of wind pressure change (Figure 4-4) resulting in Figure 4-5. This figure shows the changes in the 10-year and 100-year wind pressures for London, Ontario. The inverse of Equation (27) is used to translate 10-year and 100-year level wind pressures to wind velocities (i.e. $\bar{V}_{10}$ and $\bar{V}_{100}$). These values are then substituted in Equation (4-21) to determine the probabilistic distributions of the annual maximum wind speeds. To compute the parameters of wind load effect distribution, the procedure explained in Section 4.3.2.3 is applied. Finally, Equation (4-2) is used to calculate the time-varying annual reliability indices and probabilities of failure, according to the changes in annual wind load statistical parameters for each climate change scenario.
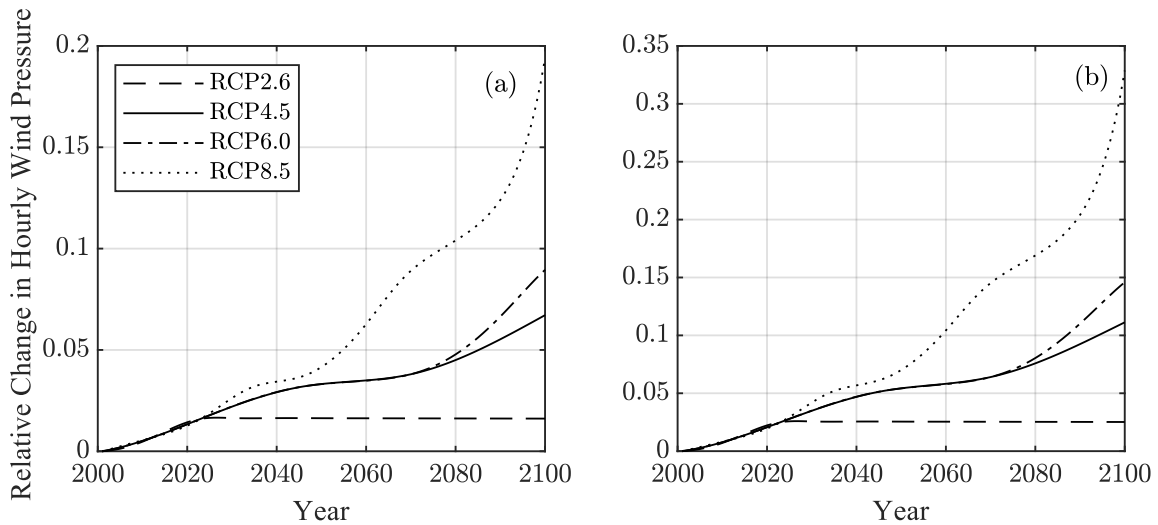
Figure 4-5. Changes in wind pressures for London, Ontario in the 21st century. (a), 10-year wind pressures, and (b), 100-year wind pressures.

4.4 Results

4.4.1 Annual Probability of Failure

Figure 4-6 illustrates the annual failure probability of the structure under nonstationary increasing wind loads associated with various RCP scenarios throughout the service life of a structure built in the Year 2000. It is noteworthy that the curve for RCP4.5 is omitted as it closely aligns with the RCP6.0 curve. As anticipated, RCP2.6 and RCP8.5 result in the least and greatest changes in reliability, respectively. Across all scenarios, the probability of failure initiates at $4.6 \cdot 10^{-5}$ in the initial year of service in the Year 2000 and consistently rises through 2023 to $5.6 \cdot 10^{-5}$. Subsequently, while the RCP2.6 curve remains constant until the end of this century, the RCP6.0 and RCP8.5 curves continue to ascend, reaching $1.6 \cdot 10^{-4}$ and $4.7 \cdot 10^{-4}$,

corresponding to a growth of 248% and 921%, respectively, compared to the beginning of the service life.
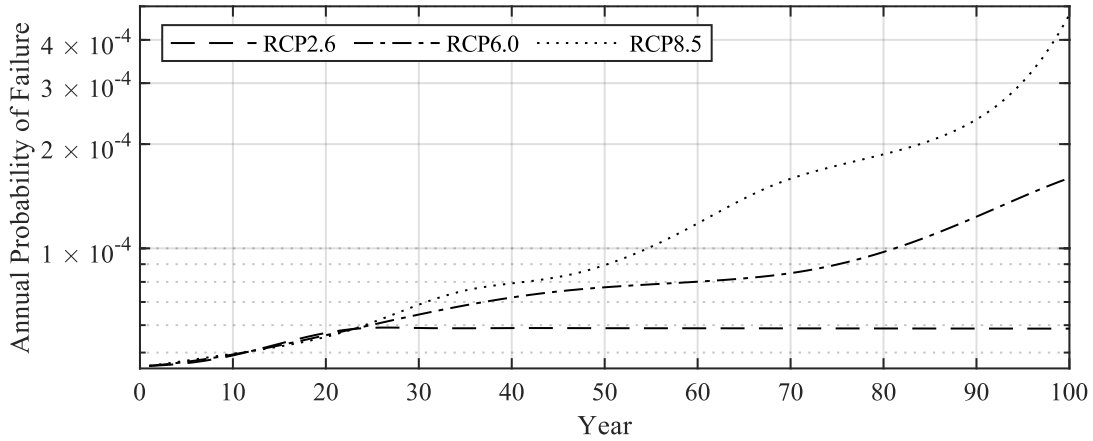
Figure 4-6. Annual probability of failure for the case study flexural member in London, Ontario.

4.4.2 Cumulative Probability of Failure

The lifetime reliability of the structure, $\mathcal{L}(T)$, is calculated using Equation (4-6). As reliability is defined as the probability of survival, the cumulative probability of failure through the jth year of service (P_{T_j}) can be easily computed using the following equation:

$$P_{T_j} = 1 - \mathcal{L}(T) = 1 - EXP(-\sum_{i=1}^{j} \lambda P_i) \tag{4-22}$$

Figure 4-7 depicts the cumulative probability of the structure experiencing failure versus time. In these illustrations, solid green lines serve as a benchmark, representing a scenario where wind loading remains stationary and unchanged for 100 years. The additional lines correspond to various RCP scenarios. It is evident that the cumulative probability of failure, under all global warming scenarios, surpasses

70

that assumed under the stationary wind loading scenario throughout the analysis period. For instance, considering a structure established in the Year 2000 with a design service life of 75 years, the total probability of failure for RCP8.5 is $6.48 \cdot 10^{-3}$, which is 1.89 times greater than the probability under the stationary scenario ($3.43 \cdot 10^{-3}$).
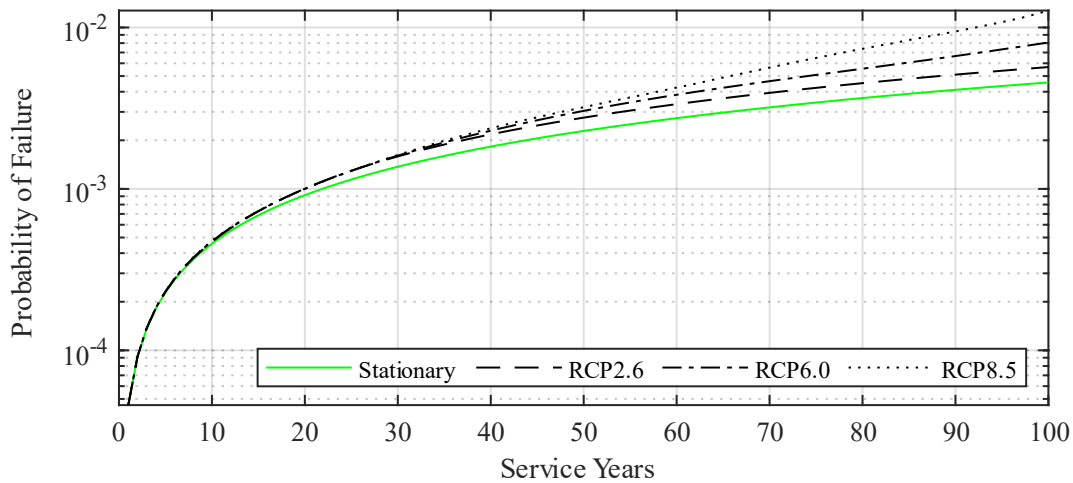
Figure 4-7. Cumulative probability of failure for different RCPs.

To assess the impact of the nonstationary (wind) to stationary (dead) load ratio on the probability of failure, a sensitivity analysis was conducted, and the findings are illustrated in Figure 4-8. In this figure, two sets of curves in green and black respectively depict the cumulative probability of failure under the stationary and RCP8.5 scenarios. Within each set, four curves correspond to different values of the wind-to-dead load ratios (WDR), ranging from 0.5 to 5, with the upper limit reflecting realistic values for aluminum structures designed for lightweight purposes. It is evident that for both groups, structures with larger WDRs (indicated by thicker curves) exhibit higher probabilities of failure, suggesting a relatively greater susceptibility to failure despite having the same design basis across all WDRs.

71

However, structures with lower WDRs demonstrate slightly greater sensitivity to future climate changes. For instance, at the 75th year of service, the probability of failure for a structure with WDR = 5 increases by 80% (from $6.93 \cdot 10^{-3}$ to $1.25 \cdot 10^{-2}$) under the RCP8.5 scenario compared to the stationary climate. Meanwhile, for a structure with WDR = 0.5 under the same conditions otherwise, the change is 98% (from $1.67 \cdot 10^{-3}$ to $3.30 \cdot 10^{-3}$).
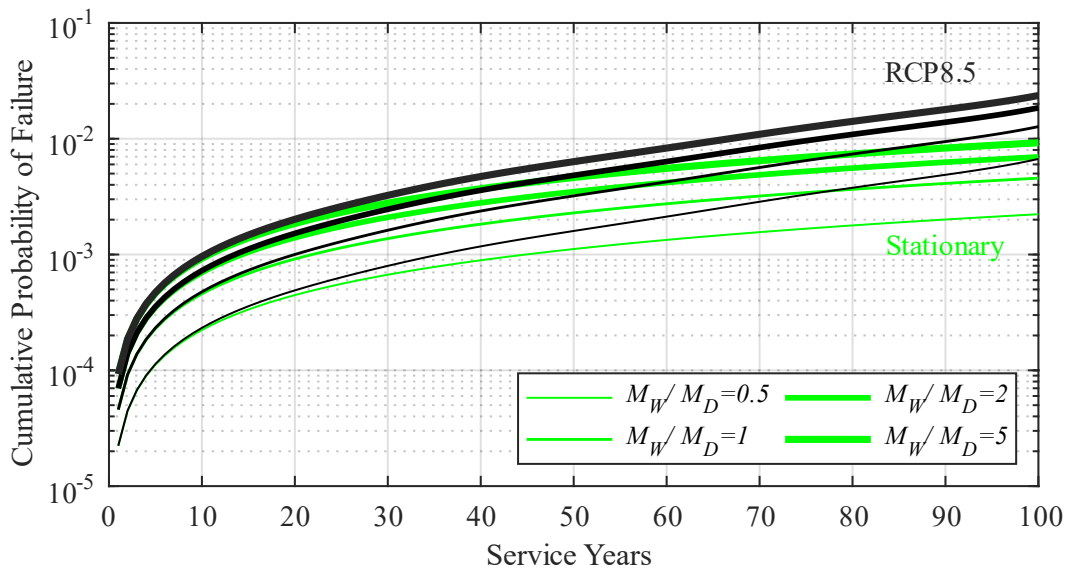
Figure 4-8. Comparison of cumulative probability of failure of various structures with different wind/dead load ratios under stationary load conditions and RCP8.5 scenario.

Figure 4-9 illustrates the sensitivity of the probability of failure to variations in the mean and standard deviation of the annual maximum wind speed. In this sensitivity analysis, a wind-to-dead load ratio of 1:1 is assumed. The solid green line represents the probability of failure under a stationary climate. The other lines consider a linear annual increase to reach a change in the parameter of interest in Year 100 (i.e. a 10 or 20% increase). As observed in this figure, the curve for a 10%

increase in the standard deviation is positioned above the curve for a 10% increase in the mean. The same holds true for the 20% increase curves. This implies that the probability of failure is more responsive to changes in the standard deviation of the wind speed than to changes in its mean.
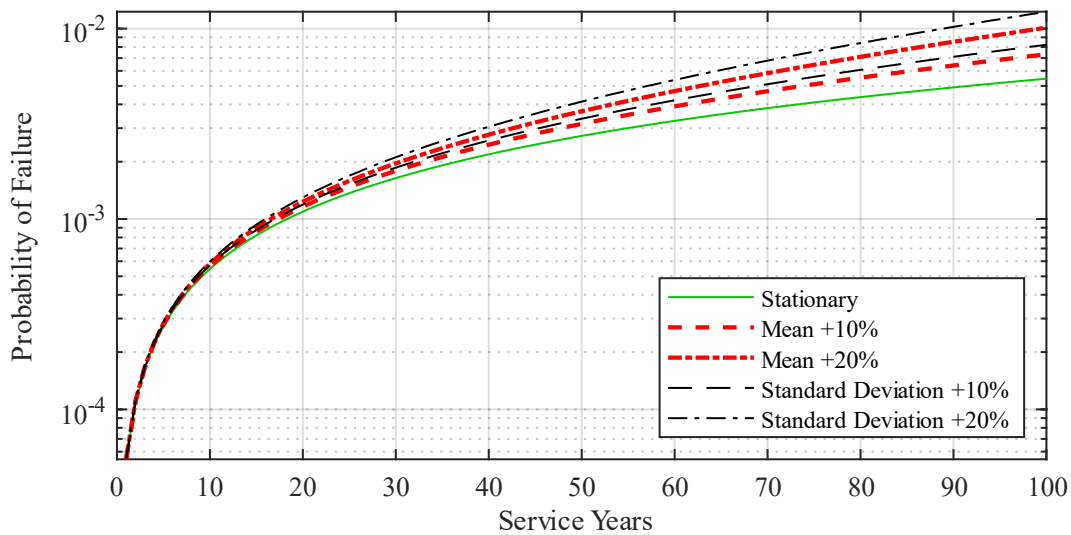
Figure 4-9. Sensitivity to the increase in annual maximum wind speed parameters.

All the preceding analyses were conducted using the mathematical approach outlined earlier, which employs closed-form expressions. This method, however, disregards the correlation between the load and resistance parameters from one year to the next. To assess the impact of this correlation across successive years of service, a Monte Carlo simulation (MCS)-based approach was employed, and the outcomes are presented in Figure 4-10, specifically for the RCP8.5 climate change scenario.

The applied MCS involves numerous trials, with each trial assessing the limit state function for every single year of service. The correlation of variables in different years is modeled by a correlation matrix, $\mathcal{R}(X)$, where $X = [x_1, x_2, ..., x_n]$ represents

the vector of random variables in different years (e.g., wind load effect in successive years of service), and the element $r_{x_i x_j}$ defines the correlation between variables in the ith and jth year. Treating the structure as a non-repairable system, the first service year in which the loads exceed the resistance is recorded as the failure year for that trial. Subsequently, the generated data for the failure year is used to capture the cumulative distribution function of failure time.

In Figure 4-10, the black dot and black dash lines respectively represent the cumulative and annual probabilities of failure predicted by the mathematical approach. The other four curves depict the cumulative probabilities of failure generated by MCS under various assumptions about the correlation of random variables (i.e., resistance, wind load effect, and dead load effect) across successive years of service.
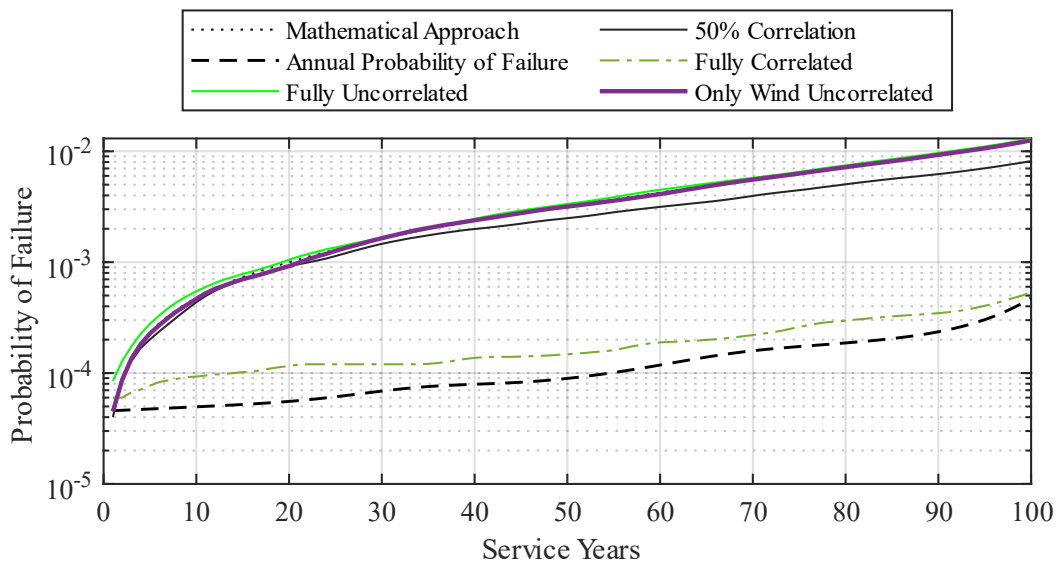
Figure 4-10. Effect of correlation of random variables between adjacent years (RCP8.5).

Generated under the assumption of complete independence between loads and resistance in different years, the "Fully Uncorrelated" curve aligns precisely with the outcome derived from the mathematical approach. This alignment serves as a validation of both the mathematical and simulation-based methodologies. The "Only Wind Uncorrelated" curve closely resembles the mathematically generated curve assuming no correlation. In this scenario, the assumption is that the dead load and resistances in different years of service are fully correlated, while the maximum annual wind loads are independent. This is a reasonable assumption in cases where values for resistance and dead loads remain constant throughout the service life of the structure.

The "Fully Correlated" and "50% Correlation " curves assume 100% and 50% correlation between random variables in successive years of service (i.e., non-diagonal elements of the correlation matrix are 1 and 0.5, respectively, for 100% and 50% correlations). As observed, an increase in correlation leads to a decrease in the cumulative probability of failure, eventually nearing the annual probability of failure curve obtained through the mathematical approach.

4.5 Concluding Remarks

In summary, this example presents various approaches to evaluate the influence of climate change on the reliability of structures during their service life. The study focuses on the nonstationary impact of wind load on a basic structural element situated in London, Ontario. The outcomes over a 100-year assessment period reveal that considering climate change effects can result in a lifetime probability of failure up to 1.9 times higher than the baseline analysis that assumes stationarity. Moreover,

the annual probability of failure in the final year of service is nearly four times greater than that in the initial year (Year 2000).

The example demonstrates that as the WDR (wind design ratio) increases, the structure becomes relatively more susceptible to failure, despite maintaining the same design basis. A sensitivity analysis highlights that the overall probability of failure is more sensitive to the coefficient of variation (COV) of annual maximum wind speed than its mean. This underscores the importance of incorporating variability of projected climatic design values in future research.

Lastly, Monte Carlo simulation (MCS) is employed to investigate the effects of the correlation of random variables across different years of service. The results indicate that as correlation increases, the probability of failure curve shifts downward, suggesting a lower probability of failure for a given year. For some scenarios, the difference is minimal, suggesting that fully correlated analysis may be adequate in practical situations.

Chapter 5. Evaluating the Methodology: Corrosion Management

5.1 Introduction

Composite concrete and steel slab-on-girder systems are commonly used in bridges throughout North America. In recent years, some bridge owners have become aware of an unexpectedly large amount of corrosion degradation of some of their weathering steel highway structures. Weathering steel contains small amounts of nickel, chromium, and copper; it is available as Type A or Type AT, as designated in CAN/CSA G40.21 (*Commentary on CAN/CSA-S6-00, Canadian Highway Bridge Design Code*, 2000). Under repeated cycles of wetting and drying, weathering steel forms a thin, adherent oxide patina in 18 to 36 months (*Commentary on CAN/CSA-S6-00, Canadian Highway Bridge Design Code*, 2000), which afterwards protects it from further penetration of oxygen and moisture that leads to corrosion. However, it appears that under certain conditions this patina does not form as previously supposed. In these cases, the patina tends to flake off, sometimes in large pieces, exposing a new steel surface to corrosion (Damgaard, 2009; Damgaard & Walbridge, 2009).

This extensive corrosion is believed to be due to microclimate conditions which result in extensive exposure of the steel element to a combination of moisture from melting snow, road salt, and sulfur dioxide. Factors that can affect microclimate conditions are the amount of de-icing salt usage, the number of wetting-drying cycles, the effectiveness of the drainage system, the design of structures (for example, the exposure to water splash from traffic), etc. Therefore, considerable variability can be seen in the condition of the environment surrounding different bridges in a city and even different locations on a single bridge. Typically, the corrosion degradation in

weathering steel structures is concentrated at the piers and abutments, where leaky joints permit water contaminated with salt to run onto the weathering steel girders, or at the midspan, where the draft of traffic passing underneath the overpass splashes the girders with salt-contaminated water. Both cases can be troubling, especially for simply supported girder bridges. For these types of bridges, the highest shear and moments forces occur at the supports and midspan respectively (Damgaard, 2009; Damgaard & Walbridge, 2009). Moreover, due to climate change effects, anticipating the amount of salt usage for employing a static corrosion protection measure can be difficult.

Climate change, as evidenced by various studies (Arvidsson et al., 2012), results in temperature fluctuations that affect the quantity of road salt used. Regions with harsh winters, like Alberta or Manitoba, currently use less salt due to its limited effectiveness in extremely low temperatures (Evans & Frick, 2001). In contrast, milder regions like Ontario or New York use more road salt. However, with rising temperatures due to climate change, provinces with severe winters may see an increase in salt usage as road salt becomes more effective. Conversely, regions with mild climates may reduce salt usage due to the temperature rise.

This high level of uncertainty, where the probability of future projections is undetermined, is referred to as deep uncertainty, or ambiguity, mostly in economics literature (Etner et al., 2012). Deep uncertainty can be treated as a non-probabilistic quantity, as opposed to traditional probabilistic random variables. Deep uncertainty challenges the traditional expected utility decision theory, the gold standard for normative models in rational decision making. Traditional decision and risk analyses make extensive use of models to predict the probable consequences of alternative risk

management decisions, but this approach faces four major obstacles when dealing with deep uncertainty of underlying state or scenario probabilities (Cox, 2012).

Considering the deep uncertainties of predicting the conditions of the environment, it would be very difficult to make decisions about employing typical corrosion protection measures. However, over time, one can observe the corrosion performance of the bridge and speculate on the actual degradation process. In this situation, resorting to fixed strategies with no consideration of information update may not be the best choice. In these "predict and then design" approaches, while the costs of a rust protection measure are clear and immediate, the benefits are uncertain and less obvious.

The focus of the study is on investigating the developed framework in determination of the optimum strategy for preservation of weathering steel highway structures when the possibility of formation of adverse microclimates is undetermined. Here a strategy is comprised of choosing among a set of engineering options (e.g., Whether Adaptation or not) and determining an action time for exercising that choice. The developed framework is a combination of RM, and dynamic programing, allowing for providing a solution that works on a wide range of possible futures instead of preparing for an expectation point.

In what follows, first, an analysis is performed for finding the optimal corrosion management strategy for a typical weathering steel highway structure. Then, a sensitivity study is performed, and the results are interpreted. Finally, a conclusion is provided, based on the presented work.

5.2 Problem Description

To illustrate the framework, an analysis is performed for finding the optimal corrosion management strategy for a typical weathering steel highway structure in the province of Ontario, Canada. The properties of the bridge are briefly described here. For a more detailed description of the loads, resistance, and reliability calculations the reader is referred to (Damgaard, 2009; Damgaard & Walbridge, 2009).

5.2.1 Bridge Model

The considered bridge is a typical single-span simply supported box girder overpass. A typical section of bridge girder is shown in Figure 5-1. Using a macro-based Excel program, the bridge was designed in a previous research study on the reliability of corroding roadway bridges (Damgaard, 2009; Damgaard & Walbridge, 2009).

Figure 5-1. Cross section of a typical box girder

In the program, at predetermined time intervals, corrosion penetration is calculated, and the geometrical, and structural properties of the bridge are modified accordingly. Here, it is assumed that corrosion occurs on the web and flange together,

and the general corrosion model is intended to replicate the thickness loss across the whole surface of a structural plate. In so doing, over time, when the resistance falls below the load effect, the program stops and records the time of failure. A total of four failure modes are considered here; each of these failure modes or "limit states" are identified and quantified by the Canadian Highway Bridge Design Code (*CAN/CSA-S6-06: Canadian Highway Bridge Design Code*, 2006):

1) Shear ($V_f/V_r \leq 1$; Clause 10.10.5.2 (a) in (*CAN/CSA-S6-06: Canadian Highway Bridge Design Code*, 2006))
2) Moment ($M_f/M_r \leq 1$; Clause 10.10.5.2 (b) in (*CAN/CSA-S6-06: Canadian Highway Bridge Design Code*, 2006))
3) Shear + moment ($727M_f/M_r + 0.455V_f/V_r \leq 1$; Clause 10.10.5.2 (c) in (*CAN/CSA-S6-06: Canadian Highway Bridge Design Code*, 2006))
4) Bearing ($B_f/B_r \leq 1$; Clause 10.10.8.1 in (*CAN/CSA-S6-06: Canadian Highway Bridge Design Code*, 2006))

These limit states are checked at eleven equidistant points along the length of the bridge (except for bearing, which is only checked at the supports). Typically, dead, and live (i.e., traffic-induced) loads dominate the design of short- and medium-span bridges. Therefore, only these load types are considered in the current study. Two kinds of dead load are distinguished: dead load and superimposed dead. The former refers to the slab and steel girder self-weight while the latter refers to the sidewalk and wearing surface. The live load is the greater of a five-axle truck load and a truck-plus-lane load.

5.2.2 Corrosion Models

The corrosion rate of weathering steel is mainly affected by three factors: the presence of chloride pollution, the presence of sulfur dioxide pollution, and the time of wetness of the steel. Based on measurements on field specimens Albrecht and Naeemi (Albrecht & Naeemi, 1984) categorized corrosion rates into three main regimes: rural, urban/industrial (henceforth referred to as urban), and marine. In this study, these three categories are considered as the potential corrosion rates due to microclimates undetermined during the design phase, and it is assumed the probability of each scenario is unassigned.

As described in (Albrecht & Naeemi, 1984), for modeling corrosion penetration, thickness loss over time, t, (in years) is assumed to follow the power function:

$$C = A \cdot t^B \tag{5-1}$$

where C is the thickness loss in mm $\times 10^{-3}$, A and B are constants. The values used for these constants in this study are given in Table 5-1, and are based on corrosion penetration tests performed in England, Germany, and the United States (Albrecht & Naeemi, 1984; Kayser, 1988). Using these values, a projection of thickness loss according to the three scenarios is presented in Figure 5-2.

Table 5-1. Corrosion Rates (Kayser, 1988)

Environment	Parameter	Distribution Type	Mean	Coefficient of Variation
Rural	A	Lognormal	33.3	0.34
	B	Lognormal	0.498	0.09
Urban	A	Lognormal	50.7	0.30
	B	Lognormal	0.567	0.37
Marine	A	Lognormal	40.2	0.22
	B	Lognormal	0.557	0.10
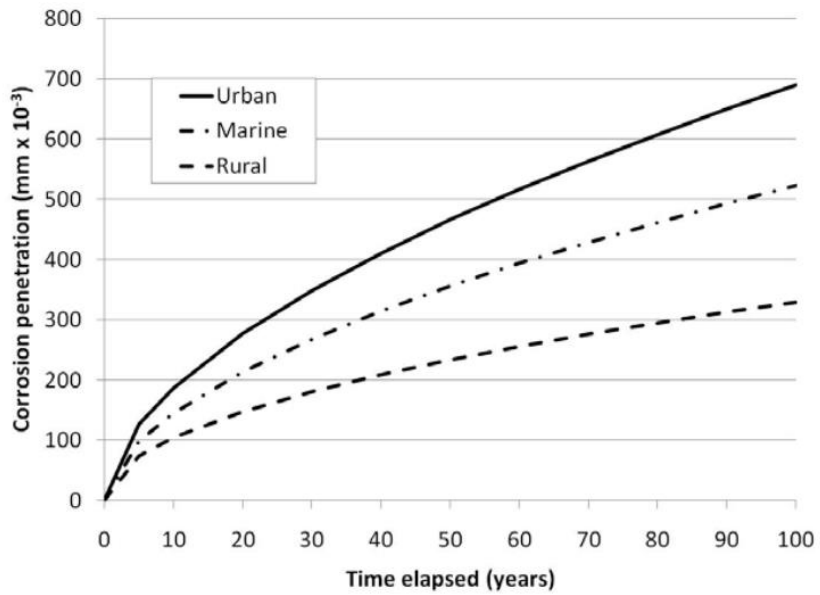
Figure 5-2. Mean corrosion penetration over time for different environments.

5.2.3 Identification of Potential Strategies and Flexibilities

In this example, metalizing and its time of application are considered as the potential protection strategies. When a protective cover is applied, it is assumed that it will prevent further progress of the corrosion until the end of the cover life. Here With the above-mentioned considerations, the probability of failure of the bridge is calculated for cover lives of 40 and 70 years. The former is reasonable for Metalizing, and the latter is considered only for sensitivity studies.

The probability of failure under each action and adaptation/application timing is performed using Monte Carlo simulation (MCS). A 100-year bridge planning horizon period is simulated. For each 100-year trial or "episode", failure can occur once, assuming no repairs. In this analysis, one million trials were performed for each strategy. To reduce computational costs and memory usage, adaptation strategies at 10-year intervals were simulated. Then linear interpolation is used to capture the lifetime cost of adaptation inside those intervals. For illustration, the annual probability of failures under the urban scenario are computed and depicted in Figure 5-3.
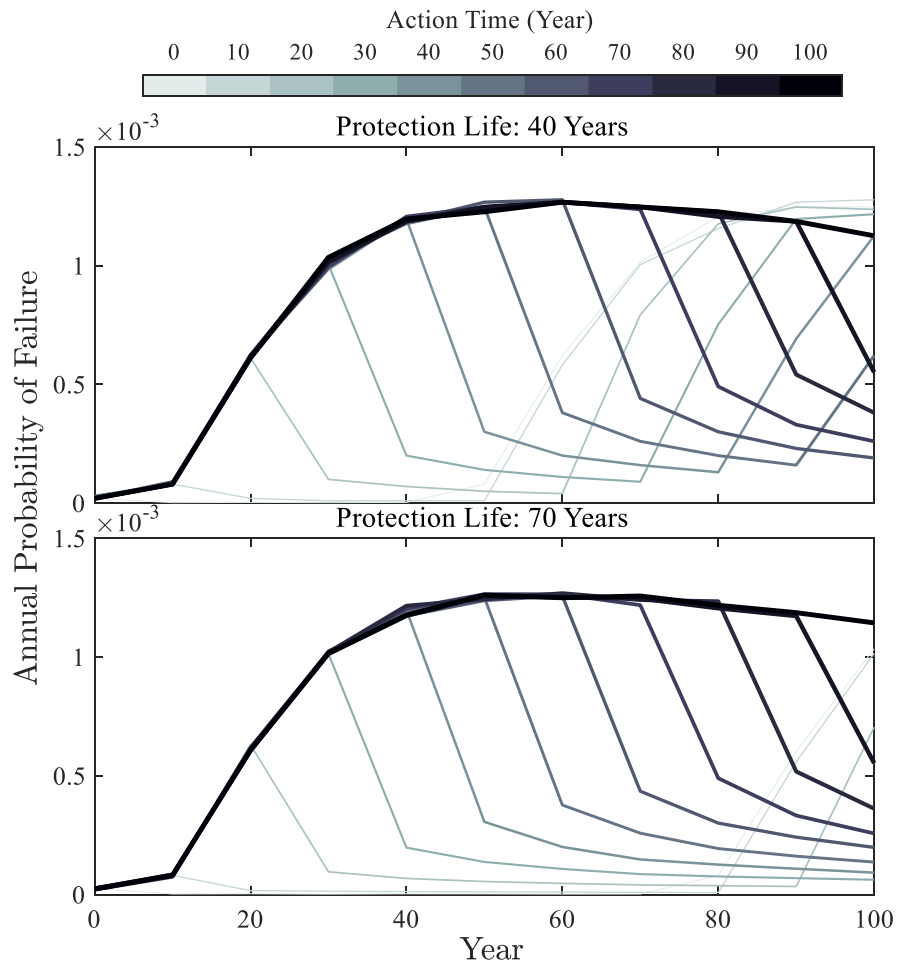
Figure 5-3. Annual probability of failure due to corrosion under the urban scenario for Protection lives of 40 and 70 years.

5.2.4 Economic Analysis of Adaptation Options

After probability of failure analysis, the life cost of failure is calculated. The life costs were then used in the developed frameworks to draw conclusions regarding appropriate management strategies. Based on the perspective of the decision-maker, different failure costs could be considered. In this sense, only the failure costs accruing after the bridge failure are considered and other costs, for example due to the bridge closure for maintenance are ignored. In order to illustrate the methodology, the expected lifetime failure cost under the worst scenario is defined as "disaster cost", and all the monetary values are presented as its portions.

For a point analysis, the elements of failure cost calculation are presented in Table 5-2. It is assumed that the corrosion protection measure involves a metallizing process with a relative cost of 0.2, which hinders further corrosion of the steel components up to the end of life of the cover layer. The accessibility cost involves field application costs such as permits, scaffolding, sand blasting and transportation of the equipment, which is mostly avoided for a construction phase application. In the next section, the framework is illustrated and interpreted.

Table 5-2. Assumed values for cost and life of a corrosion protection measure as well as the information update probability distribution.

| Parameters | Disaster cost | Metallizing cost | Accessibility cost | Discount rate | Protection Life years | I | | |
						Mean (years)	COV	Dist.
Values	1	0.2	0.15	0.02	40	5	0.5	LN

5.3 Results and Discussion

Based on the probability of failure of the bridge and values of Table 5-2, the LCC matrix is evaluated in the second step of the methodology and is presented in the form of Figure 5-4. Here, $c_{s_i a_j}$ curves represent the LCC of acting on either $a_1 =$ *Metallizing* or $a_2 = Not\ Metallizing$ at a given time under scenarios $s_1 = Urban$ and $s_2 = Rural/Marine$ (Note that Rural and Marine are put under the same scenario as they generate almost similar outcomes); The first jumps is due to the accessibility cost for in-service application of the protection measure. Over time, LCC of metallizing is declining for $s_2 = Rural/Marine$ due to the discounting effect, while under $s_1 = Urban$, it is increasing due to the increased risk.

Subsequently, in the third step of the methodology, the regret matrix and then the regret values of employing the various methods are computed. The regret of various methods is compared in Figure 5-5. Furthermore, the values of the regret matrix ($R_{s_i a_j}$ curves) are provided for context. As can be seen, the regret of the classical MR, $R^c(t)$, is increasing except over an initial period as well as beyond $t = 72$ years. Here, R^d shows the regret of delaying decision-making until a given time on the horizontal axis when the information update is assumed to occur, whereas R^s denoted

the regret of employing the stochastic method. It can be proved that R^c and R^d are the upper and lower bounds of R^s until a time t_0 after which the outcome the methods become similar. As can be seen, t_0 occurs at intersection the curves of regret of metallizing under scenarios 1 and 2.

The added value of the deterministic, V^d, and stochastic, V^s, methods is presented in Figure 5-6. V^d show the value of waiting until a given time when exact information will be available. The high initial value of V^d is since exact information can prevent unnecessary investment on metallizing. V^s at a given time is the value of waiting longer for possible information arrival in the future instead of acting according to classic MR in that considered time. V^s can also be interpreted as the maximum reasonable value of the fund that can be assigned at t to field-testing that may results in information update sometime in the future, instead of acting blindly according to $R^c(t)$. As can be seen, V^s begins with a relative value of 9% with having the option of metalizing during the construction. However, immediately after construction, this option is removed and the incentive of investing on testing and waiting info update increases.

For the various approaches, the design and management plan is presented in the form of Figure 5-7. The plan is comprised of two sections: *Before and after information arrival*. The horizontal axis is the time since construction (with the consideration of $t = 0$ as the construction phase), and vertical axis represents the set of possible actions. On the *before information* section on the top, the recommendation of the classical MR is plotted for comparison. Here, the curves represent the appropriate action for management of an unmetallized bridge at a certain age on the horizontal axis. As can be seen, in case of no information, during the construction

phase, $t = 0$, the classical MR suggests instantaneous metallizing, while the stochastic method suggests waiting. However, for an existing bridge (when $t > 0$), the recommendations of the two methods are similar until an information on the validity of either of the scenarios is arrived. For example, at $t = 15$, information arrival on validity of $s_1 = Urban$ would result in immediate metallization.

In general, here, the plan based on the stochastic information arrival suggests metallizing after waiting for information update for $t_0 = 23$ years. Otherwise, indicating the time of information arrival with I, in the case of realization of $s_1 = Urban$ at time $I < t_0$, the method suggests acting according to the s_1 case in Figure 5-7:

- when $0 < I \leq 10$ years, adapt at action time $\tau = 10$ years.

- when $I = 0$ or $I > 10$ years, adapt instantaneously at $\tau = I$.

However, in the case of realization of $s_2 = Rural/Marine$, not metallizing is suggested. In summary, the conditions of the example problem imply Category 3 according to the flowchart in the appendix. To cover all the categories a sensitivity study is performed in what follows.
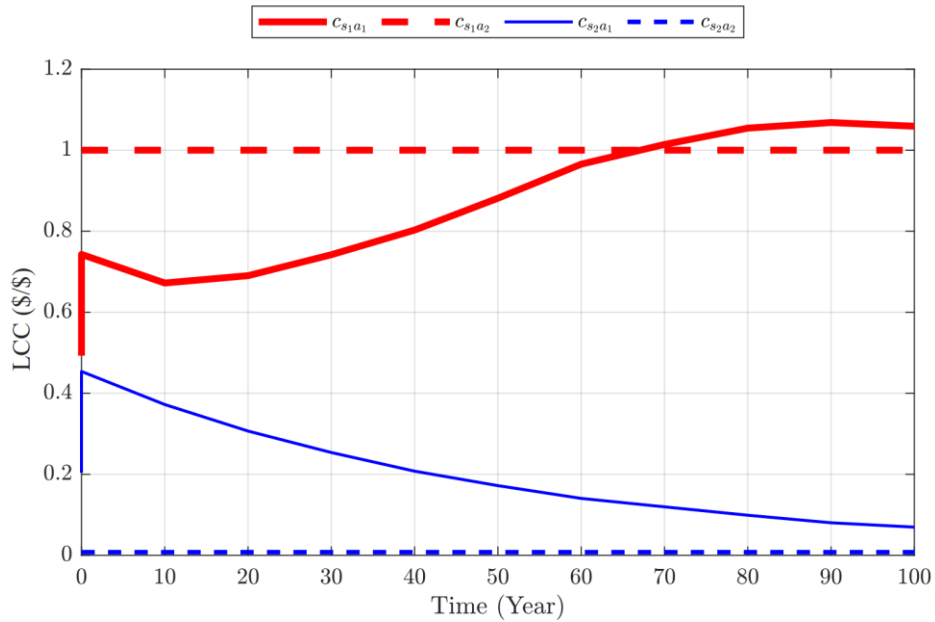
Figure 5-4. LCC of taking various actions at a considered time under different scenarios.

t_0: Time after which all methods have similar outcomes

$R_{s_i a_j}$: Regret of taking action a_j at a given time under scenario s_i

R^c, R^d, R^s : Regret of Classical MR, Deterministic and Stochastic methods
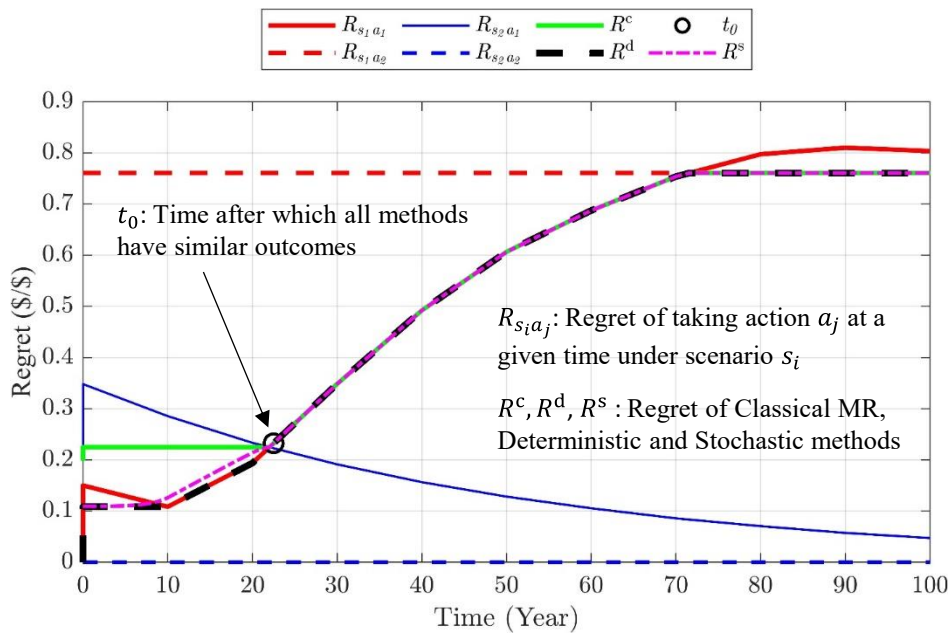
Figure 5-5. Regret values for various strategies and plans associated with accessibility cost of 0.15, metalizing cost of 0.2, and discount rate of 0.02.
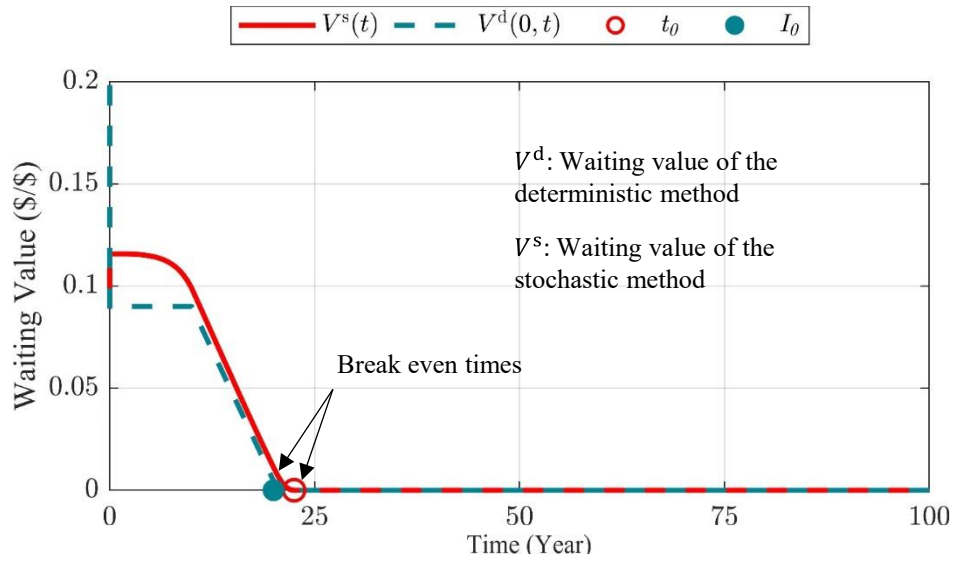
Figure 5-6. Deterministic and probabilistic value of waiting associated with accessibility cost of 0.15, metalizing cost of 0.2, and discount rate of 0.02.
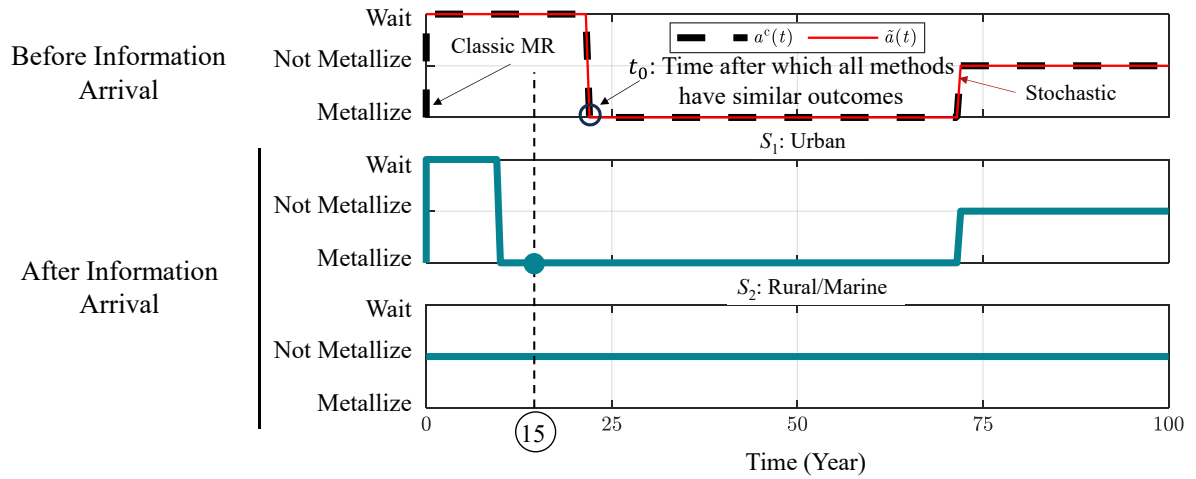
Figure 5-7. Summary of the policy to whether adapt, not adapt, or wait at time t after construction under no and full information of occurrence of each scenario.

5.4 Sensitivity Studies

In this section the sensitivity of the policies and plans to the variation of the following parameters is evaluated:

- Life of protective layer
- Discount rate
- Accessibility cost
- Metalizing cost

5.4.1 Map of Policy Categories

To interpret the value of waiting, adaptation policies are categorized into 7 types. For protection life of 40 and 70 years and discount rate of zero and two percents maps of region of these categories is presented in Figure 5-8. For clarification, an explanation is provided in the following for the case of metalizing with protection life of 40 and zero discount.

The bottom region of the figure begins with category 3 in the left due to low accessibility costs. With the increase in the accessibility cost, it becomes more reasonable to avoid accessibility cost by metalizing during construction. Therefore, the decision type changes to category 1, crossing a 45-degree straight border. At the 45-degree border, regret of decision making before construction without information (i.e., $R^c(t)$) is equal to the regret of decision-making based on full scenario information immedietly after construction (i.e., $R^d(0^+)$). In the category 1 region, when the opportunity of metalizing is missed, e.g., in the case of an existing structure, it is still reasonable to metalize with a total cost of metalizing plus the accessibility cost. The maximum total cost of metalizing in this case is equal to the accessibility cost in the bottom right corner of the triangle. Finally, with the increase in the accessibility cost,

the decision transform to category 2 by crossing a 135-degree border. Along the 135 degrees border the total cost of metalizing is constant.

Entering the mid horizontal region with the increase in the metalizing cost along the vertical axis, the decision type transforms from categories 2 and 3, to Categories 5 and 6 respectively. In category 5 region, the decision-maker is willing to invest on testing, and metalizing only if the test shows an adversary scenario. Whereas in category 3 the purpose of testing is avoiding unnecessary early investment on metalizing. As can be seen, category 3 is the smallest for discount rate of 2%. In Category 6 region, metalizing is reasonable only when information on the realization of the extreme scenario arrives during construction. Finally, in the category 7 at the top region, metalizing is too expensive to be considered as a reasonable protection measure.

Consideration of discounting affects decision category map. A major change is the addition of the Category 4 region between Category 3 and 5. In Category 4, the decision-maker is willing to invest on testing to support metalizing as early as possible. Also, it can be seen that increasing the life of the protective layer will scale up the extent of the regions. In the following sections, the category map is overlaid the figures to help interpreting the results.
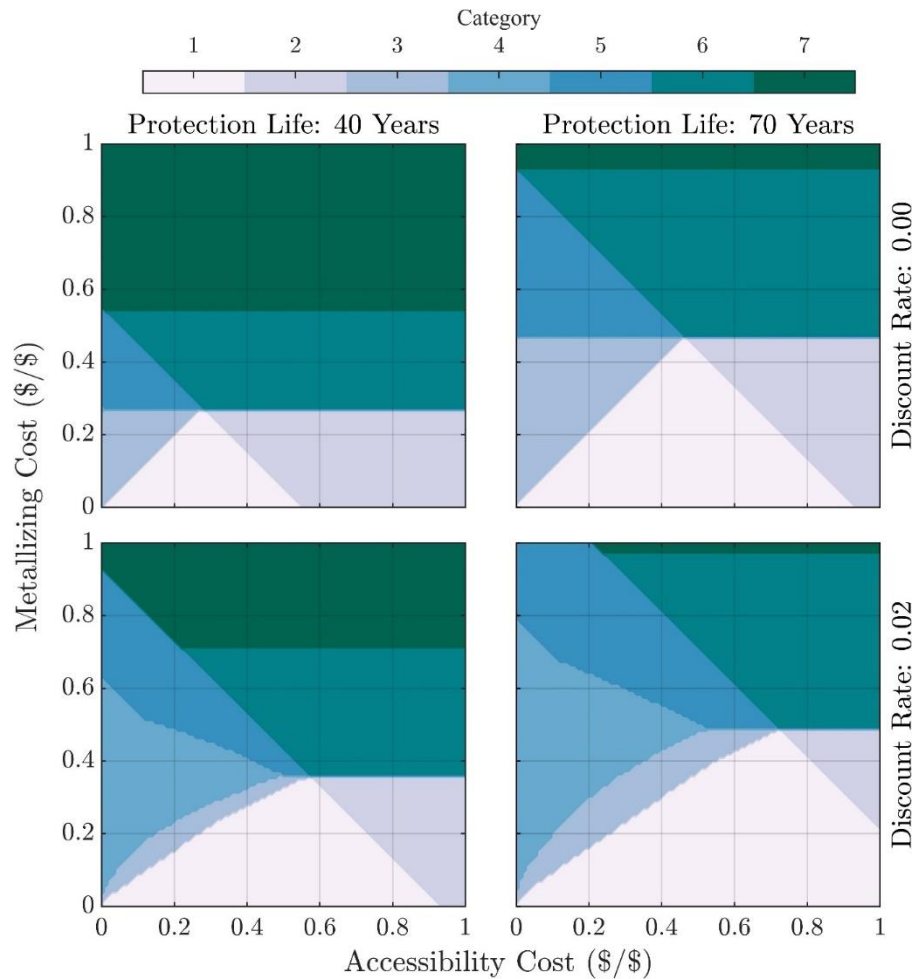
Figure 5-8. Map of Policy Categories

5.4.2 Classical MR

When employing the classical MR approach, the decision outcome falls in one of the three categories: Immediate metallization over construction, in-service metallization, or no metallization. An assessment on the category of these outcomes is presented in Figure 5-9. It can be seen that When discounting is ignored, classical application of regret suggests either immediate metalizing in regions 1-3 or not metalizing over regions 5-7. However, with the consideration of the discounting,

some portion of regions 3 and 5 transforms to region 4, in which metalizing is planned between 1 to 6 decades after construction.
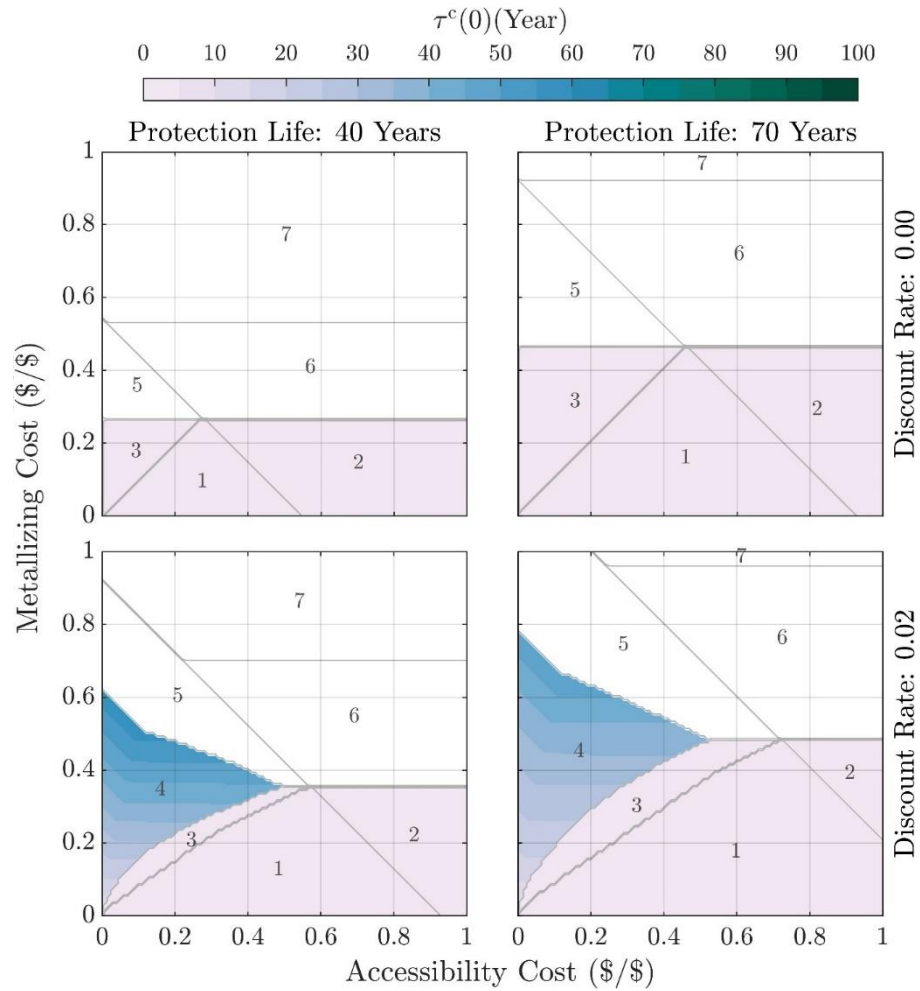
Figure 5-9. Optimal action time – Classical MR.

5.4.3 Deterministic Information Arrival

At time 0 (i.e., construction phase), the value of waiting until information arrival at I is depicted in Figure 5-10. Here, the subfigure with $I = 0$ represents the value of information update before/during the construction. Having information at this time point is valuable over regions 1 to 6, and the location of maximum values occurs at the horizontal border between 2 and 6 regions, which is between metalizing and not metalizing for classical MR. This seems reasonable as in practice in this region, decision-making should be more difficult for a manager. In this sense, this sub figure acts as a measure of the difficulty of decision-making. After construction, the waiting value over regions 1, 2, and 6 vanishes. Therefore, this subfigure confirms that in a new construction project, receiving information during construction (or earlier) is helpful for categories 1 to 6, and information received after construction is useful only for categories 3 to 5. Furthermore, the figure shows an increase in sensitivity of waiting value for $I > 30$ years.
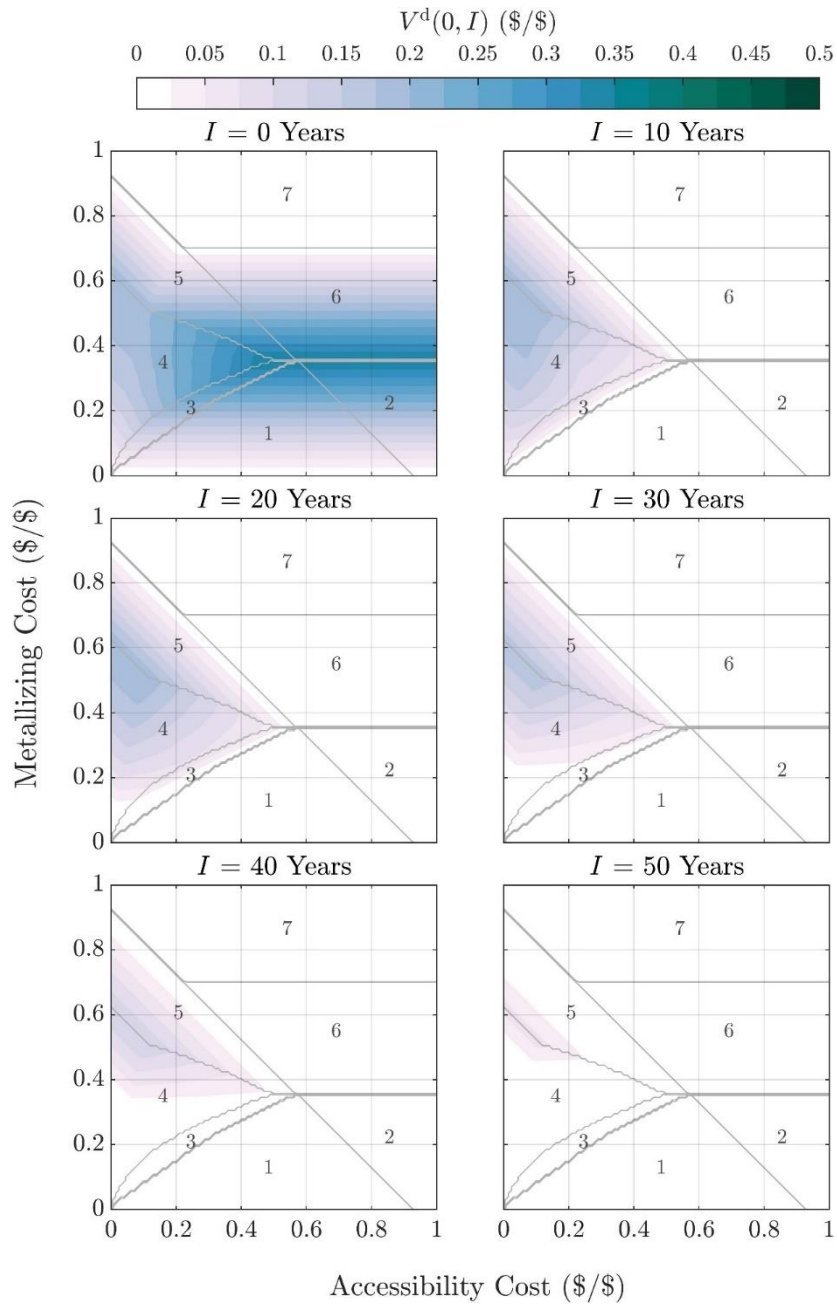
*Figure 5-10. The value of waiting until information arrival at **I** based on available action choices at time 0 (i.e., construction phase)*

5.4.4 Stochastic Information Arrival

For evaluating the value of the probabilistic option plan, Figure 5-11 to Figure 5-12 are provided. Figure 5-11 presents the added value of taking the stochastic information arrival method when considering a lognormal probability distribution for arrival time of information with mean of $\bar{I} = 5$ years and COV of 0.5. As can be seen, the maximum expected value is increased (from 0.28 to 0.45 for discount rate of 0, and from 0.20 to 0.30 for discount rate of 2%) with increase in protection life and decrease in the discount rate. However, the extent of region with positive expected waiting value is increased with the discount rate. The sensitivity of the results to the mean time of information arrival is present in Figure 5-12 for protection life of 40 years and discount rate of 2%. The sensitivity of the results to the COV of the arrival time can be inferred by comparing Figure 5-10 and Figure 5-12. From this comparison it is obvious that the waiting value shows little sensitivity to COV for the first 3 decades after construction. This comparison indicates that in this study waiting value is more sensitive to the discount rate than the supposed time of information arrival.
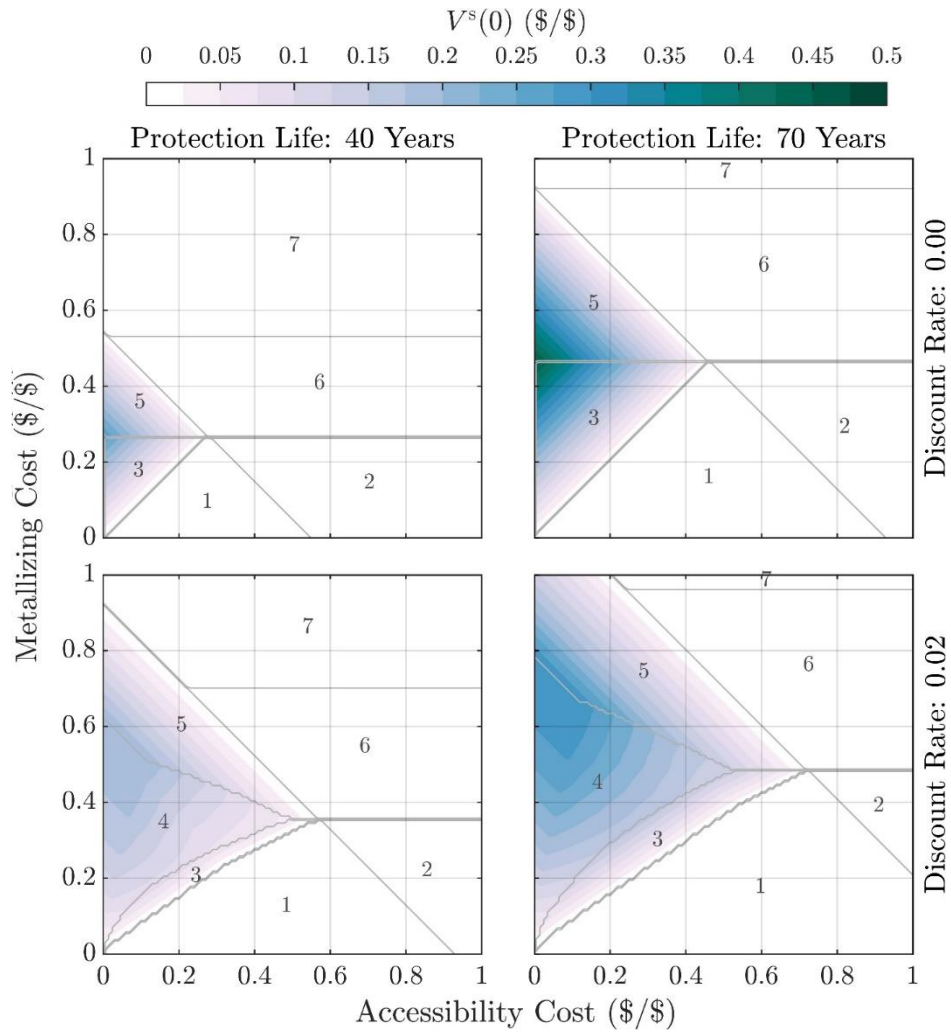
Figure 5-11. Expected waiting value when considering a lognormal probability distribution for arrival time of information with mean of 5 years and COV of 0.5
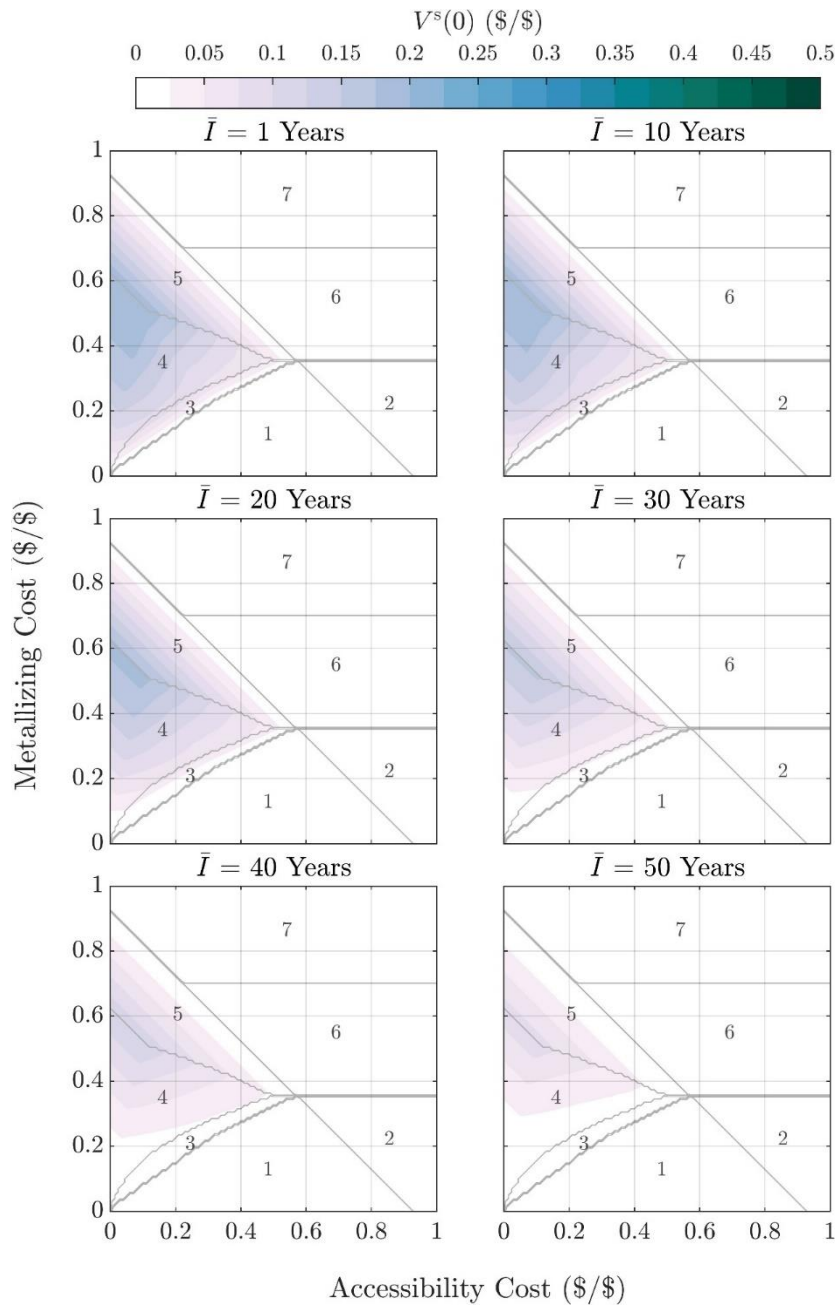
Figure 5-12. Expected information value for different lognormally distributed arrival time of information with COV of 0.5 for discounting of 2%

5.5 Concluding Remarks

This study employs the proposed framework for evaluation of various strategies for protection of steel bridges against corrosion. Composite concrete and steel slab-on-girder bridges are commonly used throughout North America. In recent years, some bridge owners have become aware of an unexpectedly large amount of corrosion degradation occurring to a number of their weathering steel highway structures. While in a mild environment weathering steel might show little degradation, in case of realization of a severe environment, for example, due to extensive use of de-icing salt during winter, using this material without protection can be found problematic as doing so might result in higher management costs or even catastrophic failures. On the contrary, the realization of a mild or moderate environment after utilization of the expensive preventive measures would also be suboptimal.

On this basis, the proposed method is used based on an assumption that the information on the state of the microclimate somehow becomes available over time, which makes delaying application of a protection measure valuable. The framework resorts to an adaptive solution, beginning with a less expensive option until the actual condition of the environment is more evident. Willing to minimize the maximum sense of loss, regret is combined with dynamic programming and implemented in the decision-making framework. The monetary added value of waiting for information is determined by comparing the outcomes for two cases of having and not having an expectation of a future information of microclimates is provided. As the optimal plan and efficacy of the method depend on the cost parameters, a procedure for classifying

the optimal plans into 7 categories is introduced. The method is illustrated using a problem of a single-span simply-supported box girder bridge.

Following the illustration, sensitivity studies are performed. Sensitivity studies show that the added value of the waiting for information is more sensitive to the discount rate than the expected time of information update. Furthermore, it was shown that the maximum expected value is increased (from 0.28 to 0.45 ($/$) for a discount rate of 0%, and from 0.20 to 0.30 ($/$) for a discount rate of 2%) with increase in protection life and decrease in the discount rate. However, the extent of region shrinks as the maximum value increases with the change in these variables. As such, the provided framework can help bridge owners more effectively target their resources on safety investments. Here the methodology was applied to corrosion management of steel bridges without explicitly considering the effect of climate change projections on the de-icing salt usage. However, the importance of climate change warrants such considerations in future studies.

Chapter 6. Bridge Scour Design and Adaptation to Climate Change

6.1 Introduction

The uncertainties associated with climate change pose challenges to bridge managers in investing in flood protection measures for safeguarding vulnerable bridges. One of the primary reasons for bridge failure globally is scour, or the removal of riverbed material from the bridge foundations caused by water flow. This issue is expected to be exacerbated by the impacts of climate change, which will affect local climate patterns and river flow regimes. So far, accurate prediction of these climate change effects has been elusive. Deterministic approaches are appropriate for defining optimum management plans for a clear and relatively certain future, which is not the case in this context, with very different and uncertain projections of river flow processes. Future climate projection is a complex task due to the interplay of various factors, including solar radiation, greenhouse gas emissions, and natural variability. However, In the context of climate change, the uncertainty around climate change will eventually decrease as a result of scientific advancements, statistical data, and monitoring weather patterns (van der Pol, van Ierland, et al., 2017). For example, some studies suggest meaningful learning about some important aspects of climate change will take 20–50 years to occur (Lee et al., 2017; Urban et al., 2014).

This possibility leads to some questions. One question is whether inaction and waiting for such information is worth the risk of adverse climate change driven events. Another important question is around the value of implementation of costly design flexibilities. To answer these questions around the bridge scour safety investments, the proposed framework is employed for designing a bridge in BC,

Canada. In the provided framework, the information arrival is modelled as a stochastic event with a predefined probability distribution. This chapter demonstrates how the methodology can be used to evaluate the trade-offs between different design options and to determine the optimal course of action, given the deep uncertainties associated with climate change.

6.2 Problem Statement

A multi-span bridge is planned for a railway crossing of Thompson River, BC Canada. Some of the details of the problem are adopted from (Neill, 1980) and inspired by the bridge wash out of events in BC. The problem involves decision-making about the length of a bridge on the river subject to climate change.

6.3 Identification Of Potential Strategies and Flexibilities

Three main options for bridge construction are:

- **Long Bridge:** Full length 230 m bridge over the entire width of the river.

- **Extensible Short Bridge:** Building an extendable shorter 150 m bridge over the main channel and filled overbanks and increasing the length if needed in the future.

- **Short Bridge:** Building a less expensive short bridge, which is not economically extendible.

The bridge cross-sections are depicted in Figure 6-1. For hydraulic modelling of the flow the Hec-Ras software is used (U.S. Army Corps of Engineers, 2022). More details on bridge dimensions for hydraulic analysis is provided in the next section.

104
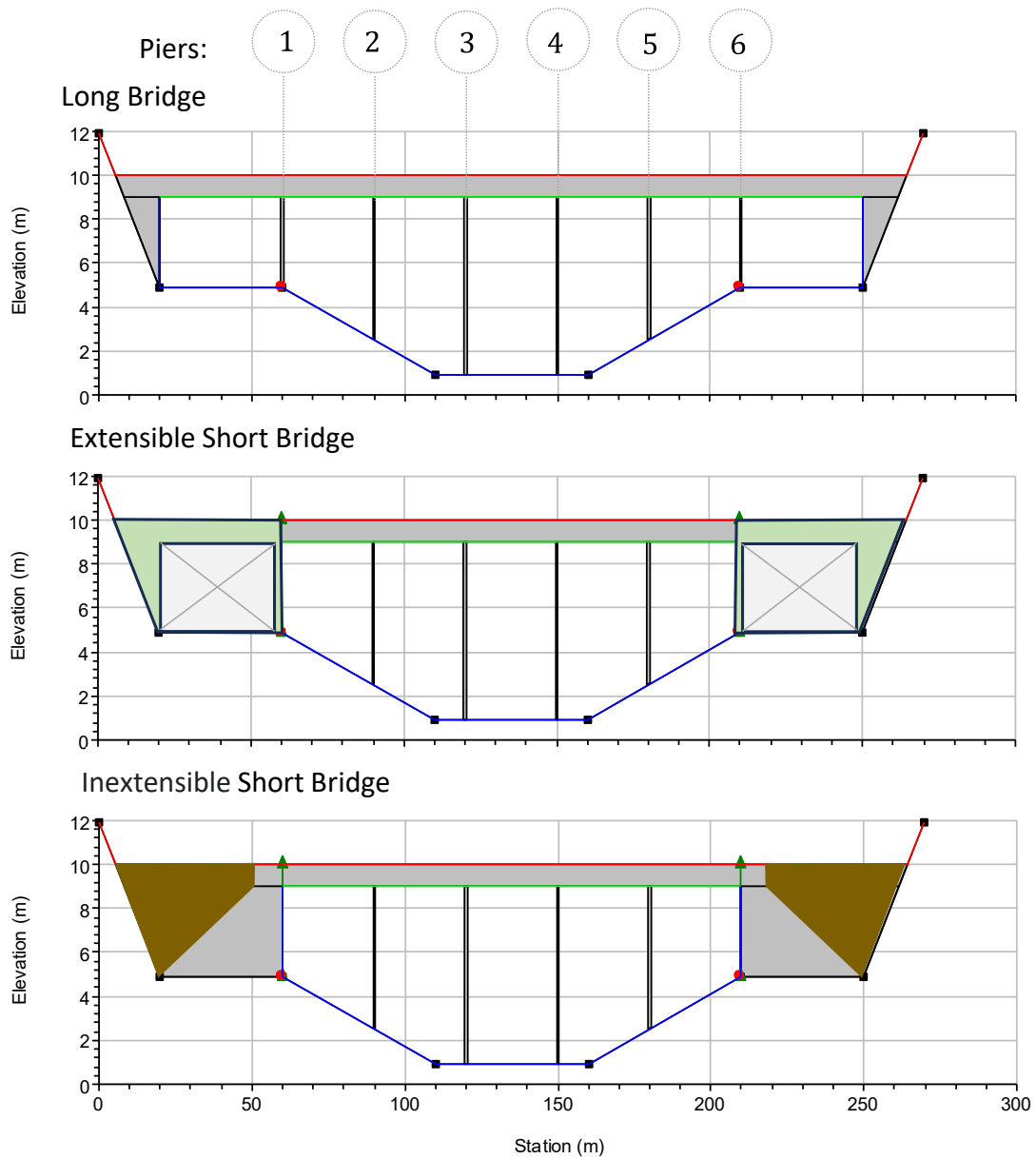
Figure 6-1. Bridge cross sections.

105

6.4 Bridge Modelling Details

The abutment is spill-through with an embankment having 2:1 side slope and a top width of 12 m. The bridge is supposed to be broad crusted with weir coefficient of 2.6. The elevation of the top of the bridge deck is 10 m, and the low chord elevation of the bridge is 9 m. The bed sediment is a relatively uniform medium sand having a median sieve diameter of 2.0 mm. For hydraulic modelling of the flow the Hec-Ras software is used (U.S. Army Corps of Engineers, 2022).

The bridge centreline is located at a river station (RS) equal to 1150 m. Ineffective flow areas in the left and right floodplains are located to the left and right, respectively, of the two vertical lines connecting the triangular symbols. The ineffective areas are valid for free flow and submerged orifice flow, but they become active or effective for overtopping flow. Lateral streambank stations for the main channel are shown at 60 m and 210 m stations, and the stream has a constant bed slope of 0.0014 m/m. Manning's n values are 0.035 for the entire cross section. The piers are dual square columns each with a width of 0.90 m. Piers are numbered from left to right beginning with #1. The pier positions are located at lateral stations of 60, 90, 120, 150, 180, and 210 m. The in-service design flexibility for an adaptable short bridge includes designing columns at stations of 60 and 210 m station such that they can sustain the increase load of adding the new spans.

Furthermore, preinstalling load bearing elements at the location of long bridge abutments would insure faster adaptation and less service interruption. The toe of the left abutment is at a lateral station of 20, and the toe of the right abutment is at a station of 250 m. The bridge routines in HEC-RAS allow the modeler to analyse the bridge

flows by using different methods with the same geometry. The different methods are: low flow, high flow, and combination flow. Low flow occurs when the water flows only through the bridge opening and is considered as open channel flow (i.e., the water surface does not exceed the highest point of the low cord of the bridge). High flow occurs when the water surface encounters the highest point of the low cord of the bridge. Finally, combination flow occurs when both low flow or pressure flow occur simultaneously with flow over the bridge. Here, For the low flow the "WSPRO" method used with the assumption of no wing walls, and for the high flow the "Pressure and/or Weir Flow" method with a coefficient of 0.8 for the "Submerged inlet + Outlet Cd".

HEC-RAS cross sections are shown in Figure 6-2, in which the differences between river stations represent the actual flow lengths, although it is only necessary to order the stations in ascending numerical value in the upstream direction. Actual flow lengths are entered elsewhere in the input data table. Station 1300 is the approach flow section (APPR) and Station 100 is the bridge exit section (EXIT). These stations are approximately one bridge length upstream and downstream of the bridge using the WSPRO methodology (Shearman et al. 1986, Sturm 2009). Bridge bounding sections are Station 1162 at the upstream toe of the embankment and Station 1138 at the downstream toe.
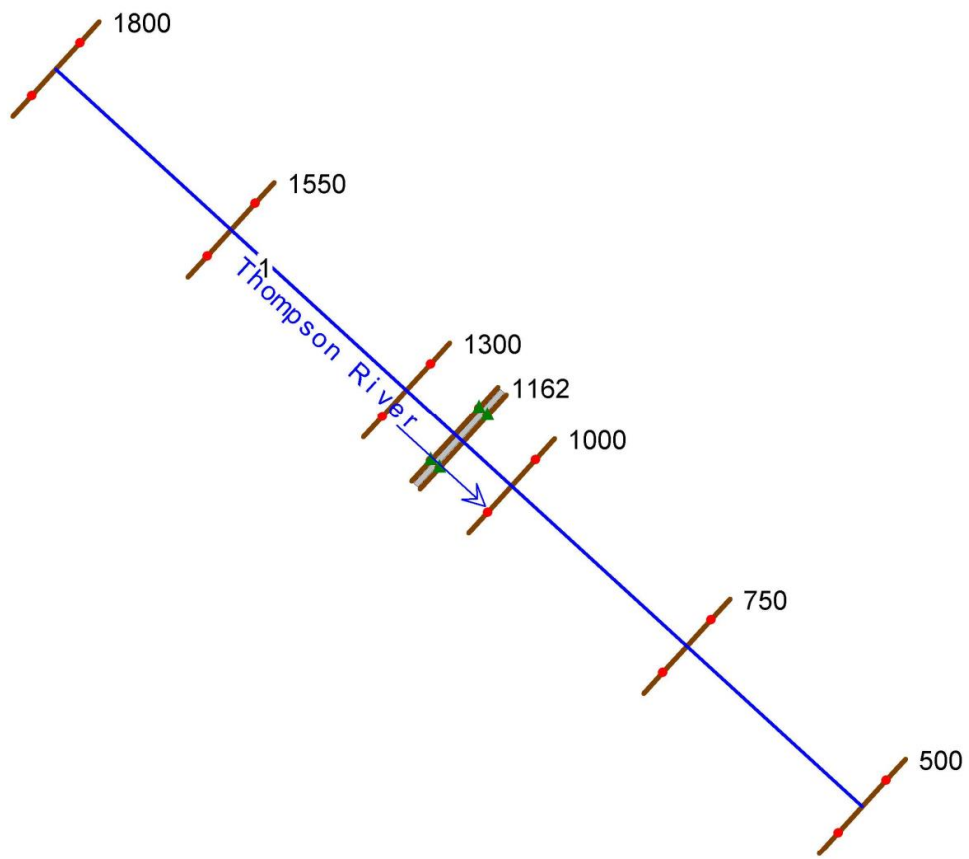
Figure 6-2. Cross-section layout along main stem for HEC-RAS analysis.

6.5 **Breakdown of Costs**

Table 6-1 provides a breakdown of construction and adaptation costs to components and their types for all bridge construction options. In this table "*" indicates that the cost occurs at the time of initial construction, whereas "+" indicates that cost occurs at the time of adaptation. The following cost types can be considered:

- Essential: costs that are present in all construction options, which includes:

    o Short Bridge Superstructure

    o Short Bridge Substructure

- Adaptation: is the cost of construction and installation of components for extending the bridge at the time of adaptation.

- Accessibility: is a cost that occurs only for in-service adaptation, and it includes:

    o Clearing of overbanks for extra waterflow

    o Transportation of equipment, permit applications and similar reworks

- Adaptation Capacity: is the cost of adjustments and installation of components that allow extension of the bridge.

    o In this example, to establish a short extendible bridge, with extra cost, the abutments of the short bridge should be built such that they can carry the load from installation of extension decks.

    o To reduce railway service interruptions, the abutment of the long bridge can be installed during the initial construction.

- Temporary: is the cost of installation of a system that will be removed in the case of adaptation. Here it includes:

    o Filling the river overbanks to create support for the road.

Table 6-1. Breakdown of construction and adaptation costs to components and their types for all bridge construction options.

Cost Type	Cost Components	Bridge Options		
		Short	Extensible	Long
Essential	Short Bridge Superstructure	*	*	*
	Short Bridge Substructure	*	*	*
Adaptation	Extension of Bridge Superstructure		+	*
Accessibility	Clear Overbanks		+	
	Rework and Permits		+	
Adaptation Capacity	Build Extra Capacity in Short Bridge Abutments		*	*
	Long Bridge Abutments Installation		*	*
Temporary	Fill Overbanks	*	*	

Note: In this table "*" indicates that the cost occurs at the time of initial construction, whereas "+" indicates that cost occurs at the time of adaptation.

Although investigation of the value of incorporating adaptation capacity is essential in discussion of the advantages of the proposed methodology, as a simplification in this illustrative example the adaptation capacity costs are ignored alongside the cost of employing temporary measures that would allow the adaptation.

6.6 Economic Analysis of Adaptation Strategies

The economic analysis of each action and adaptation timing is performed using Monte Carlo simulation (MCS). A 100-year bridge planning horizon period is simulated beginning year 2020. For each 100-year trial or "episode", failure can occur each year, assuming instant repairs. In this analysis, 10,000 trials were performed for each strategy. To reduce computational costs and memory usage, adaptation strategies at 10-year intervals were simulated. Then linear interpolation is used to capture the lifetime cost of adaptation inside those intervals.

6.7 Hydroclimate Projections and Expectations of Future Streamflow

The Pacific Climate Impacts Consortium (PCIC) (Consortium, 2020) provides access to simulated streamflow data for locations throughout British Columbia, Canada. The streamflow data were simulated using runoff and baseflow generated with an upgraded version of the Variable Infiltration Capacity (VIC-GL) model coupled with a glacier model (Schnorbus, in prep) and routed with RVIC (Hamman et al., 2016; Lohmann et al., 1996, 1998). For illustration purposes, in this example, the simulated streamflow of the Thompson River station near Spences Bridge is used without any further processing. A list of the twelve stream projection models is provided in Table 6-2 (Consortium, 2020). Similar to (Sims & Null, 2019) the historical period is selected as 1950-2000 and the calibration period is 2000-2100.

These simulations should not be treated as if they exactly represent the sequence of future events. Instead, their characteristic is extracted here to stress test the designs under some variations in the MCS trials. To do so, similar to (Sims & Null, 2019), a mean reverting stochastic process is calibrated with each of the annual

maximum of simulated stream flow time series. The stochastic differential equation has the following form:

$$d(X - \mu t) = \alpha(\bar{X} + \mu t - X)dt + \sigma dz \qquad (6\text{-}1)$$

where, dz is the increment of a standard Winner Process:

$$dz = \varepsilon\sqrt{dt} \qquad (6\text{-}2)$$

Here, ε is a random variable following the normal distribution:

$$\varepsilon \sim N(0,1) \qquad (6\text{-}3)$$

α is the instantaneous drift rate of the stochastic streamflow process, and σ is the instantaneous variance. This process is designed so that the random stream flow process revolves around a non-stationary trend, $\bar{X} + \mu t$. To illustrate the difference of the projections and importance of the methodology, extreme cases among the 12 projections (i.e., Scenarios 2 and 6) are presented in Figure 6-3 alongside their corresponding mean-reversion levels.

To calibrate the model to the data, the equation is rearranged according to Equation (6-4):

$$d(X) = \alpha(L(t) - X)dt + \sigma dz \qquad (6\text{-}4)$$

in which L is the mean reversion level of the process.

$$L(t) = \frac{\mu}{\alpha} + \bar{X} + \mu t \qquad (6\text{-}5)$$

For calibration, it was assumed that the process begins at year 2000 with $L(t = 0) = 2643$ m³/s, which is equal to the stationary mean reversion level of the 1950-2000 period. The calibrated value of the $\bar{X}$ is approximately 2.64×10^3 m³/s for the 12

112

simulated streamflow time series parameters while the other parameters are calibrated according to Figure 6-4. Mean-reversion levers are presented in Figure 6-5. To generate new samples of stream flow time series, SDEMRD objects(*SDE with Mean-Reverting Drift (SDEMRD) Model - MATLAB*, n.d.) are created based on the calibrated parameters. For illustration of the generated simulations, a sample simulation of 120 years (2000-2120) based on the parameters calibrated to Scenario 2 is presented in Figure 6-6 alongside their mean-reversion level.

Table 6-2. List of Stream Projection Models

Scenario	Base Model Name
1	ACCESS1_0_rcp45_r1i1p1
2	CanESM2_rcp45_r1i1p1
3	CCSM4_rcp45_r2i1p1
4	CNRM_CM5_rcp45_r1i1p1
5	HadGEM2_ES_rcp45_r1i1p1
6	MPI_ESM_LR_rcp45_r3i1p1
7	ACCESS1_0_rcp85_r1i1p1
8	CanESM2_rcp85_r1i1p1
9	CCSM4_rcp85_r2i1p1
10	CNRM_CM5_rcp85_r1i1p1
11	HadGEM2_ES_rcp85_r1i1p1
12	MPI_ESM_LR_rcp85_r3i1p1
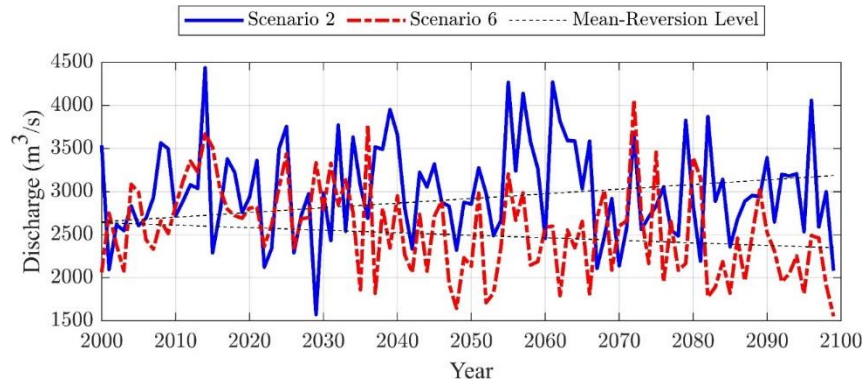
Figure 6-3. Comparison of Model 2 and Model 6 projections
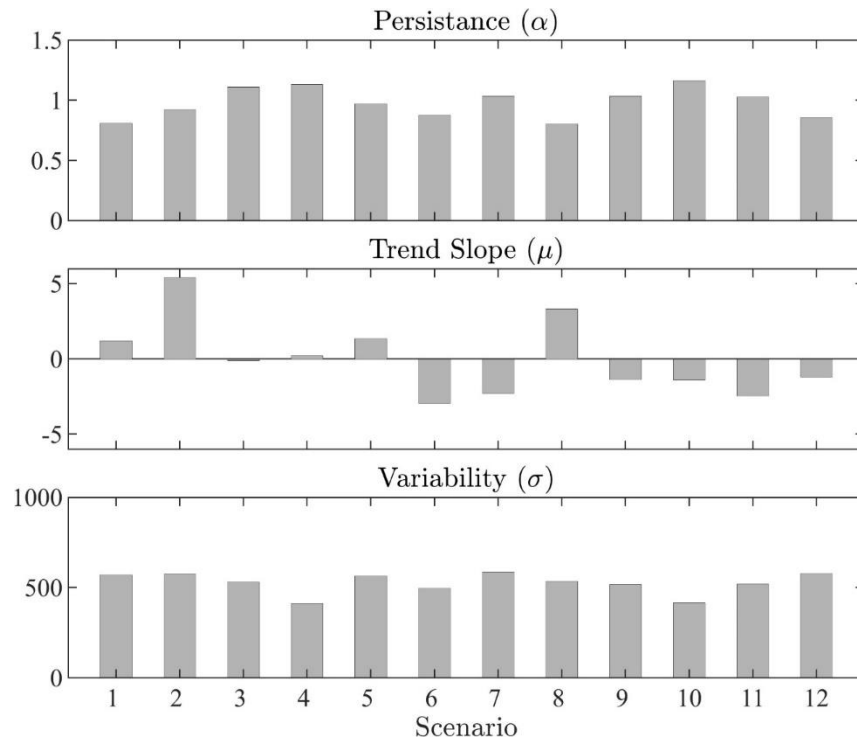
Figure 6-4. Streamflow Parameter Values for various Climate-Driven Streamflow

Projections (2001–2100) Created by 6 GCMs Each Run under Two Different RCPs.

114
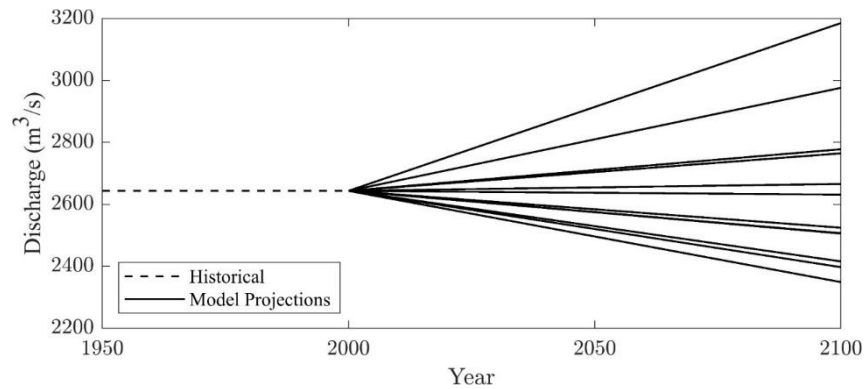
Figure 6-5. Mean-reversion levels of annual maximum discharge.
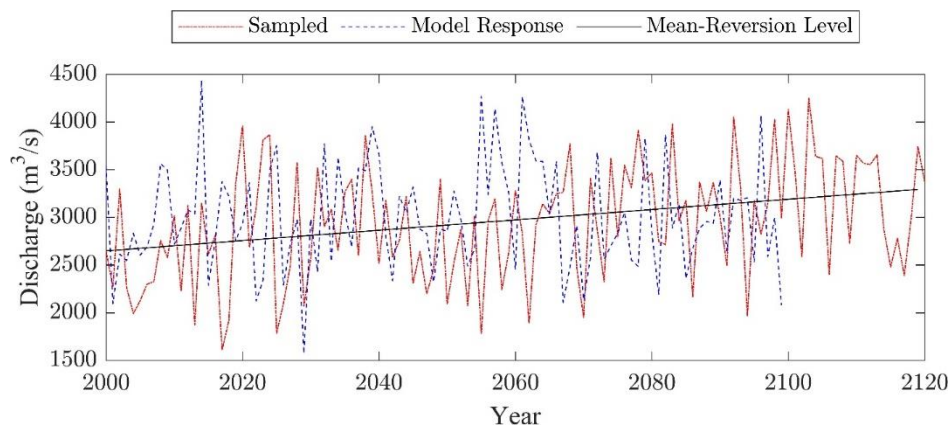
Figure 6-6. Mean-reversion level fitted to one of the GCMs hydrologic responses (Scenario 2 base model) and a sample time Serie based on the calibrated parameters.

6.8 Scour Analysis

Given the hydraulic properties of the stream determined by HEC-RAS, and the dimensions of the bridge components, scour depth is determined at the location of Piers 3 and 4 as they are more susceptible to scouring. In the damage cost analysis, it is assumed that undermining these piers incurs a damage cost equivalent to rebuilding the 150 m bridge. In the next section, an overview of the procedure used to calculate the scour depth is provided.

6.8.1 Scour and Foundation Failure

Total scour is comprised of a combination of various processes, which can happen simultaneously i.e.: channel degradation and instability, contraction scour, and local scour at piers and abutments. The sum and interaction of all these river processes create a very complex phenomenon that has, so far, eluded definitive mathematical modelling. Thus, a conservative approach is summing the different factors (Lagasse P.F. et al., 2013). Most of the dominant frameworks are based on two strong assumptions. The first assumption is that the scour depth resulting from exposure to a single flood event is independent of past events. Although the scour accumulation associated with multiple floods has been documented as a compelling cause of multiple bridge failures, very few studies (e.g. (Khandel & Soliman, 2019; Pizarro & Tubaldi, 2019)) have relaxed the assumption of independence of scouring events.

The other simplifying assumption is the consideration of a stationary hydrograph of infinite duration in the calculation of bridge scour depth during flood events. This assumption allows for the use of equilibrium scour depth, which is the stable scour depth around a bridge pier or abutment when the erosive forces of the flowing water and the resistive forces of the sediment are in balance. By assuming a stationary hydrograph of infinite duration, the dynamic changes in flow rate and scour depth over time can be ignored, making calculations simpler and more straightforward. However, it is important to note that this assumption may not accurately represent actual flood events, which can have rapidly changing flow rates and scour depths over time. In this study, a simplified version of the approach used in (Sturm et al., 2018) for combining pier scour and vertical contraction scour was

considered, in which these components are calculated separately and summed together. An overview of the methods for calculating the local and contraction scour components is provided herein while channel degradation is ignored.

6.8.2 Local Scour:

Local scour is caused by the reduction of flow around piers or abutments. Estimating pier local scour is commonly done using the Hydraulic Engineering Circular HEC-18 pier scour equation (Arneson et al., 2012), which considers factors such as the shape of the pier nose, the angle of flow attack, bed condition, and Froude number. According to HEC-18, scour due to an exposed pier stem in flow is determined as:

$$y_{s,pier} = 2.0k_1k_2k_3(\frac{a_{pier}}{h_u})^{0.65}Fr^{0.43}h_u \qquad (6\text{-}6)$$

where K_1, K_2, and K_3 are the correction factors for pier nose shape, the flow angle of attack, and bed condition respectively, h_u is the upstream channel flow depth, and Fr is the Froude number:

$$Fr = \frac{v}{\sqrt{gh_u}} \qquad (6\text{-}7)$$

where g is the gravitational constant. In more complex pile foundations, local scour depth is estimated by superimposing various scour components, including those from the pier, $y_{s,pier}$, pile cap, $y_{s,pc}$, and pile group, $y_{s,pg}$. These individual scour components are calculated based on the methods described by Arneson et al. (Arneson et al., 2012) and then summed according to Equation (6-8) to obtain the total local scour depth as demonstrated in Figure 6-7-a.

$$y_{s,local} = y_{s,pier} + y_{s,pc} + y_{s,pg} \tag{6-8}$$

6.8.3 Contraction Scour

The phenomenon known as contraction scour refers to the erosion of material across the width of a stream that occurs due to flow constriction. Typically, the constriction of channel width at a bridge is considered as the primary cause of this scour. However, submerged flow also induces scour by forcing flowing water under the bridge deck, as illustrated in Figure 6-7-b. Submerged flow contraction scour, $y_{s,SFCS,}$ is estimated through the following equation, which is the product of several variables, including the effective average approach velocity under the bridge (V_{ue}), the effective approach flow depth under the bridge (h_{ue}), a constant factor (K_u = 11.17 ft²/s), the median grain size (D_{50}), the flow depth above the bottom of the bridge superstructure (h_t), Vertical bridge opening height before scour (h_b), and the height of the weir flow overtopping the bridge (h_w) (Shan et al., 2012):

$$y_{s,SFCS} = (\frac{V_{ue}h_{ue}}{K_uD_{50}^{1/3}})^{6/7} + \left[0.2\left(\frac{h_bh_t}{h_u^2}\right)^{0.2}\left(1 - \frac{h_w}{h_t}\right)^{-0.1} - 1\right]h_b \tag{6-9}$$

When assessing the capacity of a pier, the total scour depth must consider both submerged flow contraction scours and local scour as the primary sources of sediment removal:

$$y_{s,total} = y_{s,SFCS} + y_{s,local} \tag{6-10}$$

In the present example, for simplicity, it is assumed that the foundation fails when $y_{s,total}$ is larger than foundation depth. For the considered case study, the relevant scour analysis parameters are provided in Table 6-3.
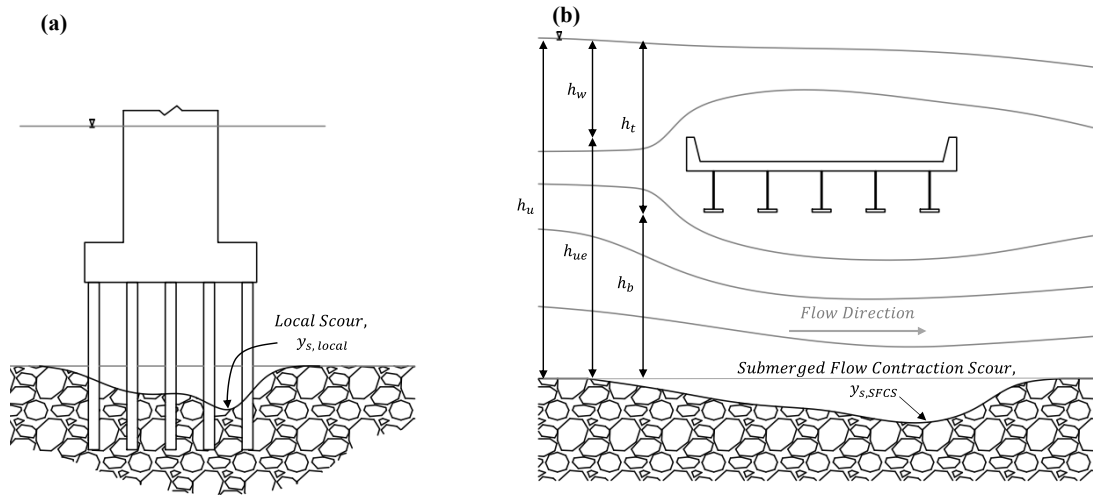
Figure 6-7. Contributions to the total scour depth include (a) local scour due to local obstructions in flow and (b) contraction scour due to submerged flow conditions.

Table 6-3. Scour analysis parameters.

Parameter	Value	Parameter	Value
Pier length along river	10 m	Angle of attack correction factor, k_2	1
Pile cap width	4 m	Correction factor for bed	1.3
Length of pile cap	12 m	Effective unit weight of soil	15000 N/m³
Thickness of pile cap or footing	3 m	D_{50}	2 mm
Hight of bottom of pile cap above bed	-3 m	Effective width of the pile group	4 m
Pile cap nose coefficient, k_1	0.9		

6.9 Results

An analysis is performed for a case where accessibility = $4M, marginal construction cost = 9000 $/m², indirect cost of failure = $100M, discount rate = 1%, and $\bar{I}$ = 20 years. The marginal construction cost is also used to determine the cost of elongation, minus the accessibility and design flexibility costs. An illustration of the second step, economic analysis of adaptation options, for determining the LCC matrix is presented in Table 6-4 for only Scenarios 2 and 6 as the extreme cases. According to the third step of the methodology, the regret matrix is computed. The element of the regret matrix, $R_{s_i a_j \tau}$, denotes the regret value of choosing action $a_j \in \{a_1 = Adapt, a_2 = Not\ Adapt\}$ at time τ under the realization of Scenario s_i. The variation of $R_{s_i a_j \tau}$ over τ is depicted Figure 6-8 for the two actions, a_1 and a_2, and two extreme scenarios, 2 and 6. As can be seen, $a_2 = Not\ Adapt$ would result the largest regret value of around $47M under the realization of the worst scenario.

The rest three curves in Figure 6-8 depict $R^c(t)$, $R^d(t)$, and $R^s(t)$ as the regret of employing the classic MR, deterministic method, and stochastic methods. Note that here $R^s(t)$ is computed with an assumption of information arrival at lognormal distributed time t with mean of $\bar{I} = 20$ years and COV = 0.5. It can be seen that $R^s(t)$ falls between $R^c(t)$ and $R^d(t)$ for decision-making times before t_0. Beyond this time, the value of these three approaches coincides, indicating that information arrival no longer can help improving the decision making.

The added value of the deterministic, V^d, and stochastic, V^s, methods is presented in Figure 6-9. V^d show the value of waiting until a given time when exact information will be available. The high initial value of V^d ($8M) is since exact

information can prevent unnecessary investment building the long bridge. V^s at a given time is the value of waiting longer for possible information arrival in the future instead of acting according to classic MR. Note that the Adaptation Capacity cost for building design flexibilities is not explicitly accounted in the analysis (see Section 6.5). Therefore, V^s can also be interpreted as the upper bound of the Adaptation Capacity costs. As can be seen, V^s begins with a value of \$2.4M with having the option of building the long bridge initially. However, immediately after construction, this option is removed and hope of gaining value through information arrival increases. Subsequently, V^s decreases overtime in case of no information arrival.

For classical MR and the stochastic methods, the design and adaptation police is presented in the form of Figure 6-10. For the stochastic methods the policy is comprised of two sections: *Before and after information arrival*. The horizontal axis is the time since construction (with the consideration of $t = 0$ as the construction phase), and vertical axis represents the set of possible actions. On the *before information* section on the top, the recommendation of the classical MR is plotted for comparison. Here, the curves represent the appropriate action for management of a bridge at a certain age on the horizontal axis. As can be seen, in case of no information, during the construction phase, $t = 0$, the classical MR suggests instantaneous adaptation (meaning to build the long bridge initially), while the stochastic method suggests waiting. However, for an existing extensible bridge (when $t > 0$), the recommendations of the two methods are similar until an information on the validity of either of the scenarios is arrived. For example, at $t = 15$, information arrival on validity of Scenario 5 would result in immediate adaptation of the extensible bridge.

Here, for instance during construction, the classical MR results in immediate adaptation according to $a^c(t)$, while the stochastic method results in waiting for information arrival according to $\tilde{a}(t)$. If the information of the occurrence of a scenario has arrived, Figure 6-10 is used, which provides a summary of the policy of whether to adapt, not adapt, or wait at time t after construction under the revealed scenario.
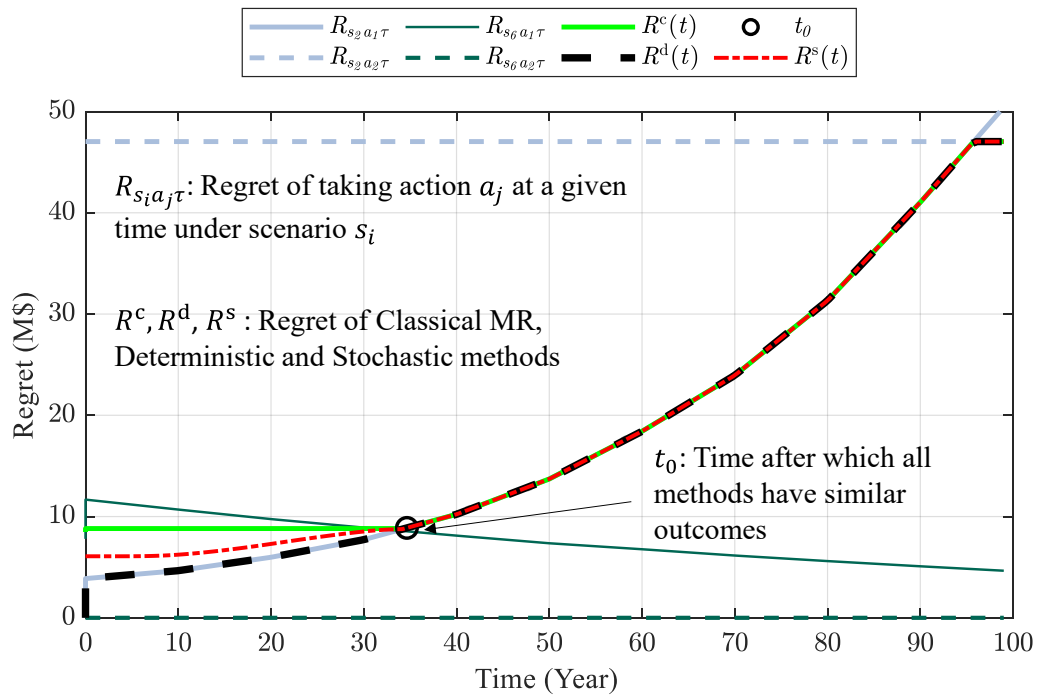
Figure 6-8. Regret values for various strategies and plans associated with Accessibility = $4 M, Construction cost = $9000 /m², Indirect cost of failure = $100 M, Discount rate = 1%, and $\bar{I}$ = 20 years.

Table 6-4. Lifetime cost and regret of various options under two extreme scenarios for the bridge adaptation example.

Adapt at (year)	Cost ($M)		Classical Regret ($M)	
	S_2	S_6	S_2	S_6
0	186.3	26.0	0.0	7.8
0$^+$	190.2	29.9	3.9	11.7
10	191.0	28.9	4.7	10.7
20	192.3	28.0	6.0	9.7
30	194.1	27.1	7.8	8.9
40	196.6	26.4	10.3	8.1
50	200.3	25.6	13.9	7.3
60	205.0	25.0	18.6	6.7
70	210.5	24.4	24.2	6.1
80	217.8	23.8	31.5	5.6
90	227.4	23.3	41.1	5.1
100	236.7	22.9	50.4	4.6
Never	233.4	18.2	47.0	0.0

Note: The 0$^+$case represents adaptation right after construction, which results in inclusion of accessibility costs.

Figure 6-9. The deterministic and stochastic value of waiting associated with Accessibility = $4 M, Construction cost = $9000 /m², Discount rate = 1%, and $\bar{I}$ = 20 years

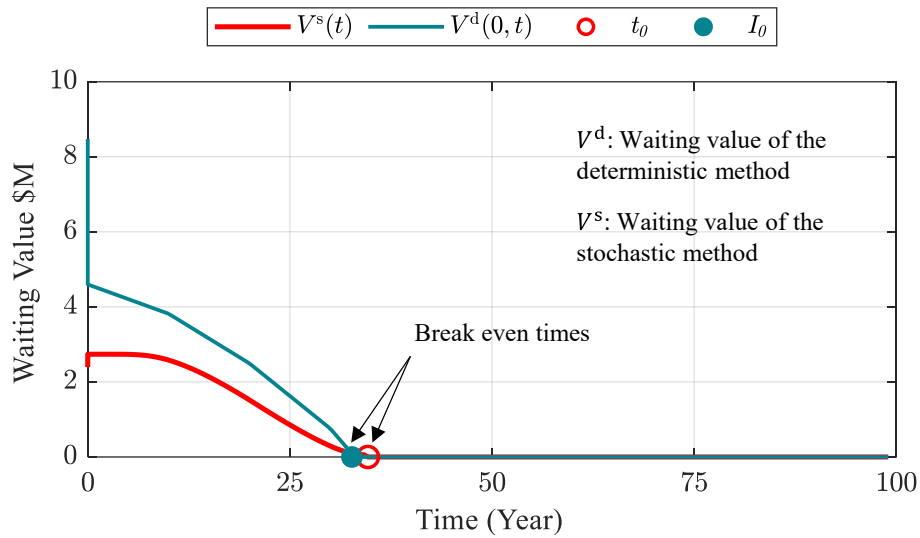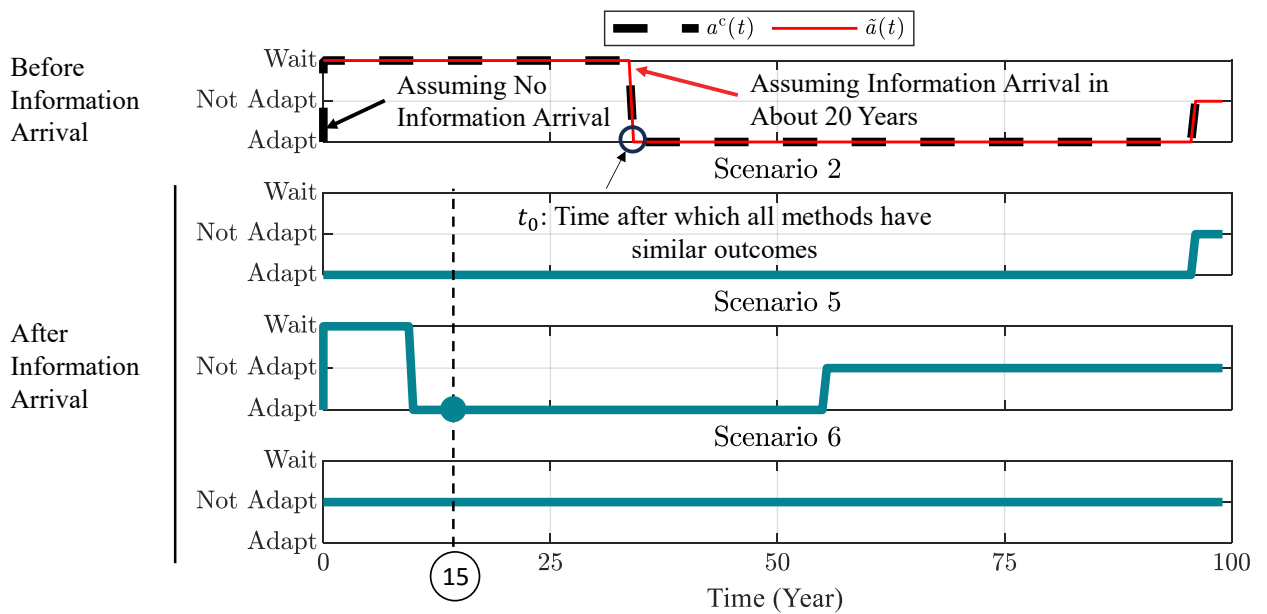*Figure 6-10. Summary of the adaptation policy to whether adapt, not adapt, or wait at time t after construction when no learning has happened yet, as well as under full knowledge of occurrence of each scenario in this time for Scenarios 2, 5, and 6.*

6.9.1 Comparison of Methods

A comparison of the regret of employing different methods is provided in Figure 6-11. In generating the results of this figure, a discount rate of 1% and indirect cost of failure of 10 M$ are considered.

Robust method refers to lifetime cost minimization based on the worst possible scenario. The method suggest adaptation immediately at the construction stage for almost all the values of accessibility and construction costs except for projects with high construction ($> \sim\$5000/m^2$) and low accessibility costs ($< \sim\$1M$), in which case, delaying adaptation is recommended due to the discounting effect. As can be seen, the robust method results in the highest values of regret, especially for large construction costs.

SEU method is employed assuming equal probabilities for all possible scenarios. For low construction costs ($< \sim\$1000/m^2$), it suggests immediate adaptation and for higher values it suggests doing nothing. As can be seen, in comparison with the Robust method, taking this approach results in lower regret values for mid to high range of construction cost.

Finally, in the bottom two rows, the Classic MR and stochastic methods are evaluated. Here, under the stochastic method case a mean time of information arrival of 30 years with COV of 0.5 is considered, and the decision categories are provided instead of the adaptation decision. The regret of employing these last two methods is drastically less than SUE and Robust methods. Also, the regret values of the Stochastic method are less than those of the Classical MR over the regions of decision categories of 3, 4 and 5. The Classical MR suggests immediate adaptation during construction

over regions 1, 2, and 3, delaying adaptation for some time over region 4 and doing nothing for the remaining regions. For the Stochastic method, however, as the time of adaptation depends on the information arrival, it is not possible to provide a predetermined adaptation date.

The difference between Stochastic and Classical MR is captured in terms of the Waiting Value. A more detailed assessment of the Waiting Value and planning under the Stochastic method is provided in the following section.
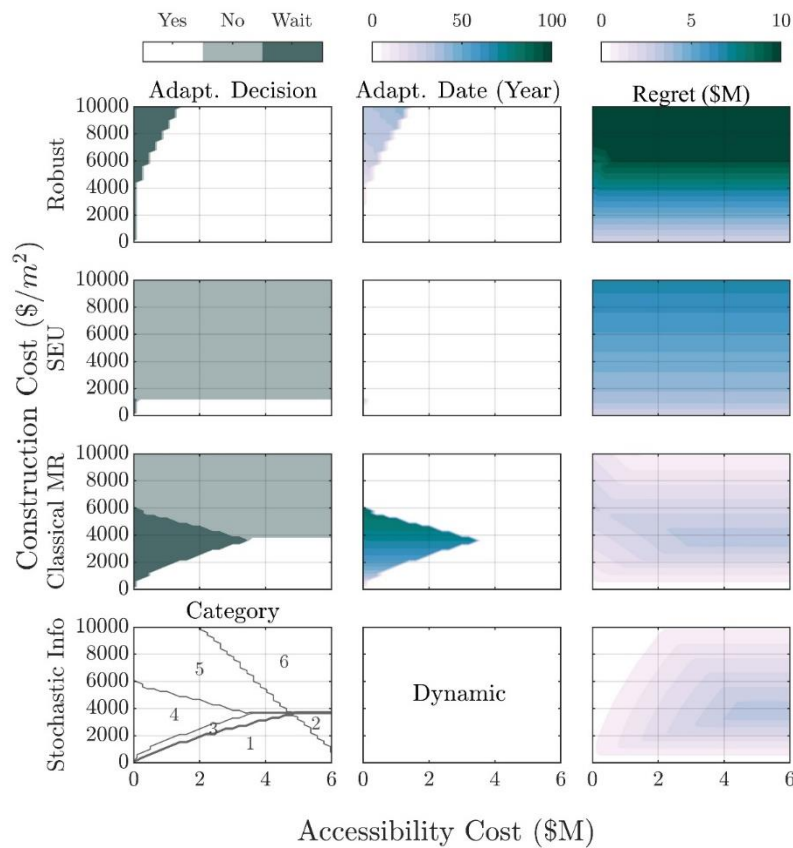

Figure 6-11. Comparison of various design and management methods in terms of adaptation decision, timing, and regret. In generating the results of this figure, a Discount rate is 1% and Indirect cost of failure of 10 M$ is considered.

126

6.10 Categories and Waiting Value Sensitivity Study

For the developed methodology, adaptation planning can be categorized into 7 types, depending on the various cost values of the project. More detail of the definition of these categories is provided in section 3.8. Accordingly, A sensitivity study is performed, and the coverage of the 7 categories coverage is depicted in Figure 6-12 for a range of construction and accessibility costs, various discount rates, and indirect failure costs under three assumptions on the mean time of information arrival. Each point in this figure identifies the planning category of a project with a certain discount rate, construction and accessibility costs. Knowing the category helps identifying the reason behind benefits of waiting values for a project.

The shades in this figure represent the waiting values. This figure shows that the waiting values can be more than \$5 M in some cases, assuming $\bar{I} = 10$ years for the expectation of time of information arrival. However, the values decrease as, $\bar{I}$ grows. Region 3 represents the cases where adaptation during construction is recommended. Region 4 includes cases where adaptation is planned for some time in the future to benefit from discounting, but an arrival of information indicating an adverse scenario may result in earlier adaptation. Region 5 includes cases where adaptation is not recommended unless arrival of information indicates an adverse scenario. The values in this region can also be interpreted as the value of implementing flexibility in design for future adaptation.

Waiting values are the largest at the border of 4-5 regions and increase with the construction cost and a decrease in the accessibility cost. The reason is that this border is the line between doing the adaptation or not in case of no information arrival.

However, at the region 3-4 border, the question is to whether do adaptation earlier during construction or wait for a predetermined period for information arrival. Therefore, it should be obvious that the implications of making a poor decision are more intense in the former case. Furthermore, based on this observation, it can be concluded that the provided method is more beneficial in decisions whether to invest on design flexibilities rather than adaptation postponing decisions.

Consideration of discount rate in the face of climate change can be controversies (Goulder & Williams, 2012). In one hand, most investments for damage prevention due to climate change would be beneficial many years in the future, while discounting the future values can aggressively shrinks those benefits. Here, three values for the discount rate have been considered – 0%, 1% and 2%. As obvious, category 4 is absent for the case of 0% discount rate and the size of category 3 is at its maxima. With the increase in discount rate, the size of category 4 and 5 regions increase, whereas the size of category 3 region decreases. For a discount rate of 0%, and an expectation time of learning of 30 and 50 years, (which would be more likely than the case of $\bar{I} = 10$ years), there are points in category 3 region that suggest waiting for information would result in up to $3 M of benefit in the case of an indirect cost of failure of $10 M.

The change in the indirect cost of failure drastically changes the borders of the regions. Especially, it increases the size of region 3 inside the limits of the figure. The figure shows that for a discount rate of 1 % and high construction and accessibility costs, the benefits of waiting can be around $4 M for indirect cost of failure of $100 M when early information arrival is expected (i.e., $\bar{I} = 10$).
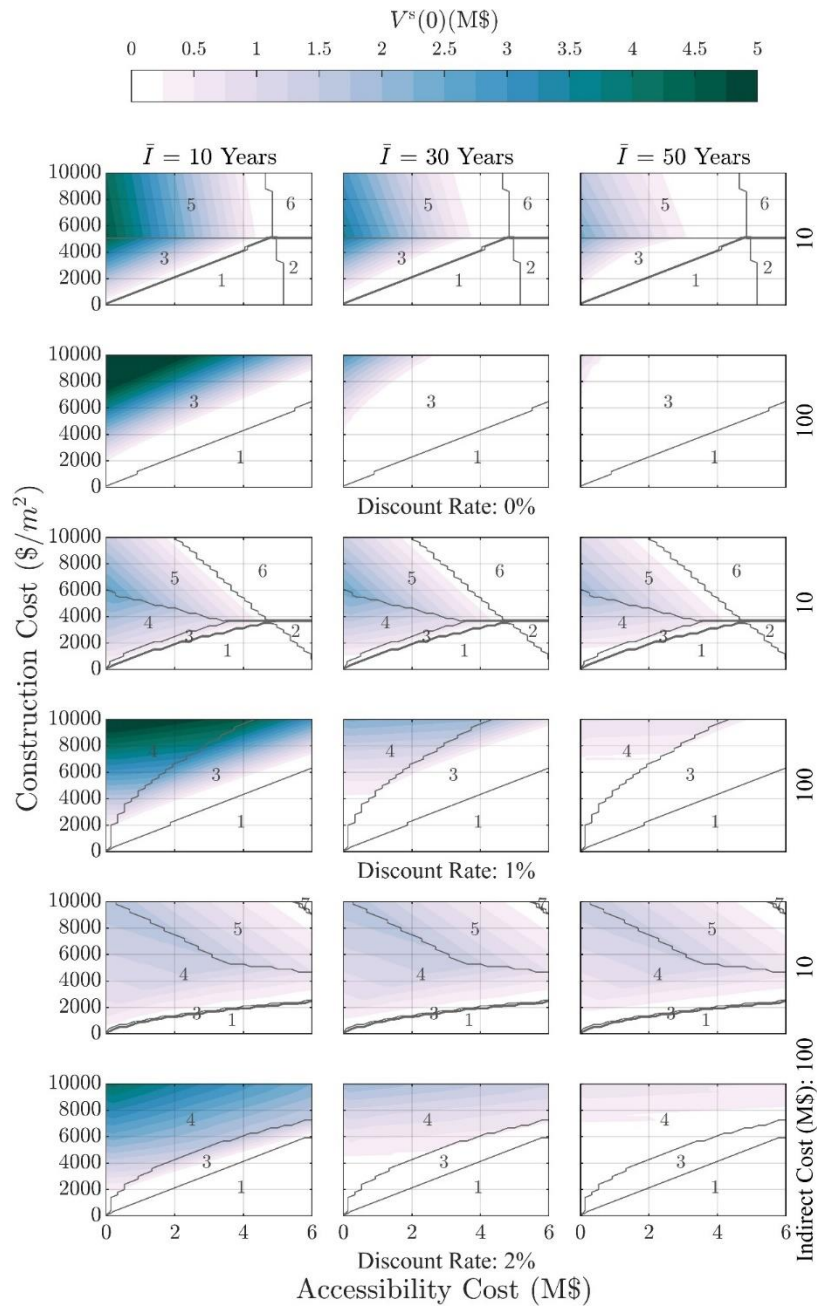
128

Figure 6-12. Waiting value for a range of construction and accessibility costs, various discount rates, and indirect failure costs under three assumptions on the mean time of information arrival. The numbers on each subfigure identify the planning category of the regions separated by gray lines.

129

6.11 Concluding Remarks

This study analyses bridge scour design and climate-change adaptation investment using a new theoretical framework incorporating climatic volatility. The provided framework is a contribution to the literature on adaptive management of infrastructure by applying dynamic programming and the minimum regret decision criterion to adaptation strategies under emerging information on climate change. The central feature of the analysis is the way it models the change in uncertainty about future climate change through information arrival. The framework does not require the likelihood of the possibility of the climate change scenarios and values the timing of information arrival in postponing adaptation projects or implementation of flexibility in the initial design.

Additionally, the approach is intuitively more inline with the nature of human behaviour in the face of uncertainties through minimizing regret instead of utility maximization. This framework contributes to the implementation of a new design paradigm considering the evolving information around climate change. In a traditional design paradigm, the infrastructure is designed and built once and expected to serve society for the next many decades under supposedly stationary or known trends of demand. In the context of climate change, where the future trend is uncertain, this design paradigm can be improved through the consideration of future adaptation flexibility in the initial design.

In the case study considered in this paper, optimal design and adaptation management of a multi-span river-crossing bridge were analysed, and benefits the developed method were illustrated. In the case study, the decision was between

constructing a safer, longer span bridge or an adaptable shorter span bridge. It was shown that a traditional application of minimum regret approach results in immediate construction of the longer bridge. However, the application of the development method revealed that building the shorter bridge and waiting for information arrival can yield a value of $2.5M in terms of reducing regret from poor decision-making under uncertainty.

A comparison of different decision-making methods for adaptation showed that the robust maximin utility method resulted in the highest regret values, especially for large construction costs. The subjective expected utility method suggested immediate adaptation for low construction costs and doing nothing for higher values, resulting in lower regret values for mid to high range of construction cost. Implying the classical Minimax Regret can result in up to millions of dollars of saving in terms of regret depending on project costs, discount rate and the prospect of time of information arrival.

A comprehensive sensitivity study was performed with various outcomes. This study showed that the discount rate has a drastic effect on the waiting value. On one hand, most investments for damage prevention due to climate change would be beneficial many years into the future, while discounting the future values can aggressively shrink these benefits. For a discount rate of 0%, waiting for information can result in up to 3 M$ of benefit for an indirect cost of failure of 10 M$. However, with an increase of the discount rate to 2% the benefits would shrink to zero. A study on the effect of indirect cost of failure revealed that increasing the indirect cost by one order of magnitude will not yield a change in the magnitude of the value of waiting for information. Furthermore, it was shown that the provided method is more

beneficial in decisions whether to invest on design flexibilities rather than adaptation postponing decisions.

Chapter 7. Conclusion and Recommendation for Future studies

7.1 Conclusions

Based on the research presented in the previous chapters of this thesis, the following conclusions are drawn:

Chapter 4:

To evaluate the potential danger of climate change to infrastructure, a structural reliability assessment was conducted using several methods under the impact of climate change. The analysis included a case study of nonstationary effects of wind load on a simple structural element located in London, Ontario. Based on this analysis the following conclusions are drawn:

- Results from the 100-year analysis period indicate that the lifetime probability of failure can be as much as 1.9 times greater than the baseline (stationary) analysis if the worst climate change scenario effects are considered. Furthermore, the annual probability of failure in the final year of service is almost four times that of those in the beginning year (Year 2000).

- While the reliability methods demonstrate the potential threat of climate change to infrastructure, they do not provide means of appropriate decision-making among alternative design and adaptation options, which is crucial given the uncertainties surrounding climate change.

 Chapters 5 and 6:

Traditional optimization-based probabilistic approaches fall short in the face of climate change uncertainties, where no likelihood of the various possible scenarios

is available. Employing subjective probabilities leads to subjective design suggestions with unknow performance and a potential of being regretful in the future. Therefore, based on Minimax Regret, a non-probabilistic decision-making approach, a framework was developed in this thesis. The framework requires no likelihood of climate change scenarios. Additionally, the approach is robust and captures the nature of human behavior better than the traditional expected utility approach in the face of uncertainties through regret minimization.

As the information around climate change is evolving over time, a new design paradigm was considered in the developed framework. In a traditional design paradigm, the infrastructure is designed and built once and is supposed to serve society for the next many decades under supposedly stationary conditions or known trends of demand evolvement. In the context of climate change, where the future trend is uncertain, this design paradigm can be improved through the consideration of future adaptation flexibility in the initial design. On this basis, the proposed method is founded on an assumption that the information on the environment forcings somehow becomes available over time, which might make delaying expensive safety investments valuable. The framework resorts to adaptive solutions and dynamic programming, beginning with a less expensive option until the actual condition of the environment is more evident. In this regard, the monetary added value of waiting for information is determined by comparing the outcomes for two cases of having and not having an expectation of a future information.

As opposed to the classical minimax regret, the developed method does not provide a predetermined adaptation procedure or plan. Instead, it provides design and adaptation policies or strategies on choosing the most appropriate set of action as

time passes and more information on the environmental conditions is revealed. As the optimal design and adaptation policy and efficacy of the method depend on the cost properties of projects. In this regard the possible design and management behaviour can be classified into seven distinct categories. An algorithm was introduced that classifies the projects into those seven categories. Based on the case studies in chapter 5 and 6, the following conclusions are drawn:

- It was shown that the classical minimax regret suggests immediate adaptation during construction if a project falls under Categories 1, 2, and 3; in-service adaptation for projects under Category 4; and doing nothing if a project falls under the remaining categories.

- It was shown that consideration of information arrival through applying the developed methodology is beneficial only for projects falling in Categories 3, 4, and 5. For a new construction project, consideration of the information arrival is the most critical if the project falls under categories 3 and 5. For a Category 3 project, the developed method may suggest avoiding immediate safety investments on the contrary to the recommendation of the classical minimax regret. If a project falls under Category 5, consideration of future flexibilities in the initial design can be beneficial, which is against the recommendation of the classical minimax regret. However, for a Category 4 project, arrival of information may only expedite adaptation investments, which happens automatically even without consideration of information arrival in the initial design. Therefore, in the case of climate change, where information arrival is not at the control of the decision-maker, the developed method has no edge over the classical minimax regret. However, when information arrival is at the control of the decision-maker,

(like in the case of bridge corrosion management), waiting value for information can also be interpreted as the value of testing for information gathering, making the developed method valuable even for category 4 projects.

- Sensitivity studies for the case study of corrosion management (Chapter 5) also show that the added waiting value for information is more sensitive to the discount rate than the expected time of information arrival. Furthermore, it was shown that the maximum expected waiting value is increased with increase in protection life and decrease in the discount rate (from 24% to 44% of disaster cost for discount rate of 0%, and from 19% to 29% for discount rate of 2%, where disaster cost is defined as the lifetime cost of no system modification under the worst scenario). However, the extent of region shrinks as the maximum value increases with the change in these variables.

- It was shown that in the absence of information, the implications of making poor decision of not implementing flexibility in design (around the border of Categories 4 and 5) can be more than early adaptation investments during construction for Category 3 projects.

- In the case study of bridge scour adaptation, a comparison of different decision-making methods for adaptation showed that the robust maximin utility method resulted in the highest regret values, especially for large construction costs. The subjective expected utility method suggested immediate adaptation for low construction costs and doing nothing for higher values, resulting in lower regret values for mid to high range of construction cost. Implying the classical minimax

136

regret can result in up to millions of dollars of saving in terms of regret depending on project costs, discount rate, and the prospect of time of information arrival.

- It was shown that the discount rate has a drastic effect on the waiting value. On one hand, most investments for damage prevention due to climate change would be beneficial for many years into the future, while discounting the future values can aggressively shrink these benefits. For a discount rate of 0%, waiting for information can result in up to 3.5 M$ of benefit for an indirect cost of failure of 10 M$. However, with an increase in the discount rate to 2% the benefits would shrink to zero.

- A study on the effect of indirect cost of failure revealed that increasing the indirect cost by one order of magnitude will not yield a change in the magnitude of the value of waiting for information.

7.2 Future Studies

The following is a list of possible areas of future work stemming from the presented research:

- *Considering multiple adaptation steps and magnitudes:* The current study considers only one adaptation step with a predetermined magnitude. Although considering multiple adaptation steps and magnitudes would result in more complicated approaches, it would better indicate the value of waiting for information and design flexibility and perhaps more accurately reflect the full range of possibilities actually available to infrastructure managers.

137

- *Optimizing initial design based on possible adaptations in the future:* This study only considers the value of modification of an existing design. In practice, the designer would be faced with various design options, and the waiting value and design flexibility should be assessed considering all these options.

- *Investigate a method that adjusts prior initial belief for least regret and allows for smooth learning:* This study assumes that information emerges in a sudden event, which can be improved for more compliance with reality. To achieve this, a probabilistic method can be used to represent the state of belief in the possible scenarios and update the probabilities using a Bayesian updating scheme based on observations. To avoid the issue of imposing subjective probabilities in the initial design phase, where there is no information on the probability of the scenarios is available, the initial probabilities can be adjusted so that they lead to the minimum possible regret. In this way, the advantages of both non-probabilistic and multiple-prior methods could be captured in one framework.

- *Employ the method on case studies to better investigate the value of flexibility in design:* In the case studies used for this work, although the value of design flexibility was inferred from the waiting value, it was not directly considered in the design. For example, in the case of bridge corrosion management through metalizing, no initial investment was necessary to allow metalizing in the future. Instead, it was assumed that later metalizing is always possible without prior considerations. Therefore, to better reflect on the value of design flexibility, more relevant case studies should be investigated.

- *Perform studies for simplifying the adaptive design and adaptation management process for general applications and code development*: The approaches proposed in this study are not easily applicable in day-to-day engineering practice. Therefore, to capture the benefits of design flexibility and waiting value in common engineering practice, more research studies and tool developments are needed.

- *Develop frameworks for considering the budget and monetary limitation along with waiting value and design flexibility in the design and adaptation management process*:

  After many decades of improper management, many civil infrastructure managers are now facing budget shortages, making it challenging to maintain an inventory of already degraded assets. Therefore, any adaptation measure and implementation of design flexibility is in direct competition with maintaining the crumbling assets over a limited budget. To effectively manage this issue, frameworks need to be developed that consider both the budget and monetary limitations, as well as the waiting value and design flexibility necessary for the adaptation of infrastructure to climate change. By adopting such an approach, infrastructure managers can allocate limited resources more efficiently, ensuring that existing assets are maintained while also allowing for the development of new infrastructure that meets the changing demands and the challenges posed by climate change.

- *Investigate and implement emission reduction along with monetary values in the design and adaptation management process*: Governments and agencies are pushing toward measuring and controlling GHG emission especially in the

139

construction industry. Therefore, it is important to consider GHG emission alongside monetary values in a comprehensive framework for design and adaptation management of infrastructure.

- *Investigate the application of reinforcement learning*: Investigate the application of reinforcement learning in the design and adaptation management of infrastructure for solving complicated planning problems with various options and criteria mentioned in the previous recommendation.

Bibliography

Afroz, S., Rhodes, N., Park, J., & Crummey, E. (2022). *Costing Climate Change Impacts to Public Infrastructure: Transportation*.

Albrecht, P., & Naeemi, A. (1984). National Cooperative Highway Research Program Report 272: Performance of Weathering Steel in Bridges. *Transportation Research Board, National Research Council, Washington, DC*.

Allais, M. (1953). Le Comportement de l'Homme Rationnel devant le Risque: Critique des Postulats et Axiomes de l'Ecole Americaine. *Econometrica*, *21*(4), 503.

Arneson, L. A., Zevenbergen, L. W., Lagasse, P. F., Clopper, P. E., & (FHWA)", "Federal Highway Administration. (2012). Evaluating Scour at Bridges. Fifth Edition, Hydraulic Engineering Circular No. 18 (HEC-18). Publication No. FHWA-HIF-12-003. *U.S. Department of Transportation, Federal Highway Administration*, *April*, 340pp.

Arrow, K. J., & Hurwicz, L. (1972). An optimality criterion for decision-making under ignorance. *Uncertainty and Expectations in Economics*, *1*.

Arvidsson, A., Blomqvist, G., & Öberg, G. (2012). Impact of climate change on use of anti-icing and deicing salt in Sweden. *Winter Maintenance and Surface Transportation Weather: International Conference on Winter Maintenance and Surface Transportation Weather*, *30*, 3–10.

Baravalle, M., & Köhler, J. (2019). A risk-based approach for calibration of design codes. *Structural Safety*, *78*(September 2017), 63–75.

Bastidas-Arteaga, E., & Stewart, M. G. (2019). Climate change impact for bridges subjected to scour and corrosion. In *Climate Adaptation Engineering: Risks and Economics for Infrastructure Decision-Making 1st Edition* (p. 387).

Bellman, R. (1952). On the Theory of Dynamic Programming. *Proceedings of the National Academy of Sciences*, *38*(8), 716–719.

Binmore, K. (2008). Rational Decisions. In *Rational Decisions*. Princeton University Press.

Broecker, W. S. (1997). Thermohaline circulation, the achilles heel of our climate system: Will man-made CO2 upset the current balance? *Science*, *278*(5343), 1582–1588.

CAN/CSA-S6-06: Canadian Highway Bridge Design Code. (2006). Canadian Standards Association.

Canadian Standards Association. (2009). *Risk Management: Guideline for Decision-Makers, CAN/CSA-Q850-97 (R2009)*. https://www.scc.ca/en/standardsdb/standards/6777

Cannon, A., Jeong, D. Il, Zhang, X., & Zwiers, F. W. (2020). *Climate-resilient buildings and core public infrastructure: an assessment of the impact of climate change on climatic design data in Canada*.

Coles, S. (2001). *An introduction to statistical modeling of extreme values*. https://www.researchgate.net/profile/Joan-Del-Castillo/publication/39434099_Comentaris_de_llibres/links/55102c250cf2a95b5b426dd8/Comentaris-de-llibres.pdf

Commentary on CAN/CSA-S6-00, Canadian Highway Bridge Design Code. (2000). Canadian Standards Association.

Consortium, P. C. I. (2020). *VIC-GL BCCAQ CMIP5 RVIC: Station Hydrologic Model Output*. University of Victoria. https://www.pacificclimate.org/data/station-hydrologic-model-output

Cox, L. A. (2012). Confronting Deep Uncertainties in Risk Analysis. *Risk Analysis*, *32*(10), 1607–1629.

CSA. (2007). *Calibration report For CAN/CSA-S6-06 canadian highway bridge design code* (Issue August).

CSA Group. (2019). *CSA S6:19, Canadian Highway Bridge Design Code*. Canadian Standards Association (CSA).

Damgaard, N. (2009). *Prediction and Prolongation of the Service Life of Weathering Steel*

Highway Structures. University of Waterloo.

Damgaard, N., & Walbridge, S. (2009). Service life prediction for weathering steel highway structures. *Proceedings of the 2009 Structures Congress - Don't Mess with Structural Engineers: Expanding Our Role*, 2189–2198.

de Neufville, R. (2019). Engineering Options Analysis (EOA). In *Decision Making Under Deep Uncertainty. From Theory to Practice*. Springer.

Dittrich, R., Wreford, A., & Moran, D. (2016). A survey of decision-making approaches for climate change adaptation: Are robust methods the way forward? In *Ecological Economics* (Vol. 122, pp. 79–89). Elsevier B.V.

Dreyfus, S. (2002). Richard Bellman on the birth of dynamic programming. *Operations Research*, *50*(1), 48–51.

Ellsberg, D. (1961). Risk, ambiguity, and the savage axioms. *Quarterly Journal of Economics*, *75*(4), 643–669.

Etner, J., Jeleva, M., & Tallon, J. M. (2012). Decision theory under ambiguity. *Journal of Economic Surveys*, *26*(2), 234–270.

Evans, M., & Frick, C. (2001). *The effects of road salts on aquatic ecosystems*.

Gilboa, I. (2009). Theory of Decision under Uncertainty. In *Theory of Decision under Uncertainty*.

Gilboa, I., Postlewaite, A., Philosophy, D. S.-E. &, & 2009, undefined. (2009). Is it always rational to satisfy Savage's axioms? *Cambridge.Org*, *25*, 285–296.

Gilboa, I., Postlewaite, A. W., & Schmeidler, D. (2008). Probability and uncertainty in economic modeling. *Journal of Economic Perspectives*, *22*(3), 173–188.

Gilboa, I., & Schmeidler, D. (1989). Maxmin expected utility with non-unique prior. *Journal of Mathematical Economics*, *18*(2), 141–153.

Goulder, L. H., & Williams, R. C. (2012). The choice of discount rate for climate change policy

evaluation. *Climate Change Economics*, *3*(4).

Guthrie, G. (2019). Real options analysis of climate-change adaptation: investment flexibility and extreme weather events. *Climatic Change*, *156*(1–2), 231–253.

Haasnoot, M., Kwakkel, J. H., Walker, W. E., & ter Maat, J. (2013). Dynamic adaptive policy pathways: A method for crafting robust decisions for a deeply uncertain world. *Global Environmental Change*, *23*(2), 485–498.

Haasnoot, M., van Aalst, M., Rozenberg, J., Dominique, K., Matthews, J., Bouwer, L. M., Kind, J., & Poff, N. L. R. (2020). Investments under non-stationarity: economic evaluation of adaptation pathways. *Climatic Change*, *161*(3), 451–463.

Hallegatte, S. (2009). Strategies to adapt to an uncertain climate change. *Global Environmental Change*, *19*(2), 240–247.

Hallegatte, S., Shah, A., Lempert, R., Brown, C., & Gill, S. (2012). Investment Decision Making Under Deep Uncertainty: Application to Climate Change. *Policy Research Working Paper*, *6193*, 41.

Hamman, J., Nijssen, B., Brunke, M., Cassano, J., Craig, A., DuVivier, A., Hughes, M., Lettenmaier, D. P., Maslowski, W., Osinski, R., Roberts, A., & Zeng, X. (2016). Land Surface Climate in the Regional Arctic System Model. *Journal of Climate*, *29*(18), 6543–6562.

Hawkins, E., & Sutton, R. (2011). The potential to narrow uncertainty in projections of regional precipitation change. *Climate Dynamics*, *37*(1), 407–418.

Heal, G., & Millner, A. (2014). Uncertainty and decision making in climate change economics. *Review of Environmental Economics and Policy*, *8*(1), 120–137.

IPCC. (2007). Climate Change 2007: The Physical Science Basis. Contribution of Working Group I to the Fourth Assessment Report of the Intergovernmental Panel on Climate Change. Summary for Policymakers. In *Intergovernmental Panel on Climate Change*.

ISO. (2015). *ISO 2394:2015 General principles on reliability for structures*. ISO Geneva.

Issues - Global Warming | Impact Zones - U.S. Alaska. (n.d.). https://www.markey.senate.gov/imo/media/globalwarming/impactzones/alaska.html

Johnson, B. W. (2005). *After The Disaster: Utility Restoration Cost Recovery*. www.eei.org

Judd, A. (2021). *New photos of Coquihalla Highway flood damage released*. Globalnews.Ca. https://globalnews.ca/news/8381003/bc-flooding-new-photos-coquihalla-highway-damage/

Katz, R. W., Craigmile, P. F., Guttorp, P., Haran, M., Sansó, B., & Stein, M. L. (2013). Uncertainty analysis in climate change assessments. *Nature Climate Change 2013 3:9*, *3*(9), 769–771.

Kayser, J. (1988). *The effects of corrosion on the reliability of steel girder bridges*.

Khandel, O., & Soliman, M. (2019). Integrated Framework for Quantifying the Effect of Climate Change on the Risk of Bridge Failure Due to Floods and Flood-Induced Scour. *Journal of Bridge Engineering*, *24*(9), 1–14.

Klibanoff, P., Marinacci, M., & Mukerji, S. (2005). A smooth model of decision making under ambiguity. *Econometrica*, *73*(6), 1849–1892.

Knight, F. H. (1921). *Risk, uncertainty and profit* (Vol. 31). Houghton Mifflin.

Knutti, R. (2010). The end of model democracy? *Climatic Change*, *102*(3), 395–404.

Knutti, R., Furrer, R., Tebaldi, C., Cermak, J., & Meehl, G. A. (2010). Challenges in combining projections from multiple climate models. *Journal of Climate*, *23*(10), 2739–2758.

Knutti, R., & Sedláček, J. (2012). Robustness and uncertainties in the new CMIP5 climate model projections. *Nature Climate Change 2012 3:4*, *3*(4), 369–373.

Kupper, L. L. (1971). Probability, statistics, and decision for civil engineers. *Technometrics*, *13*(1), 211–211.

Kwakkel, J. H., Walker, W. E., & Haasnoot, M. (2016). Coping with the Wickedness of Public Policy Problems: Approaches for Decision Making under Deep Uncertainty. *Journal of Water Resources Planning and Management*, *142*(3), 01816001.

Lagasse P.F., Ghosn M., Johnson P.A., Zevenbergen, L. W., & Clopper, P. E. (2013). Risk-based approach for bridge scour prediction: Final report. In *Transportation Research Board of the National Academies*.

Lee, B. S., Haran, M., & Keller, K. (2017). Multidecadal Scale Detection Time for Potentially Increasing Atlantic Storm Surges in a Warming Climate. *Geophysical Research Letters*, *44*(20), 10,617-10,623.

Li, Q., Wang, C., & Ellingwood, B. R. (2015). Time-dependent reliability of aging structures in the presence of non-stationary loads and degradation. *Structural Safety*, *52*(PA), 132–141.

Lohmann, D., Nolte-Holube, R., & Raschke, E. (1996). A large-scale horizontal routing model to be coupled to land surface parametrization schemes. *Tellus, Series A: Dynamic Meteorology and Oceanography*, *48*(5), 708–721.

Lohmann, D., Raschke, E., Nijssen, B., & Lettenmaier, D. P. (1998). Regional scale hydrology: I. Formulation of the VIC-2L model coupled to a routing model. *Hydrological Sciences Journal*, *43*(1), 131–141.

Maccheroni, F., Marinacci, M., & Rustichini, A. (2006). Ambiguity aversion, robustness, and the variational representation of preferences. *Econometrica*, *74*(6), 1447–1498.

Malik, A., Rothbaum, J., & Smith, S. C. (2010). *Climate Change, Uncertainty, and Decision-Making*.

Marchau, V., Walker, W., Bloemen, P., & Popper, S. (2019). Decision Making Under Deep Uncertainty. From Theory to Practice. In *Springer*.

Mills, E. (2012). Electric Grid Disruptions and Extreme Weather. *US Disaster Reanalysis Workshop National Climatic Data Center*, *2012*.

Mondoro, A., Frangopol, D. M., & Liu, L. (2018). Multi-criteria robust optimization framework for bridge adaptation under climate change. *Structural Safety*, *74*(April), 14–23.

Morel, B. (2020). Real Option Analysis and Climate Change. In *Springer Climate*.

Neill, C. R. (1980). Scour problems at railway bridges on the Thompson River, B.C. *CAN. J. CIV. ENGNG.*, *7*(2, Jun. 1980), 357–372.

Nowak, A. S., & Grouni, H. N. (1994). Calibration of the Ontario highway bridge design code 1991 edition. *Canadian Journal of Civil Engineering*, *21*(1), 25–35.

Pandey, M. D., & Lounis, Z. (2023). Stochastic modelling of non-stationary environmental loads for reliability analysis under the changing climate. *Structural Safety*, *103*, 102348.

Pizarro, A., & Tubaldi, E. (2019). Quantification of Modelling Uncertainties in Bridge Scour Risk Assessment under Multiple Flood Events. *Geosciences*, *9*(10), 445.

Sandink, D., & Lapp, D. (2021). The PIEVC Protocol for Assessing Public Infrastructure Vulnerability to Climate Change Impacts: National and International Application. In *Lecture Notes in Civil Engineering* (Vol. 249). Springer Nature Singapore.

Savage, L. J. (1951). The Theory of Statistical Decision. *Journal of the American Statistical Association*, *46*(253), 55–67.

Savage, L. J. (1972). *The Foundations of Statistics*. Dover Publications.

Schmeidler, D. (1989). Subjective Probability and Expected Utility without Additivity. *Econometrica*, *57*(3), 571.

SDE with Mean-Reverting Drift (SDEMRD) model - MATLAB. (n.d.). Retrieved February 13, 2023, from https://www.mathworks.com/help/finance/sdemrd.html

Shan, H., Xie, Z., Bojanowski, C., Suaznabar, O., Lottes, S., Shen, J., Kerenyi, K., & Genex Systems, L. (2012). *Submerged flow bridge scour under clear water conditions*.

Shayanfar, M. A., Barkhordari, M. A., Barkhori, M., & Barkhori, M. (2018). An adaptive

directional importance sampling method for structural reliability analysis. *Structural Safety*, *70*, 14–20.

Sims, C., & Null, S. E. (2019). Climate Forecasts and Flood Mitigation. *Southern Economic Journal*, *85*(4), 1083–1107.

Stocker, T. F., Qin, D., Plattner, G.-K. K., Tignor, M. M. B. B., Allen, S. K., Boschung, J., Nauels, A., Xia, Y., Bex, V., & Midgley, P. M. (2014). Climate change 2013: the physical science basis working group I contribution to the fifth assessment report of the intergovernmental panel on climate change. In *Intergovernmental Panel on Climate Change* (Vol. 9781107057). Cambridge University Press.

Stroombergen, A., & Lawrence, J. (2022). A novel illustration of real options analysis to address the problem of probabilities under deep uncertainty and changing climate risk. *Climate Risk Management*, *38*, 100458.

Sturm, T., Abid, I., Melville, B., Xiong, X., Stoesser, T., Bugallo, B. F., Chua, K. V., Abt, S., & Hong, S. (2018). Combining Individual Scour Components to Determine Total Scour. In *Combining Individual Scour Components to Determine Total Scour*.

U.S. Army Corps of Engineers. (2022). HEC-RAS (river analysis system). In *cedb.asce.org* (6.3.1). Hydrologic Engineering Center.

Urban, N. M., Holden, P. B., Edwards, N. R., Sriver, R. L., & Keller, K. (2014). Historical and future learning about climate sensitivity. *Geophysical Research Letters*, *41*(7), 2543–2552.

van der Pol, T. D., Gabbert, S., Weikard, H. P., van Ierland, E. C., & Hendrix, E. M. T. (2017). A Minimax Regret Analysis of Flood Risk Management Strategies Under Climate Change Uncertainty and Emerging Information. *Environmental and Resource Economics*, *68*(4), 1087–1109.

van der Pol, T. D., van Ierland, E. C., & Gabbert, S. (2017). Economic analysis of adaptive strategies for flood risk management under climate change. *Mitigation and Adaptation*

Strategies for Global Change, *22*(2), 267–285.

van der Pol, T. D., van Ierland, E. C., & Weikard, H. P. (2014). Optimal dike investments under uncertainty and learning about increasing water levels. *Journal of Flood Risk Management*, *7*(4), 308–318.

Wald, A. (1949). Statistical Decision Functions. *The Annals of Mathematical Statistics*, *20*(2), 165–205. http://www.jstor.org/stable/2236853

Walker, W. E., Marchau, V. A. W. J., & Swanson, D. (2010). *Addressing deep uncertainty using adaptive policies: Introduction to section 2*.

Wang, C., Yu, X., & Liang, F. (2017). A review of bridge scour: mechanism, estimation, monitoring and countermeasures. *Natural Hazards*, *87*(3), 1881–1906.

Wardhana, K., & Hadipriono, F. C. (2003). Analysis of Recent Bridge Failures in the United States. *Journal of Performance of Constructed Facilities*, *17*(3), 144–150.

Yager, R. R. (2004). Decision making using minimization of regret. *International Journal of Approximate Reasoning*, *36*(2), 109–128.

Appendix A.

A.1. Load Factors and Reliability Index

This section aims to calculate the proper value for the load factor, which yields a desired reliability index (β). For simplification, the lognormally distributed random variables for the resistance, R, and load, L, can be replaced by normalized variables:

$$z_R = \frac{R}{R_n}, \quad z_L = \frac{L}{L_n} \tag{0-1}$$

In Equation (0-1), the 'n' subscript denotes a nominal or design value, S and R are the actual load and resistance, and z_L and z_R are the normalized load and resistance. Therefore, the limit state function G can be written as:

$$G = z_R \cdot R_n - z_L \cdot L_n \text{ or } G = z_R \cdot L_n \cdot \alpha_L - z_L \cdot L_n \tag{0-2}$$

Failure happens when $G < 0$ or $z_R \cdot \alpha_L < z_L$. Taking the natural log of both sides:

$$LN(\alpha_L) + LN(z_R) < LN(z_L) \tag{0-3}$$

$$LN(z_L) - LN(z_R) > LN(\alpha_L)$$

As z_L and z_R are lognormally distributed, $LN(z_L)$ and $LN(z_R)$, and a new variable defined as $LN(z_L) - LN(z_R) = X$, would have normal distributions. Therefore, the limit state function can be redefined as:

$$X > LN(\alpha_L) \tag{0-4}$$

Consequently, the probability of failure can be calculated using the following formulas:

$$p(X > LN(\alpha_L)) = \Phi(-\beta) \tag{0-5}$$

From this equation one can conclude $p(X < LN(\alpha_L)) = \Phi(\beta)$, and further expand the equation to:

$$p\left(\frac{X - \bar{X}}{\sigma_X} < \frac{LN(\alpha_L) - \bar{X}}{\sigma_X}\right) = \Phi(\beta) \tag{0-6}$$

Please note that the mean value of each variable is denoted by a bar (e.g. $\bar{X}$) while their COV is denoted with a COV (e.g. COV_L), and their standard deviation is shown by σ (e.g. σ_X). In Equation (0-5), as $(X - \bar{X})/\sigma_X$ follows the standard normal distribution, one can conclude that $\frac{LN(\alpha_L) - \bar{X}}{\sigma_X} = \beta$. Therefore, the load factor can be calculated by the following formula as a function of the reliability index (β):

$$\alpha_L = EXP(\beta \cdot \sigma_X + \bar{X}) \tag{0-7}$$

where:

$$\sigma_X = \sqrt{LN\left[(1 + COV_{Z_L}^2)(1 + COV_{Z_R}^2)\right]} \tag{0-8}$$

and

$$\bar{X} = LN\left(\frac{\bar{z}_L}{\bar{z}_R}\sqrt{\frac{1 + COV_{Z_R}^2}{1 + COV_{Z_L}^2}}\right) \tag{0-9}$$

However, it is worth noting that in general design problems, the demand on the engineered component or system usually involves a combination of different loads, each of which is given its load factor in modern design codes. The simultaneous presence of dead and wind load effects on a structure is a simple example of such a condition. In this regard, the limit state function can be redefined as $G = R - (D + W)$ where D and W are random variables representing dead and wind load effects. Accordingly, a minimum resistance (R_n) is required:

151

$$\phi_R R_n = \alpha_D D_n + \alpha_W W_n \tag{0-10}$$

Here, ϕ_R, α_D, and D_n, are the resistance factor, dead load factor, and nominal dead load effect, while αw and Wn represent the wind load factor and nominal wind load effect. Given the resistance and dead load factors and parameters of the load and resistance random variables, the wind load factor can be calculated by replacing the statistical parameters of R (resistance) in Equation (0-11)) with $U = R - D$ and L with W. As a result, with the assumption of a lognormal distribution for U:

$$\alpha_W = \frac{\bar{z}_W}{\bar{z}_U} \Omega \tag{0-11}$$

$$\Omega = \left(\sqrt{\frac{1 + COV_{z_U}^2}{1 + COV_{z_W}^2}} \right) EXP\left(\beta \sqrt{LN\left[(1 + COV_{z_W}^2)(1 + COV_{z_U}^2) \right]} \right)$$

in which the normalized lognormally distributed random variable z_U, is defined according to the following formula:

$$z_U = \frac{R-D}{\phi_R R_n - \alpha_D D_n} = \frac{R_n}{U_n} z_R - \frac{D_n}{U_n} z_D \tag{0-12}$$

where $U_n = \phi_R R_n - \alpha_d D_n$. As a result, $\bar{z}_u$ and σ_{z_U}, the mean and standard deviation of z_U can be computed using Equations (0-13) and (0-14) respectively:

$$\bar{z}_U = \frac{R_n \bar{z}_R - D_n \bar{z}_D}{U_n} \tag{0-13}$$

$$\sigma_{z_U} = \sqrt{\left(\frac{R_n}{U_n} \right)^2 \sigma_{z_R}^2 + \left(\frac{D_n}{U_n} \right)^2 \sigma_{z_D}^2} \tag{0-14}$$

Therefore, the COV of z_U is:

$$COV_{z_U} = \frac{\sqrt{\left(\frac{R_n}{U_n} \right)^2 \sigma_{z_R}^2 + \left(\frac{D_n}{U_n} \right)^2 \sigma_{z_D}^2}}{\frac{R_n}{U_n} \bar{z}_R - \frac{D_n}{U_n} \bar{z}_D} \tag{0-15}$$

The other important outcome is that the reliability index can be computed through the following equation:

$$\beta = LN\left(\Omega\sqrt{\frac{1+COV_{z_W}^2}{1+COV_{z_U}^2}}\right)\Big/\sqrt{LN\big[(1+COV_{z_W}^2)(1+COV_{z_U}^2)\big]} \qquad (0\text{-}16)$$

$$\Omega = \frac{\bar{z}_R}{\bar{z}_W\phi_R}\left[\alpha_W - \frac{D_n}{w_n}\left(\frac{\phi_R\bar{z}_D}{\bar{z}_R} - \alpha_D\right)\right] \qquad (0\text{-}17)$$

A.2. Category Sample Analysis

Following the analysis in Section 5.4.1, to interpret the value of waiting, adaptation plans are categorized into 7 types. For protection life of 40 and 70 years and discount rate of zero and two percents maps of region of these categories are presented in Figure 0-1. For better understanding, for the sample points a trough i in this figure, the regrets and adaptation policy summaries are presented in Figure 0-2 to Figure 0-4. Further explanation is avoided as these figures can be interpreted in a way similar to what was provided in Section 5.3. In these figures, curves associated with the stochastic method are drawn for lognormally distributed information update with mean of $\bar{I} = 10$ years and COV of 0.5. To assess the effect of info update distribution, Figure 0-5 is provided for $\bar{I} = 40$ instead but with the same discount rate of 2%. As can be seen, with the increase in $\bar{I}$ the stochastic value of waiting is decreased and for Category 3, the initial waiting decision is changed to metalizing.
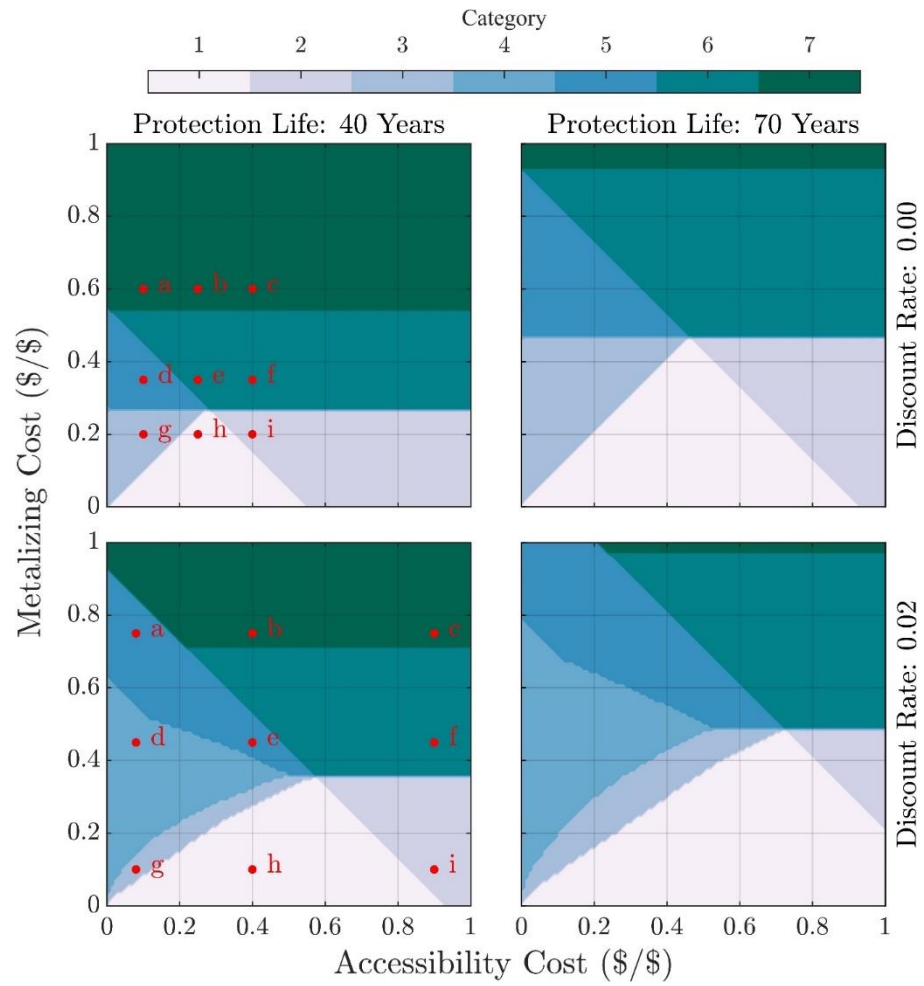
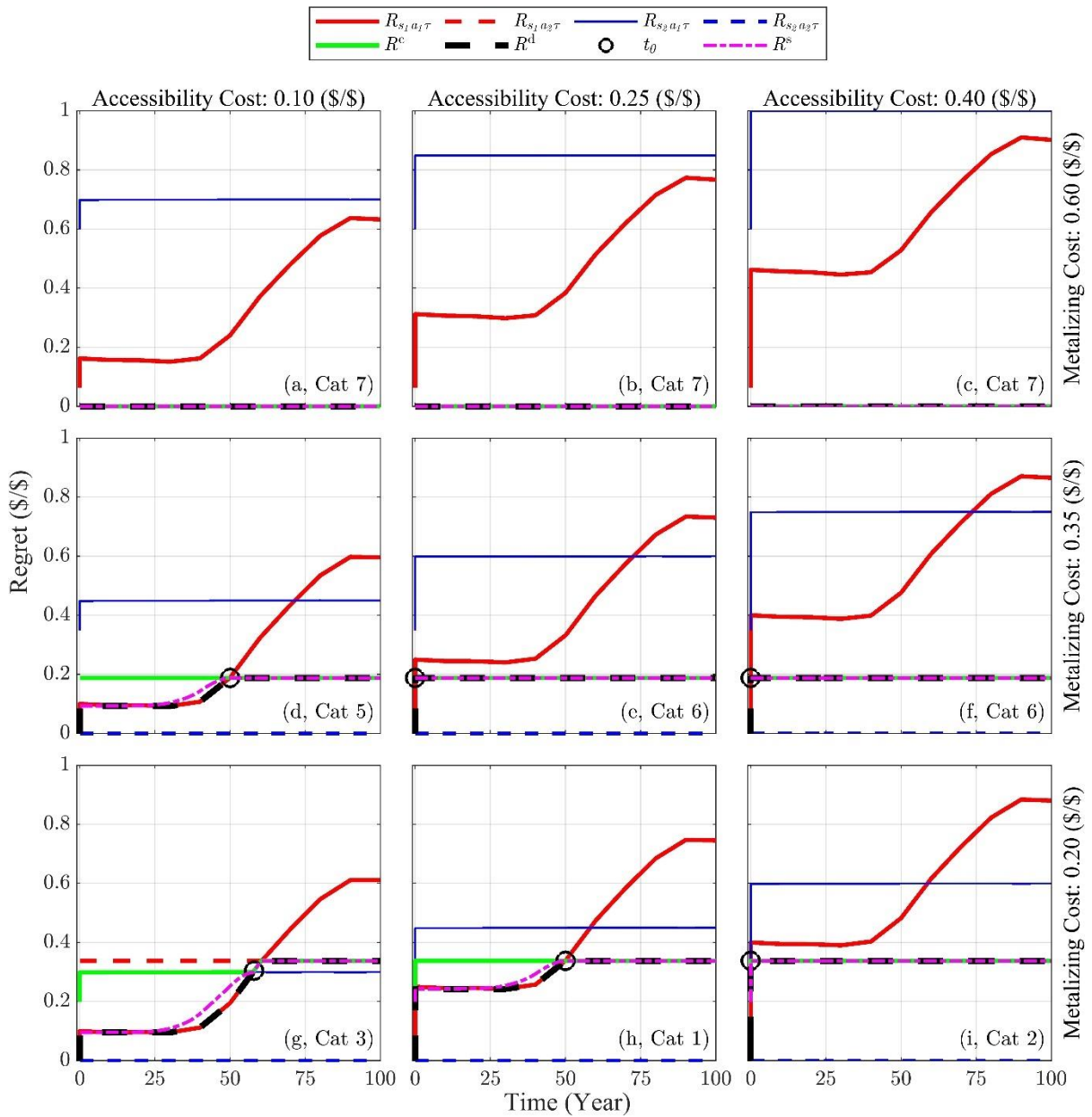*Figure 0-1. Decision category for different values of the considered parameters.*

Figure 0-2. Regret values of various strategies for the sample points a trough i with discount rate of 0% in Figure 0-1.
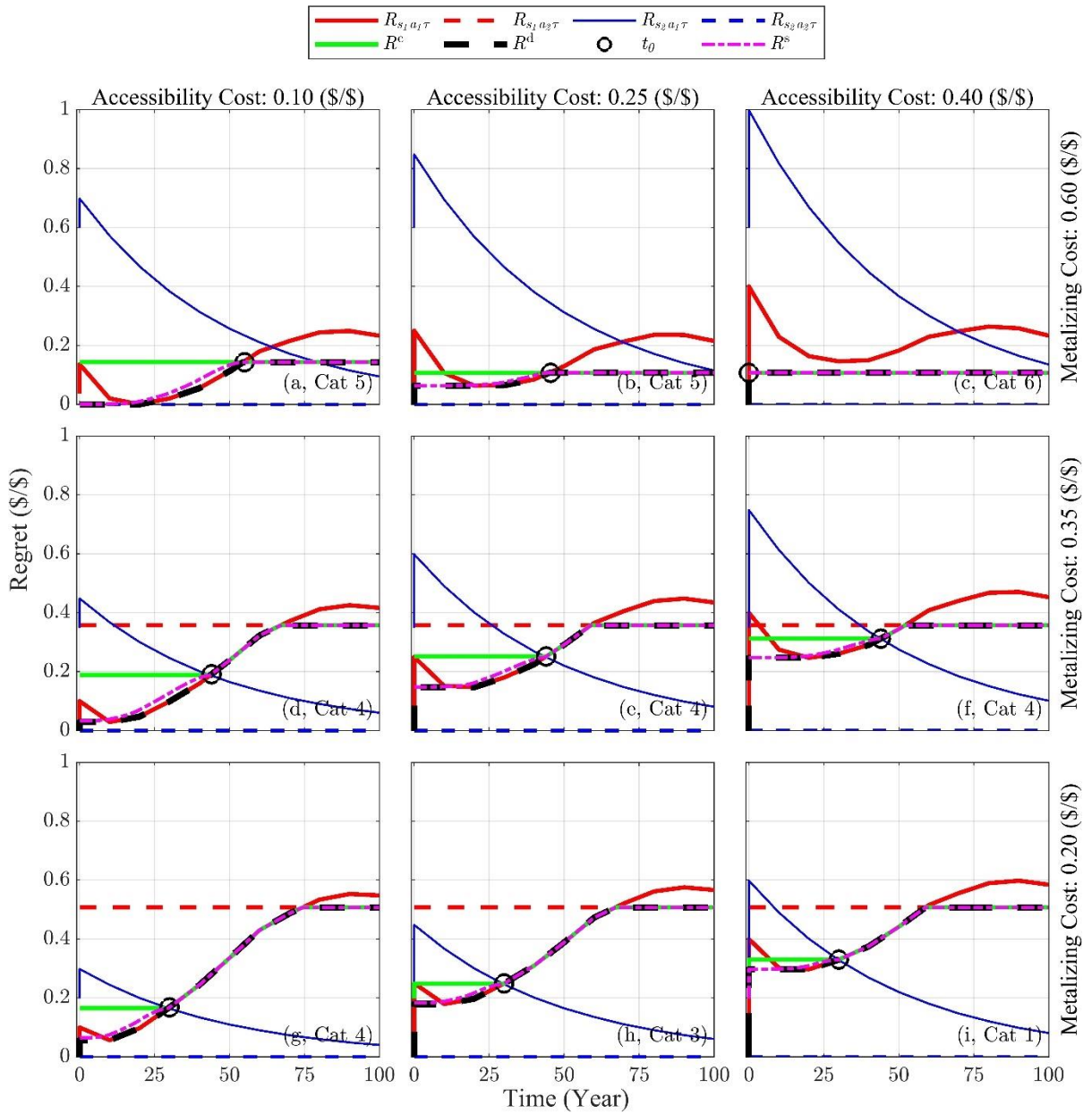
Figure 0-3. Regret values of various strategies for the sample points a trough i with discount rate of 2% in Figure 0-1.
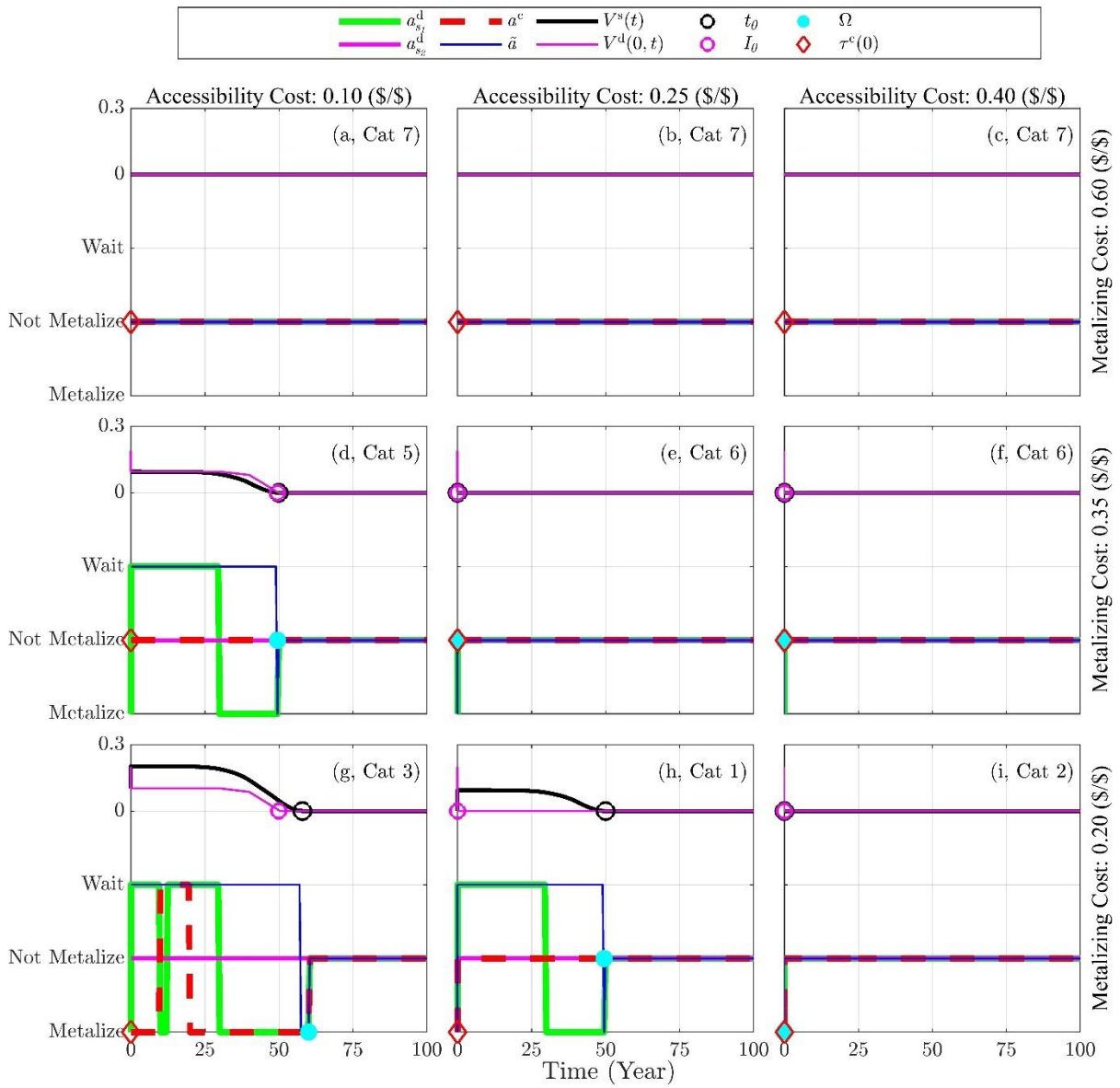
156

Figure 0-4. Summary of the plan to whether metalize, not metalize, or wait during construction and later over time, as well as the deterministic and stochastic value of waiting ($/$) for the sample points a to i with Discount rate 0%, $\overline{I} = 10$ years and COV of 0.5.
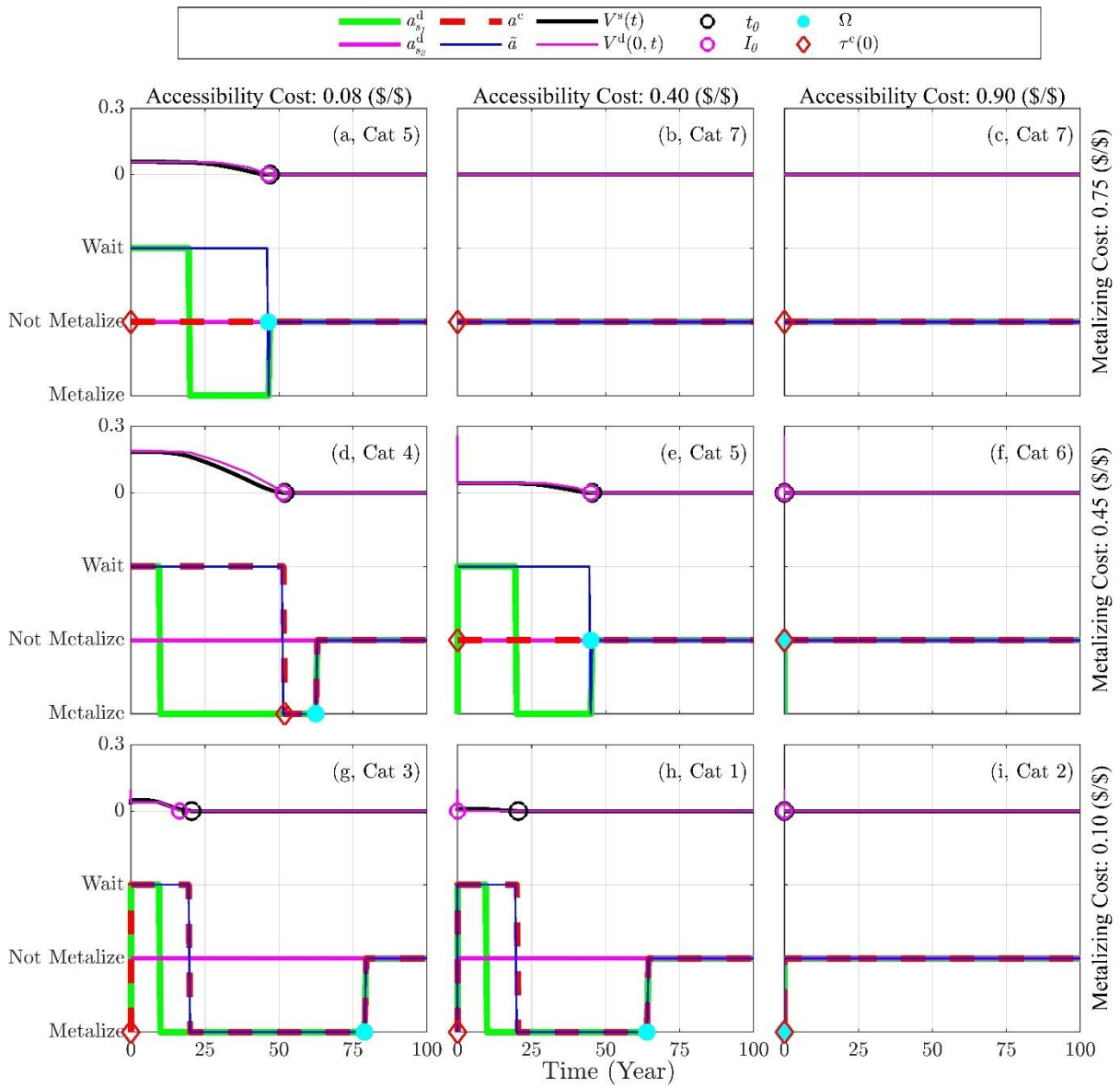
Figure 0-5. Summary of the plan to whether metalize, not metalize, or wait during construction and later over time, as well as the deterministic and probabilistic value of waiting ($/$) for the sample points a to i with Discount rate 2%, $\bar{I} = 40$ years and COV of 0.5.